Nitrogenase-Like Enzymes of Chlorophyll and Bacteriochlorophyll Biosynthesis

Von der Fakultät für Lebenswissenschaften
der Technischen Universität Carolo-Wilhelmina
zu Braunschweig
zur Erlangung des Grades einer
Doktorin der Naturwissenschaften
(Dr. rer. nat.)
genehmigte
D i s s e r t a t i o n

von Denise Wätzlich
aus Dresden

1. Referent: Professor Dr. Dieter Jahn
2. Referent: Professor Dr. Michael Steinert
eingereicht am: 09.11.2009
mündliche Prüfung (Disputation) am: 16.12.2009

Druckjahr 2010

Vorveröffentlichungen der Dissertation

Teilergebnisse aus dieser Arbeit wurden mit Genehmigung der Fakultät für Lebenswissenschaften, vertreten durch den Mentor der Arbeit, in folgenden Beiträgen vorab veröffentlicht:

Publikationen

Wätzlich, D., Bröcker, M.J., Uliczka, F., Ribbe, M., Virus, S., Jahn, D. & Moser, J. (2009). Chimeric Nitrogenase-like Enzymes of (Bacterio)chlorophyll Biosynthesis. *J Biol Chem*. **284**, 15530-15540.

Bröcker, M.J., Wätzlich, D., Uliczka, F., Virus, S., Saggu, M., Lendzian, F., Scheer, H., Rüdiger, W., Moser, J. & Jahn, D. (2008). Substrate recognition of nitrogenase-like dark-operative protochlorophyllide oxidoreductase from *Prochlorococcus marinus*. *J Biol Chem*. **283**, 29873-29881.

Walther, J., Bröcker, M.J., Wätzlich, D., Nimtz, M., Rohde, M., Jahn, D. & Moser, J. (2008). Protochlorophyllide: a new photosensitizer for the photodynamic inactivation of Gram-positive and Gram-negative bacteria. *FEMS Microbiol Lett.* **290**, 156-163.

Bröcker, M.J., Wätzlich, D., Bruchmann, S., Saggu, M., Lendzian, F., Moser, J. & Jahn, D. (2009). Biosynthesis of (Bacterio)chlorophylls:Transient Subunit Interaction and Electron Transfer of Dark Operative Protochlorophyllide Oxidoreductase.
Manuscript in Preparation

Tagungsbeiträge

Wätzlich, D., Virus, S., Uliczka, F., Bröcker, M.J., Jahn, D. & Moser, J.: Protein-Protein-Interaction Analysis of Dark Operative Protochlorophyllide Oxidoreductase (DPOR) subunits. (Poster) VAAM Jahrestagung, Frankfurt (2008).

Wätzlich, D., Bröcker, M.J., Virus, S., Ganskow, S., Schubert, W.-D., Heinz, D., Jahn, D. & Moser, J.: ATP-Driven Reduction by Dark-Operative Protochlorophyllide Oxidoreductase from *Chlorobium tepidum* mechanistically resembles Nitrogenase. (Poster) Gordon's Research Conference - Chemistry & Biology of Tetrapyrroles, Newport, RI, USA (2008).

Wätzlich, D., Virus, S., Uliczka, F., Bröcker, M.J., Jahn, D. & Moser, J.: Dynamic Protein-Protein-Interaction of Dark Operative Protochlorophyllide Oxidoreductase (DPOR). (Poster) VAAM Jahrestagung, Bochum (2009).

Meiner Familie

„Carpe Diem!“

Horaz in „Carmen“ (1,11), 23 v. Chr.

TABLE OF CONTENTS

ABBREVIATIONS

A	Ampere
A_λ	absorption at wavelength λ nm
AcsF	aerobic cyclase system Fe-containing subunit
ALA	5-aminolevulinic acid
Amp^R	ampicillin resistance
APS	ammonium peroxodisulfate
ATP	adenosine triphosphate
AU	absorption units
Bchlide	3-vinyl bacteriochlorophyllide *a*
BCIP	5-brom-4-chloro-3-indolylphosphate
bp	base pair
BSA	bovine serum albumin
Chlide	chlorophyllide *a*
COR	chlorophyllide *a* oxidoreductase
CPI	chloroform phenol isoamyl alcohol
C_V	column volume
Da	Dalton
ds	double stranded
DMF	N,N-dimethylformamide
DNA	deoxyribonucleic acid
(d)dNTP	(di)deoxynucleotide
DPOR	dark-operative protochlorophyllide oxidoreductase
DTT	1,4-dithio-D,L-threitol
EDTA	ethylenediaminetetraacetic acid
et al.	*et alteri* (and others)
FAD	flavin adenine dinucleotide
FMN	flavin mononucleotide
for	forward
FPLC	fast performance liquid chromatography
g	earth gravity
GPC	gel permeation chromatography
H_2O_{deion}	deionized water
HEPES	4-(2-hydroxyethyl)-piperazine-1-ethane sulfonic acid
HPLC	high pressure liquid chromatography
IPTG	isopropyl-β-D-galactopyranosid
kb	kilo base pair (1 kb = 1'000 bp)
λ	wavelength
l	liter
LC-MS	liquid chromatography – mass spectrometry
m	milli
MCS	multiple cloning site
MME	magnesium protoporphyrin IX monomethyl ester
M_r	relative molecular mass
NAD(P)H	nicotinamide adenine dinucleotide (phosphate), reduced
NBT	nitro blue tetrazolium
OD_λ	optical density at wavelength λ nm

ORF	open reading frame
p	pico
PBS	phosphate buffered saline
PP_{ii}	pyrophosphate
Pchlide	protochlorophyllide
PCR	polymerase chain reaction
pH	negative decadic logarithm of the H^+ concentration in a solution
PIPES	Piperazine-N,N'-bis[2-ethanesulfonic acid]
p.s.i.	pounds per square inch
PVDF	polyvinylidendifluorid
Pyro-Chlide *a*	Pyro-chlorophyllide *a*
rev	reverse
RNase	ribonuclease
rpm	rotations per minute
RT	room temperature
SAM	S-adenosyl-L-methionine
SDS	sodium dodecyl sulfate
SDS-PAGE	sodium dodecyl sulfate-polyacrylamide gel electrophoresis
sec	second
TAE	TRIS-acetate-EDTA
TE	TRIS-EDTA
TEMED	N,N,N',N',-tetramethyl ethylen diamine
TES	N-tris[hydroxymethyl]methyl-2-aminoethanesulfonic acid
Tet^R	tetracycline resistance
Triton® X-100	t-octylphenoxypolyethoxyethanol
TRIS	Tris-(hydroxymethyl)-aminomethane
Tween	Polyoxyethylensorbitanmonolaurat
U	unit
UV/VIS	ultra violet and visible spectrum of light
V	volt
v/v	volume per volume
W	watt
w/v	weight per volume
Zn-3^1-13^2-di-OH-Pheid *a*	Zn-3^1-13^2-dihydroxy-pheophorbide *a*
Zn-3-Acetyl-Pheid *a*	Zn-3 Acetyl-pheophorbide *a*
Zn-3-Formyl-Me-Pheid *a*	Zn-3-Formyl-methyl-pheophorbide *a*
Zn-3-Formyl-Pyro-Me-Pheid *a*	Zn-3-Formyl-Pyro-methyl-pheophorbide *a*
Zn-BPheid *c*	Zn-bacteriopheophorbide *c*
Zn-Pyro-Pheid *a*	Zn-Pyro-pheophorbide *a*
°C	centigrade

1 INTRODUCTION

1.1 Photosynthesis

Photosynthesis is the most fundamental biochemical process for life on earth. By this process, energy from sunlight is converted into chemical energy. The reduction of carbon dioxide to organic carbon compounds by photosynthetic organisms provides the basis for most life forms. Moreover, oxygen, a by-product of photosynthesis, enabled the development of the aerobic metabolism which constitutes an important step in the evolution of higher organisms (Raymond *et al.*, 2002).

Photosynthesis is dependent on the presence of (bacterio)chlorophyll molecules capable of absorbing light quanta. These light-sensitive pigments are arranged in so-called photosystems consisting of a reaction center performing the photochemical reactions and antennae complexes which function in light harvesting and energy transfer onto the reaction center. The photosynthetic machinery is localized in special internal membrane systems: in eukaryots photosynthesis takes place in thylakoid membranes within specialized organelles, the chloroplasts, while the pigments in prokaryots are integrated into different internal membrane structures derived from the cytoplasmic membrane or in thylakoid membranes. Chlorophylls can be found in plants, algae and cyanobacteria, whereas the other phototrophic bacteria employ bacteriochlorophylls for light absorption (Blankenship *et al.*, 1998).

The type of photosynthesis varies in the different photosynthetic organisms. Green plants, algae and cyanobacteria use water as electron donor for the reduction of carbon dioxide thereby producing molecular oxygen. Thus, this type of photosynthesis is referred to as oxygenic photosynthesis. Nowadays, it is assumed that oxygenic photosynthesis of cyanobacteria resulted in the increase of oxygen in the atmosphere, enabling the evolution of aerobic, eukaryotic life forms in the first place. On the other hand, purple bacteria, green (non-)sulfur bacteria and heliobacteria perform anoxygenic photosynthesis. Thereby, alternative electron donors like reduced sulfur sources or hydrogen are employed. While anoxygenic photosynthesis depends on one photosystem, oxygenic photosynthesis requires the sequential action of two photosystems (Xiong, 2006).

1.2 Structure and Function of Chlorophylls and Bacteriochlorophylls

(Bacterio)chlorophylls belong to the widespread family of tetrapyrroles. Tetrapyrroles play an essential role in all living organisms (Matsumoto *et al.*, 2004). They are involved in metabolic processes such as energy transfer in photosynthesis and respiration or as prosthetic groups of various enzymes. Due to their intensive color, they have been designated as "pigments of life" (Battersby, 2000). The basic structure of tetrapyrroles consists of four condensed pyrrole rings linked to a cyclic system or a linear molecule. The basic cyclic ring structure is termed porphyrin with four pyrrole rings covalently linked *via* four methine bridges (Fig. 1, *a*). The most abundant tetrapyrroles in nature are the green-colored (bacterio)chlorophylls (Grimm *et al.*, 2006). In addition to (bacterio)chlorophylls, heme, siroheme, corrinoids (e.g. vitamin B_{12}), coenzyme F_{430}, heme d_1 and linear tetrapyrroles like bilins and phycobilins are classified as tetrapyrroles based on their structure and biosynthesis (Frankenberg *et al.*, 2003).

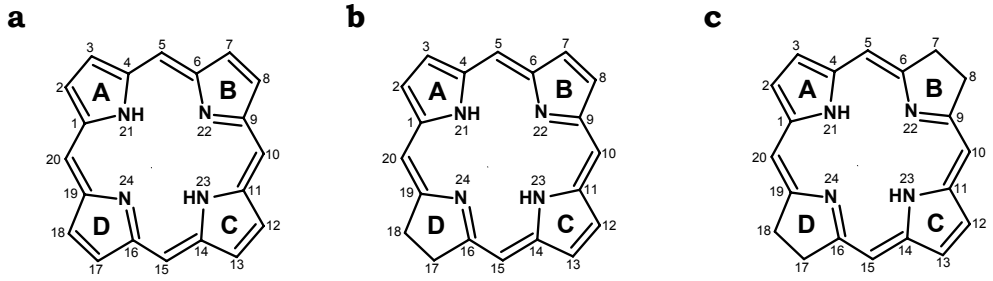

Fig. 1: Structures of tetrapyrroles: porphyrin, chlorin and bacteriochlorin.
The porphyrin ring (*a*) is the basic structure of cyclic tetrapyrroles. The four pyrrole rings are denoted clockwise A to D, carbon and nitrogen atoms are numbered. Tetrapyrroles with a single bond between C17-C18 are referred to as chlorin type (*b*) whereas molecules with a single bond between C7-C8 and C17-C18 are referred to as bacteriochlorin type (*c*).

A variety of (bacterio)chlorophylls exists in nature. However, all these molecules exhibit the same common backbone structure derived from a porphyrin ring system carrying magnesium as central atom. The heterocyclic ring structure of chlorophylls is termed chlorin whereas bacteriochlorophylls make use of a bacteriochlorin ring system (Fig. 1, *b* and *c*). A long hydrophobic side chain, in most cases a phytol chain, is linked to the porphyrin which serves to anchor the molecule within the photosynthetic membranes.

The most abundant (bacterio)chlorophylls, chlorophyll *a* and bacteriochlorophyll *a*, are illustrated in Figure 2.

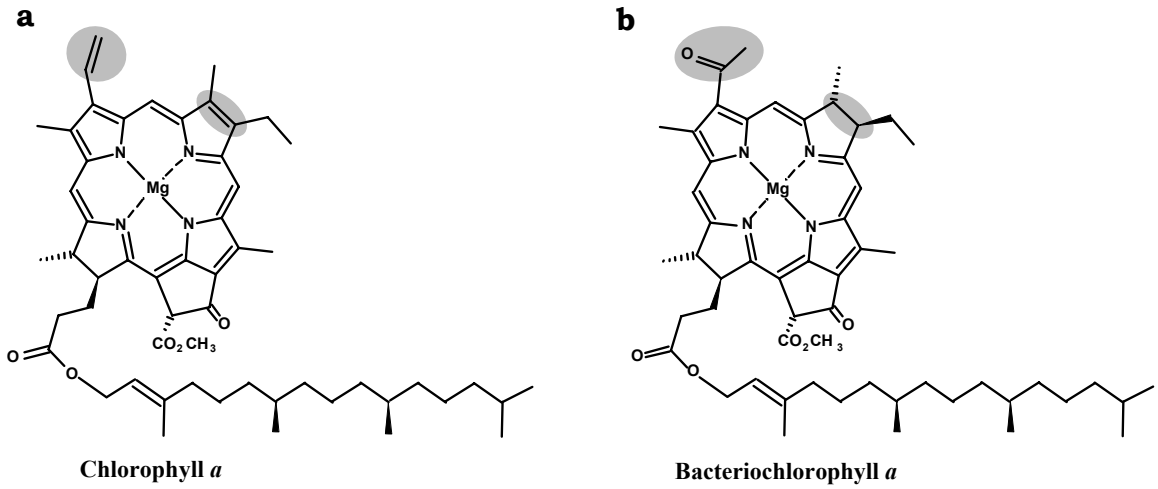

Fig. 2: Structures of chlorophyll *a* (a) and bacteriochlorophyll *a* (b).
Chlorophyll and bacteriochlorophyll are both tetrapyrroles containing magnesium as a central atom. Varying parts of the two molecules are highlighted in *gray*.

Modification of the side chains located on ring A and B of the porphyrin ring results in the diversity of (bacterio)chlorophylls. Instead of a phytol, other isoprenoid alcohols such as farnesol or geranylgeraniol can be present as hydrophobic side chain in bacteriochlorophylls.

In all organisms performing oxygenic photosynthesis, chlorophyll *a* is the primary pigment for photosynthesis. Moreover, chlorophyll *b*, *c* and *d*, divinyl-chlorophyll *a* and *b* as well as 8-hydroxy-chlorophyll are found (Chew *et al.*, 2007). Anoxygenic photosynthetic organisms contain distinct types of bacteriochlorophylls. Bacteriochlorophyll *a* and *b* are present in purple bacteria. In contrast, bacteriochlorophyll *c*, *d* and *e* are only found in green bacteria and bacteriochlorphyll *g* only in heliobacteria (Grimm *et al.*, 2006). Figure 3 gives an overview of the different (bacterio)chlorophyll structures.

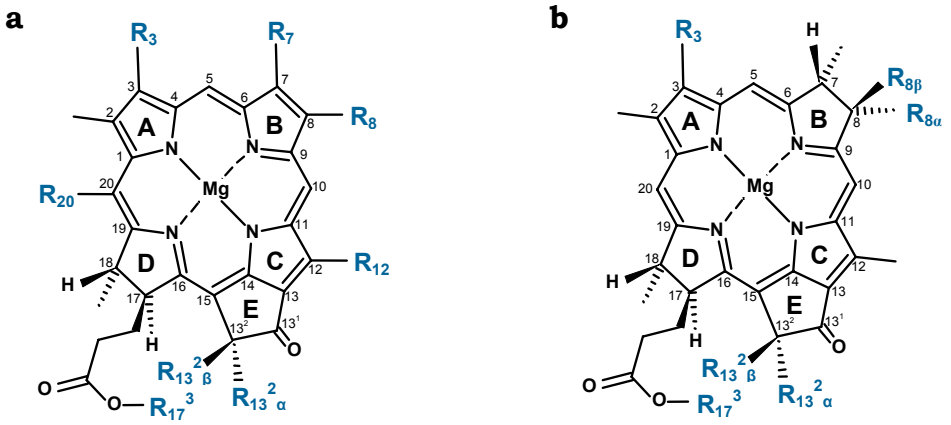

pigment	R_3	R_7	R_8 ($R_{8\alpha}$/ $R_{8\beta}$)	R_{12}	$R_{13}^2{}_\alpha$	$R_{13}^2{}_\beta$	R_{17}^3	R_{20}
chl *a*	C_2H_3	CH_3	C_2H_5	CH_3	$COOCH_3$	H	Phy	H
chl *b*	C_2H_3	CHO	C_2H_5	CH_3	$COOCH_3$	H	Phy	H
chl *c*	C_2H_3	CH_3	C_2H_5 or C_2H_3	CH_3	$COOCH_3$	H	H	H
chl *d*	CHO	CH_3	C_2H_5	CH_3	$COOCH_3$	H	Phy	H
divinyl chl *a*	C_2H_3	CH_3	C_2H_3	CH_3	$COOCH_3$	H	Phy	H
divinyl chl *b*	C_2H_3	CHO	C_2H_3	CH_3	$COOCH_3$	H	Phy	H
8-hydroxy chl	C_2H_3	CH_3	C_2H_4OH	CH_3	$COOCH_3$	H	Farn	H
bchl *a*	$COCH_3$	-	H/ C_2H_5	CH_3	$COOCH_3$	H	Phy	-
bchl *b*	$COCH_3$	-	=CH-CH_3	CH_3	$COOCH_3$	H	Phy	-
bchl *c*	CHOH-CH_3	CH_3	$CH_2CH_n(CH_3)_{3-n}$	CH_3/ C_2H_5	H	H	Farn/ others	CH_3
bchl *d*	CHOH-CH_3	CH_3	$CH_2CH_n(CH_3)_{3-n}$	CH_3/ C_2H_5	H	H	Farn/ others	H
bchl *e*	CHOH-CH_3	CHO	$CH_2CH_n(CH_3)_{3-n}$	CH_3/ C_2H_5	H	H	Farn/ others	CH_3
bchl *g*	C_2H_3	-	=CH-CH_3	CH_3	$COOCH_3$	H	GG	-

Fig. 3: Chemical structures of different (bacterio)chlorophyll molecules.
The basic structure consists of a chlorin (*a*) or a bacteriochlorin (*b*) structure, respectively, with varying ring substituents R shown in *blue*. Short names of the photosynthetic pigments and composition of the ring substituents are indicated. Chl = chlorophyll; bchl = bacteriochlorophyll; Phy = phytyl; GG = geranylgeranyl; Farn = farnesyl.

The green color of the different (bacterio)chlorophyll molecules is based on the extensive system of conjugated double bonds. This allows (bacterio)chlorophyll molecules to capture photons of light in the visible (380 - 460 nm) and far-red (600 - 850 nm) region of the spectrum (Grimm *et al*., 2006). Based on their specific substituents and the saturation of the ring system each (bacterio)chlorophyll exhibits a specific absorption spectrum. For efficient photosynthesis, various (bacterio)chlorophyll molecules are arranged in a photosystem. (Bacterio)chlorophylls act as antennae complexes which harvest large quantities of photons. They guide them towards a central pair of (bacterio)chlorophyll molecules in the reaction center. Here, the energy of photons is trapped in the form of excited electrons whose excitation energy is transferred to an electron transport chain to produce energy equivalents for the conversion of carbon dioxide into carbohydrates (Milgrom, 1997). By employing different (bacterio)chlorophyll species the photosynthetic organisms make use of the light spectrum in an optimal way.

1.3 Biosynthesis of Chlorophylls and Bacteriochlorophylls

All tetrapyrroles originate from a common biosynthetic pathway starting with the precursor 5-aminolevulinic acid (ALA) (Fig. 4). This molecule includes all carbon and nitrogen atoms required for the formation of the tetrapyrrole macrocycle. ALA is converted *via* several reaction steps into the first cyclic intermediate, uroporphyrinogen III. The pathway is branched at this point for the formation of siroheme, coenzyme F_{430}, heme d_1 and corrinoids. Hemes and (bacterio)chlorophylls are formed by conversion of uroporphyrinogen III *via* multiple decarboxylation and oxidation steps into the aromatic, colored compound protoporphyrin IX. Protoporphyrin IX represents the branching point for heme and (bacterio)chlorophyll biosynthesis. Insertion of iron into protoporphyrin IX catalyzed by a ferrochelatase directs the molecule towards the heme biosynthetic pathway (Dailey, 2002) while incorporation of magnesium is the first committed step for (bacterio)chlorophyll biosynthesis (Willows, 2003).

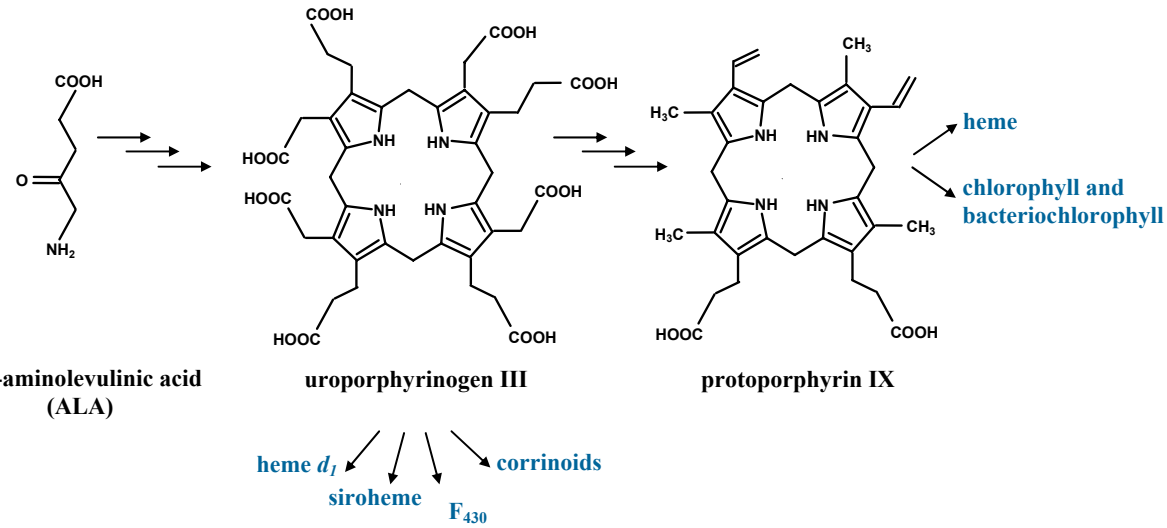

Fig. 4: Important intermediates for the biosynthesis of tetrapyrroles.
Branching points for the synthesis of different tetrapyrrole classes are indicated. The classes of tetrapyrroles are highlighted in *blue*. All tetrapyrroles are synthesized based on 5-aminolevulinic acid (ALA). The tetrapyrroles siroheme, F_{430}, heme d_1 and corrinoids derive from the first cyclic intermediate uroporphyrinogen III. The synthesis of heme and (bacterio)chlorophyll proceeds from protoporphyrin IX which is formed *via* several steps from uroporphyrinogen III.

The biosynthesis of (bacterio)chlorophylls proceeds *via* a common biosynthetic pathway for the core ring system. The required enzymes are conserved in eukaryots as well as in prokaryots. A summary of the biosynthesis of chlorophyll *a* and bacteriochlorophyll *a* starting from protoporphyrin IX is shown in Figure 5.

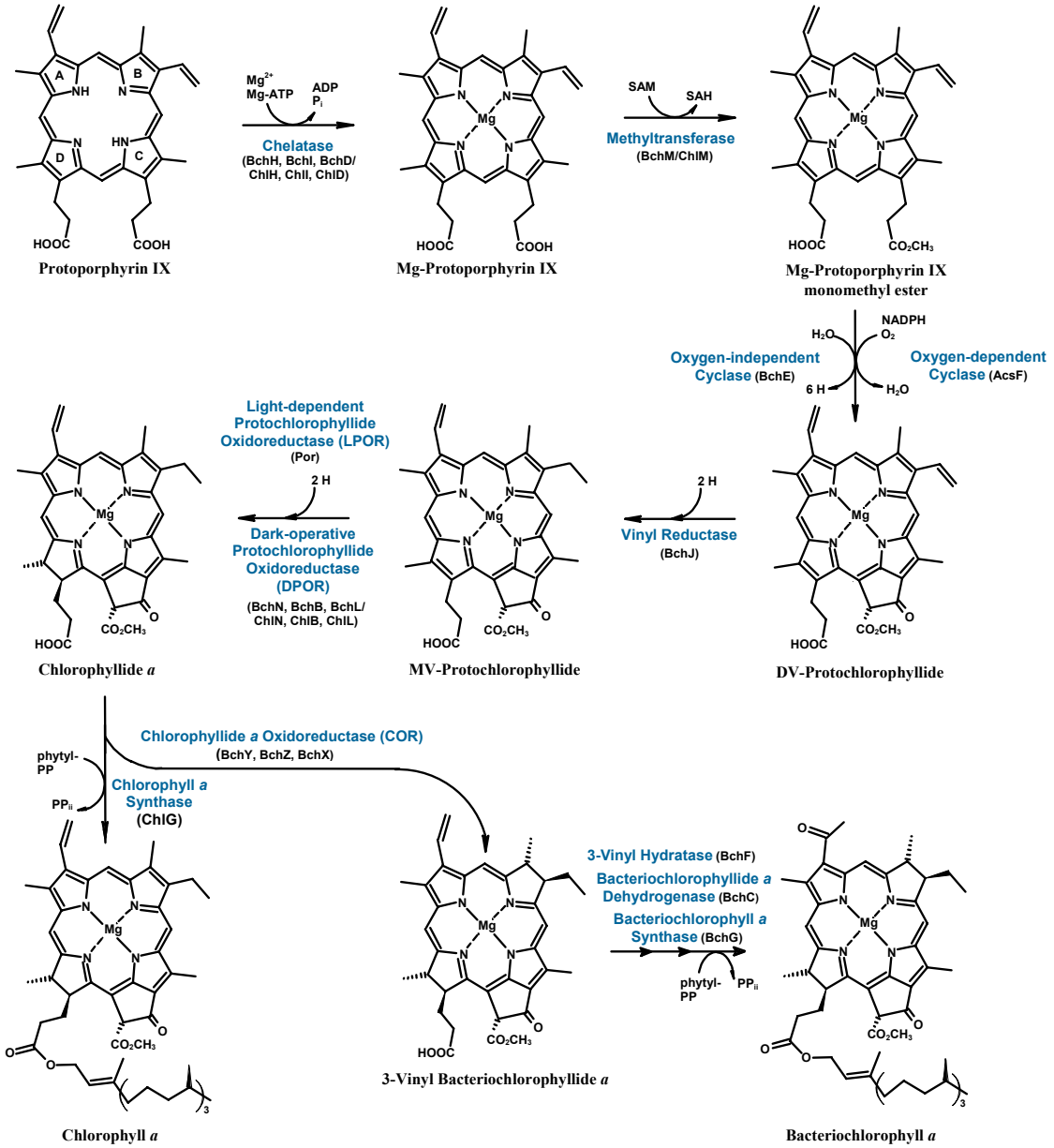

Fig. 5: Overview of the biosynthesis of chlorophyll *a* and bacteriochlorophyll *a* from protoporphyrin IX.
Short names of the enzymes are shown in *blue*, corresponding gene names are indicated. The pyrrole rings are marked in protoporphyrin IX with A - D. MV = monovinyl, DV = divinyl.

By insertion of magnesium into protoporphyrin IX catalyzed by the ATP-dependent enzyme magnesium protoporphyrin IX chelatase (BchHID/ChlHID), magnesium protoporphyrin IX is formed (Viney *et al.*, 2007). Subsequently, this molecule is converted by the S-adenosyl-L-methionine (SAM)-dependent magnesium protoporphyrin IX *O*-methyltransferase (BchM/ChlM) into magnesium protoporphyrin IX monomethyl ester (Shepherd *et al.*, 2004). From this ester, protochlorophyllide is built by the formation of the isocyclic fifth ring which is characteristic for all (bacterio)chlorophylls. This step will be

described in more detail in section 1.4. The reaction is catalyzed either by the oxygen-dependent (AcsF) or the oxygen-independent (BchE) magnesium protoporphyrin IX monomethyl ester oxidative cyclase (Bollivar *et al.*, 1996). In Figure 5, the specific reduction of the 8-vinyl side chain is depicted with divinyl protochlorophyllide as a substrate. The reaction is catalyzed by the 3-, 8- divinyl protochlorophyllide *a* 8-vinyl reductase (BchJ) leading to monovinyl protochlorophyllide (Nagata *et al.*, 2005). However, several studies indicated that this reduction step can also be performed based on protoporphyrin IX, magnesium protoporphyrin IX, magnesium protoporphyrin IX monomethyl ester and chlorophyllide (Parham *et al.*, 1995). Subsequently, the reduction of ring D of protochlorophyllide yields the chlorin chlorophyllide. This reaction can be catalyzed by two independent enzymes: by the light-dependent protchlorophyllide oxidoreductase (LPOR; Por) or by the light-independent protochlorophyllide oxidoreductase (dark-operative protochlorophyllide oxidoreductase; DPOR; BchNBL/ChlNBL) (Beale, 1999, Suzuki *et al.*, 1997). The reduction will be described in detail in section 1.5. Finally, chlorophyllide is esterificated with phytol catalyzed by chlorophyll *a* synthase (ChlG) to give chlorophyll *a* while an analogous enzyme (BchG) is present for the synthesis of bacteriochlorophyll *a* (Beale, 1999). The biosynthesis of bacteriochlorophyll *a* requires additional enzymatic steps when compared to the biosynthesis of chlorophyll. Formation of the bacteriochlorin from chlorophyllide *a* occurs by the reduction of ring B catalyzed by the chlorophyllide *a* oxidoreductase (COR; BchYZX). This enzyme shows high sequence homology at the amino acid level to the DPOR enzyme suggesting a similar reaction mechanism for D and B ring reduction (Nomata *et al.*, 2006b). The COR enzyme will be described in detail in section 1.6. The enzyme 3-Vinyl hydratase (BchF) is responsible for the addition of water to the 3-vinyl group on ring A while the [3-Hydroxyethyl]-bacteriochlorophyllide *a* dehydrogenase (BchC) subsequently oxidizes this hydroxyl group to a keto group (Bollivar, 2006). Further modifications of the tetrapyrrole backbone by several enzymes lead to the various structures of the different bacteriochlorophylls (Willows, 2003).

1.4 Formation of the Isocyclic Ring of Chlorophylls and Bacteriochlorophylls

Formation of the fifth ring (or ring E) is characteristic for all (bacterio)chlorophylls. Therefore, an oxidative cyclization of magnesium protoporphyrin IX monomethyl ester (MME) is required which is catalyzed by the enzyme magnesium protoporphyrin IX monomethyl ester oxidative cyclase (cyclase). This complex reaction includes addition of an oxygen atom at C13[1] position and a six-electron oxidation leading to the formation of protochlorophyllide (Pchlide) (Fig. 6). Depending on the origin of the oxygen atom, catalysis is performed by two structurally unrelated cyclase enzymes. Aerobic phototrophic organisms contain an oxygen-dependent form of the cyclase, AcsF (aerobic cyclase system Fe-containing subunit), while the oxygen-independent cyclase is found primarily in anoxygenic phototrophs. However, some organisms such as *Rubrivivax gelatinosus* contain both, oxygen-dependent and oxygen-independent cyclase enzymes (Ouchane *et al.*, 2004, Pinta *et al.*, 2002).

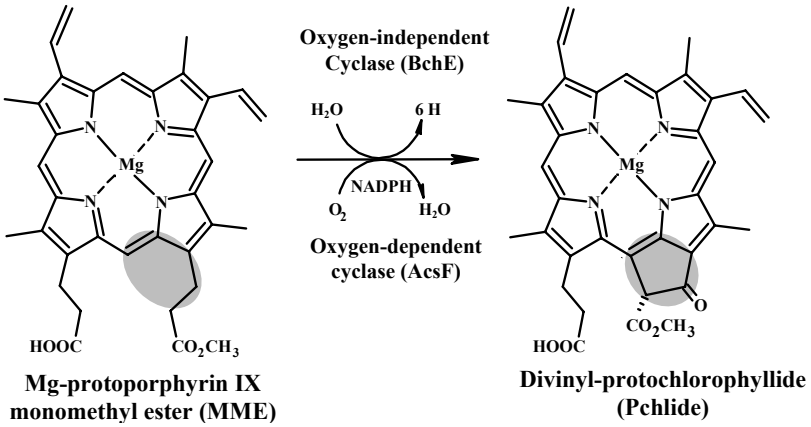

Fig. 6: Two different enzymatic systems for the biosynthesis of the isocyclic fifth ring during (bacterio)chlorophyll biosynthesis.
The oxygen-dependent or the oxygen-independent cyclase catalyzes the conversion of MME into divinyl-Pchlide. For this cyclization the carbonyl oxygen atom at position C13[1] is derived from molecular oxygen for the oxygen-dependent cyclase (AcsF), while the oxygen-independent enzyme (BchE) makes use of the oxygen from a water molecule for this reaction.

1.4.1 The Oxygen-Dependent Cyclase

Activity for the oxygen-dependent cyclase was demonstrated in plastids of cucumber (Chereskin *et al.*, 1982), wheat (Nasrulhaq-Boyce *et al.*, 1987), barley (Rzeznicka *et al.*, 2005), and the algae *Chlamydomonas reinhardtii* (Bollivar *et al.*, 1996) as well as in cell

lysates of the cyanobacterium *Synechocystis* PCC 6803 (Bollivar *et al.*, 1996). The enzyme requires oxygen and NADPH as a cofactor (Chereskin *et al.*, 1982, Wong *et al.*, 1985). By labeling experiments it was shown that the carbonyl oxygen atom at $C13^1$ is derived from molecular oxygen (Walker *et al.*, 1988). The observed cyclase activity was inhibited by Fe-chelators suggesting that a non-heme iron is involved in enzyme catalysis (Nasrulhaq-Boyce *et al.*, 1987). Furthermore, activity was only detectable in activity assays when a soluble fraction was combined with a membrane fraction. However, for *Chlamydomonas* chloroplasts it was demonstrated that cyclase activity is membrane-associated. Attempts to purify and identify the cyclase components from membrane or cytosolic fractions were not successful.

Analysis of the amino acid sequence of AcsF reveals the presence of two $EX_{(29-35)}$DEXRH motifs (Pinta *et al*., 2002). This motif is characteristic for the enzyme class of monooxygenases carrying a binuclear iron cluster. These multimeric enzymes catalyze the oxidation of their substrate in the presence of a reducing agent (NADPH or NADH) (Pinta *et al.*, 2002). This might indicate that the oxygen-dependent cyclase consists as a multi-subunit enzyme.

Three sequential enzymatic steps were proposed for the oxygen-dependent cyclase reaction (Bollivar *et al.*, 1996) as illustrated in Figure 7: first, hydroxylation of the $C13^1$ position of the 6-methyl propionate occurs, followed by oxidation of this hydroxyl group to the corresponding keto group. The activated methyl group at $C13^2$ reacts with the γ-meso carbon C15 in an oxidative reaction under removal of two protons to yield the isocyclic ring structure.

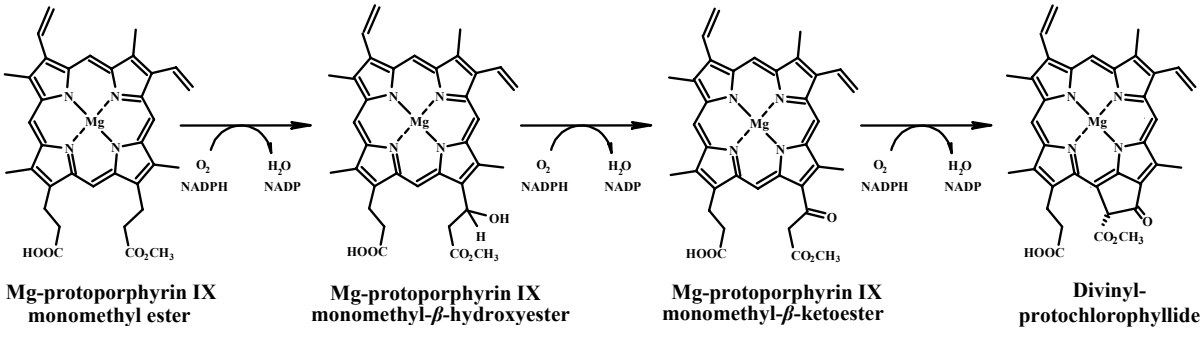

Fig. 7: Postulated reaction mechanism for the formation of the isocyclic ring by the oxygen-dependent cyclase (AcsF).
The cyclization reaction is a six-electron oxidation which occurs in three sequential steps and requires molecular oxygen and NADPH. The reaction proceeds *via* a hydroxyl- and a keto-intermediate.

The postulated reaction mechanism as well as the partial sequence homology to monooxygenases again might indicate that the oxygen-dependent cyclase is composed of several additional subunits besides AcsF. To date, none of the remaining protein subunits of the oxygen-dependent cyclase complex has been identified.

1.4.2 The Oxygen-Independent Cyclase

Many phototrophic organisms perform bacteriochlorophyll biosynthesis only under anaerobic conditions and therefore, they possess an oxygen-independent cyclase system for the conversion of MME into Pchlide. Isotope labeling experiments with the oxygen-independent cyclase showed that the oxygen at $C13^1$ position is derived from water (Porra *et al.*, 1995). Transposon mutants of *Rhodobacter sphaeroides* accumulating the substrate MME were identified and led to annotation of BchE as oxygen-independent cyclase. Homologs of BchE were only found in photosynthetic organisms, but not in algae or plants (Ouchane *et al*., 2004).

All BchE sequences show a highly conserved sequence motif consisting of three cysteines (CXXXCXXC) which is characteristic for [4Fe-4S] cluster containing proteins. BchE was grouped in the family of radical-SAM enzymes (Ouchane *et al.*, 2004). Members of this family are involved in radical reaction mechanisms associated with the cleavage of SAM. Moreover, a SAM binding domain was identified in the amino acid sequence of BchE suggesting that SAM acts as a cofactor for the enzyme (Ouchane *et al*., 2004). Based on the sequence homology to cobalamin binding domains of the enzyme P-methylase from *Streptomyces hygroscopicus* it was postulated that the oxygen-independent cyclase might require a cobalamin cofactor. Indeed, *R. capsulatus* mutants deficient in vitamin B_{12} biosynthesis have been shown to accumulate MME (Gough *et al.*, 2000). This defect in bacteriochlorophyll biosynthesis could be restored by addition of exogenous cobalamin.

Enzymatic activity for the oxygen-independent cyclase was shown so far only *in vivo* by using permeabilized *R. capsulatus* cells (Gough *et al*., 2000).

Based on these observations and the observed sequence homology a radical reaction mechanism was postulated for the oxygen-independent cyclase (Fig. 8), including a hydroxyl- as well as a keto-intermediate as for the oxygen-dependent enzyme (Gough *et al*., 2000, Wong *et al*., 1985). The proposed reaction mechanism is initiated by the formation of an adenosyl radical from adenosyl-cobalamin. This adenosyl radical

facilitates hydrogen abstraction resulting in a $C13^1$ radical of the substrate. After removal of an electron the $C13^1$ cation is formed. This cation is then hydroxylated by H_2O ($C13^1$-OH). Removal of a second hydrogen leads to the $C13^1$-keto MME. The $C13^1$-keto-$C13^2$ radical is then formed after hydrogen abstraction. This radical attacks the γ–meso-carbon C15 resulting in the cyclization of the fifth ring after abstraction of another hydrogen atom. To date, no additional protein subunits have been identified which are involved in the oxygen-independent cyclase reaction.

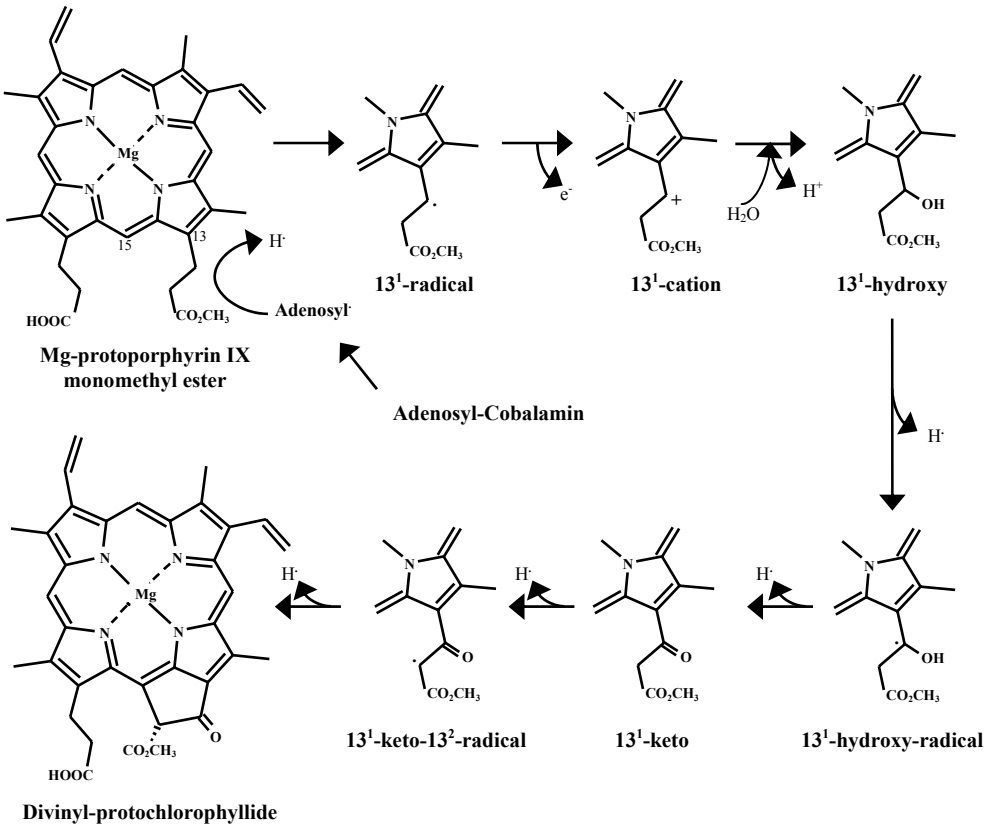

Fig. 8: Postulated reaction mechanism for the formation of the isocyclic ring by the oxygen-independent cyclase (BchE).
Radical mechanism for an adenosyl-cobalamin-dependent oxygen-independent cyclase (Gough *et al*., 2000).

1.5 Reduction of Pyrrole Ring D

A key regulatory step in (bacterio)chlorophyll biosynthesis is the stereospecific reduction of the C17-C18 double bond of ring D which converts the porphyrin Pchlide into the chlorin chlorophyllide (Chlide) (Fig. 9) (Fujita, 1996). Two completely unrelated enzymatic systems are able to catalyze this reaction: the light-dependent

protochlorophyllide oxidoreductase (LPOR; NADPH Pchlide oxidoreductase, EC 1.3.1.33). LPOR uses NADPH as a cofactor and forms a tight complex with its substrate Pchlide. LPOR catalysis is then initiated by the presence of light. Since no alternative enzyme for Pchlide reduction is available in angiosperms, LPOR is essential for the greening of these organisms in the presence of light. In contrast, the light-independent (dark-operative) Pchlide oxidoreductase (DPOR) is not dependent on the presence of light. DPOR consists of three different protein subunits (Nomata *et al.*, 2005).

Some anoxygenic bacteria only contain the DPOR enzyme while cyanobacteria, algae and gymnosperms possess both enzymes, LPOR and DPOR. DPOR enables these organisms to synthesize (bacterio)chlorophylls in the dark.

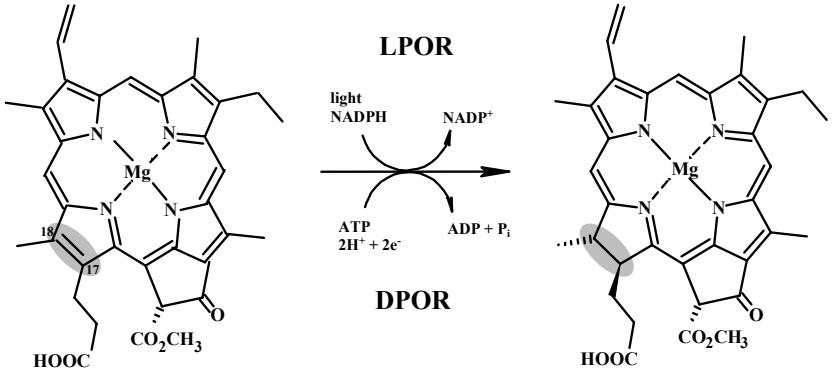

Fig. 9: Two different enzymes catalyze the reduction of ring D during (bacterio)chlorophyll biosynthesis.
The light-dependent Pchlide oxidoreductase (LPOR) catalyzes the reduction of ring D using light and NADPH as a cofactor. Angiosperms exclusively possess this type of enzyme for D ring reduction. Cyanobacteria, algae, gymnosperms and some anoxygenic bacteria possess solely the dark-operative Pchlide oxidoreductase (DPOR). The ATP-dependent DPOR catalysis is independent of light. This enzyme enables the related organisms to synthesize (bacterio)chlorophylls in the dark.

1.5.1 The Light-Dependent Protochlorophyllide Oxidoreductase (LPOR)

LPOR is a single-subunit enzyme showing protein sequence identity to the family of short-chain alcohol dehydrogenases including a variety of NAD(P)H-dependent enzymes (Baker, 1994). Members of this family contain two strictly conserved active site amino acid residues, a tyrosine and a lysine residue, both of which are essential for catalytic activity. Due to the homology of LPOR to this family, a structural homology model of the enzyme from *Synechocystis* was established (Townley *et al.*, 2001). Indeed, the two conserved residues are located in the proposed catalytic site of LPOR and were found to be essential for enzymatic activity (Wilks *et al.*, 1995). LPOR catalysis has been studied

extensively by various methods including spectroscopy, steady-state kinetics, substrate analogs and site-directed mutagenesis (Heyes *et al.*, 2006, Klement *et al.*, 1999, Griffiths, 1980).

1.5.2 The Dark-Operative Protochlorophyllide Oxidoreductase (DPOR)

DPOR enzymes consist of three subunits which are designated BchN, BchB and BchL in bacteriochlorophyll-synthesizing organisms and ChlN, ChlB and ChlL in chlorophyll-synthesizing organisms (Fujita *et al.*, 1993) (Fig. 10).

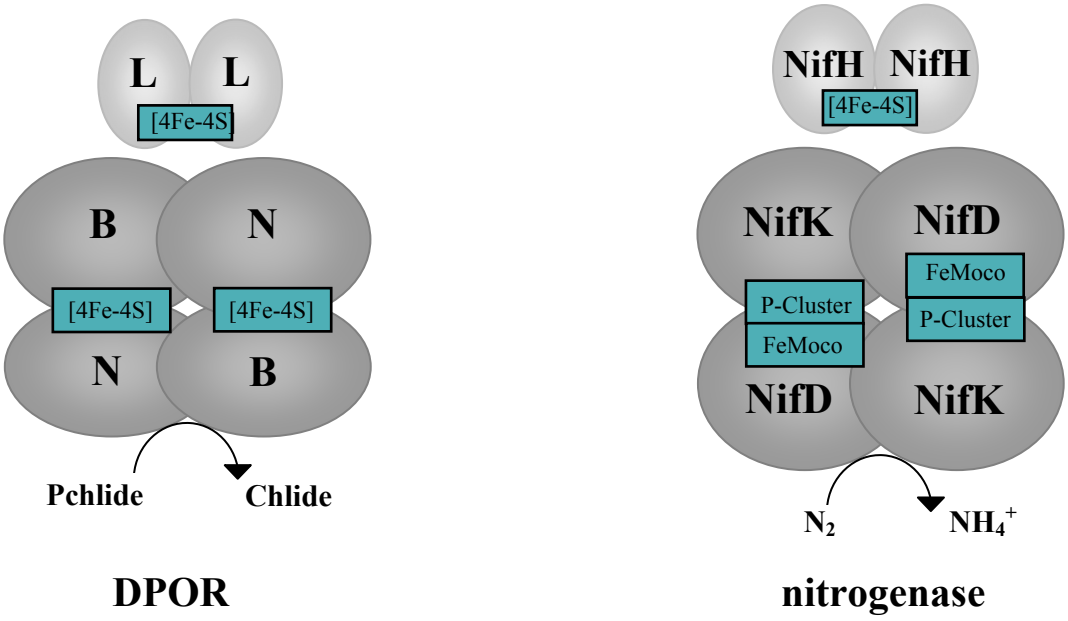

Fig. 10: Schematic model of DPOR and nitrogenase.
DPOR and nitrogenase share a high degree of protein sequence homology. Both enzymes consist of three subunits. The oligomeric structure of the individual subunits and the related metallo-clusters are illustrated for the DPOR and the nitrogenase system.

Subunits BchN/ChlN, BchB/ChlB and BchL/ChlL share significant amino acid sequence homology to the corresponding subunits NifD, NifK and NifH of the related nitrogenase system, respectively (Burke *et al.*, 1993). While subunits BchL/ChlL exhibit a protein sequence identity value of ~33 % to NifH, subunits BchN/ChlN and BchB/ChlB show lower sequence identity values of ~15 % when compared to subunits NifD and NifK. For both enzymes a common oligomeric protein architecture has been demonstrated consisting of the heterotetrameric complexes $(BchNB)_2$/$(ChlNB)_2$ and $(NifDK)_2$ which are completed

by homodimeric protein subunits $BchL_2$/$ChlL_2$ and $NifH_2$, respectively (Bröcker *et al.*, 2008a, Nomata *et al.*, 2006a, Tezcan *et al.*, 2005).

Nitrogenase is a well-characterized protein complex that catalyzes the reduction of nitrogen to ammonia in a reaction that requires at least 16 molecules of MgATP (Rees *et al.*, 2005, Peters *et al.*, 1995, Dean *et al.*, 1993). During nitrogenase catalysis, subunit $NifH_2$ (Fe protein) associates with and dissociates from the $(NifDK)_2$ complex (MoFe protein). Binding, hydrolysis of MgATP and structural rearrangements are coupled to sequential intersubunit electron transfer. For this purpose, $NifH_2$ contains an ATP binding motif and an intersubunit [4Fe-4S] cluster coordinated by two cysteine residues from each NifH monomer (Burke *et al*., 1993, Suzuki *et al*., 1997). Electrons from this [4Fe-4S] cluster are transferred *via* a [8Fe-7S] cluster (P-cluster) onto the [1Mo-7Fe-9S-X-homocitrate] cluster (MoFe cofactor). Both of the latter clusters are located on $(NifDK)_2$ where dinitrogen is reduced to ammonia (Dean *et al*., 1993). Three-dimensional structures of $NifH_2$ in complex with $(NifDK)_2$ revealed a detailed picture of the dynamic interaction of both subcomplexes (Tezcan *et al*., 2005, Schindelin *et al.*, 1997).

Based on biochemical and bioinformatic approaches, it has been proposed that the initial steps of DPOR reaction strongly resemble nitrogenase catalysis. Key amino acid residues essential for DPOR function have been identified by mutagenesis of the enzyme from *Chlorobaculum tepidum* (formerly denoted as *Chlorobium tepidum*) (Bröcker *et al*., 2008a). The catalytic mechanism of DPOR includes electron transfer from a “plant-type” [2Fe-2S] ferredoxin onto the dimeric DPOR subunit $BchL_2$/$ChlL_2$ carrying an intersubunit [4Fe-4S] redox center coordinated by Cys^{97} and Cys^{131} in *C. tepidum*. Analogous to nitrogenase, Lys^{10} in the phosphate-binding loop (P-loop) and Leu^{126} in the switch II region of DPOR were found to be essential for DPOR catalysis. Moreover, it was shown that the $BchL_2$ protein from *C. tepidum* does not form a stable complex with the catalytic $(BchNB)_2$ subcomplex. Therefore, a transient interaction responsible for the electron transfer onto protein subunit $(BchNB)_2$/$(ChlNB)_2$ has been proposed (Bröcker *et al*., 2008a).

The subsequent [Fe-S] cluster-dependent catalysis and the specific substrate recognition at the active site located on subunit $(BchNB)_2$/$(ChlNB)_2$ are unrelated to nitrogenase. The $(BchNB)_2$ subcomplex was shown to carry a second [4Fe-4S] cluster which was proposed to be ligated by Cys^{21}, Cys^{46}, and Cys^{103} of the BchN subunit and Cys^{94} of subunit BchB (*C. tepidum* numbering) (Bröcker *et al.*, 2008a). No evidence for any type of additional cofactor was obtained from biochemical and EPR spectroscopic analyses (Bröcker *et al.*,

2008b, Nomata *et al.*, 2008). Thus, despite the same common oligomeric architecture the catalytic subunits $(BchNB)_2$/$(ChlNB)_2$ clearly differ from the corresponding nitrogenase complex, as no molybdenum-containing cofactor or P-cluster equivalent is employed (Bröcker *et al.*, 2008b, Sarma *et al.*, 2008). Based on these results it was concluded that electrons from the [4Fe-4S] cluster of $(BchNB)_2$/$(ChlNB)_2$ are transferred directly onto the Pchlide substrate at the active site of DPOR.

1.6 Reduction of Pyrrole Ring B

For the conversion of the chlorin Chlide into a bacteriochlorin structure, the C7-C8 double bond of ring B is stereospecifically reduced yielding 3-vinyl bacteriochlorophyllide *a* (Bchlide) (Fig. 11). The reaction is catalyzed by another nitrogenase-like enzyme termed chlorophyllide *a* oxidoreductase (COR) (Nomata *et al.*, 2006b). The COR enzyme consists of three protein subunits designated as BchY, BchZ and BchX.

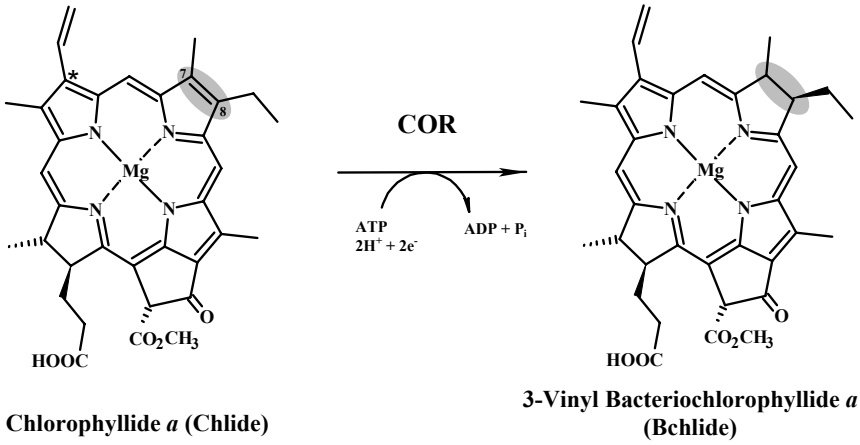

Fig. 11: Reduction of pyrrole ring B during bacteriochlorophyll biosynthesis by the chlorophyllide *a* oxidoreductase (COR).
COR catalyzes the stereospecific reduction of the C7-C8 double bond of ring B leading to the formation of Bchlide. The position marked by an asterisk carries either a vinyl or a hydroxyethyl moiety (Bollivar *et al.*, 1994).

All COR subunits share significant homology to the corresponding subunits of nitrogenase (NifD, NifK and NifH) and DPOR (BchN/ChlN, BchB/ChlB and BchL/ChlL). In amino acid sequence alignments of BchX proteins with the closely related BchL or ChlL subunits of DPOR, both cysteinyl ligands responsible for the [4Fe-4S] cluster formation and residues involved in ATP binding motifs are highly conserved (Burke *et al*., 1993).

Furthermore, all cysteinyl residues characterized as ligands for a catalytic [4Fe-4S] cluster in $(BchNB)_2$ or $(ChlNB)_2$ are conserved in the sequences of subunits BchY and BchZ of COR (Nomata *et al.*, 2006b). These data indicate that the catalytic mechanism of COR strongly resembles DPOR catalysis. *In vitro* assays for nitrogenase, DPOR as well as COR make use of the artificial electron donor dithionite in the presence of ATP and have to be performed under anaerobic conditions due to the oxygen-sensitive nature of the [4Fe-4S] clusters (Nomata *et al.*, 2006b, Fujita *et al.*, 2000, Wherland *et al.*, 1981).

Enzymatic activity for the enzymes from *R. capsulatus* (Nomata *et al*., 2006b) and *R. sphaeroides* (Kim *et al*., 2008) has been described in the literature. Moreover, in a recent study for the COR enzyme from *R. sphaeroides* it was shown by EPR spectroscopy that subunits BchX and BchY contain [4Fe-4S] cluster while subunit BchZ was proposed to carry a heme cofactor (b-type heme) and provides the substrate binding site. Furthermore, the authors presented experiments indicating that subunit BchX might carry a flavin cofactor (FMN) and they demonstrated that COR generates superoxide under low oxygen conditions (2 %) *(*Kim *et al.*, 2008).

1.7 Aim of this Study

Conversion of protochlorophyllide (Pchlide) into chlorophyllide *a* (Chlide) and chlorophyllide *a* to 3-Vinyl bacteriochlorophyllide *a* (Bchlide) represent key regulatory steps in (bacterio)chlorophyll biosynthesis. Protein-protein-interactions between the different subunits of these nitrogenase-like multi-subunit enzymes mediate the catalytically crucial electron transfer reactions. Therefore, the first objective of this work was to analyze the transient dark-operative protochlorophyllide oxidoreductase (DPOR) and chlorophyllide *a* oxidoreductase (COR) catalyses using enzymatic systems from different organisms. Thereby, first the analysis of the transient protein-protein-interaction of the dimeric DPOR subunit $BchL_2$ or $ChlL_2$ with the heterotetrameric DPOR subunits $(BchNB)_2$ or $(ChlNB)_2$ during DPOR catalysis was of particular importance. For this purpose, a strategy to identify conserved regions of the postulated docking face had to be developed and subsequently verified by a site-directed mutagenesis approach.

Secondly, all subunits of COR show a high degree of sequence identity to the related subunits of DPOR. In this study, COR enzymes from different organisms had to be recombinantly produced, purified and biochemically characterized. Moreover, for the elucidation of the potential evolution of the electron-transferring subunits of nitrogenase and nitrogenase-like enzymes, chimeric enzymes consisting of DPOR subunits $(BchNB)_2$ or $(ChlNB)_2$ in combination with subunits $BchX_2$ of the COR enzyme and with subunit $NifH_2$ of nitrogenase were to be tested for functionality.

A third aim of this work was to study the oxygen-dependent formation of the isocyclic ring characteristic for all (bacterio)chlorophylls. This conversion of magnesium protoporphyrin IX monomethyl ester (MME) into protochlorophyllide (Pchlide) is catalyzed by an oxygen-dependent cyclase from which only one subunit of the postulated enzyme complex could be identified so far. Consequently, new candidate proteins were to be analyzed.

2 MATERIALS AND METHODS

2.1 Instruments, Chemicals and Materials

2.1.1 Instruments

agarose gel electrophoresis	Agagel	Biometra
agarose gel documentation	GelDoc	BioRad
anaerobic workstations	Type B Flexible vinyl chamber	COY Laboratory Products Inc.
autoclave	LVSA 50/70	Zirbus
blotting equipment	Semidry-Blot Trans-Blot®SD	BioRad
centrifuges	Centrifuge 5804	Eppendorf
	Minispin	Eppendorf
	RC 5B Plus	Sorvall
	L7-65 Ultracentrifuge	Beckman
DNA sequencing	ABI Prism™ 310 Genetic Analyser	Applied Biosystems
filtration/degassing system		self-construction
FPLC	ÄKTApurifier™	GE Healthcare
	ÄKTAprime™	GE Healthcare
French® Press	French® Pressure Cell	SLM Aminco
	French® Pressure Cell Press	Polytec
HPLC	Jasco 1500	Jasco
luminescence spectrometer	LS50B	Perkin Elmer
pH determination	pH-Meter CG 842	Schott
photometer	Ultrospec 2000	Amersham Pharmacia
rotating evaporator	VV2000	Heidolph
scales	SBA 52	Scaltec
	BP61S	Sartorius
SDS-PAGE	Mini Protean III	BioRad
shaker	305/3020	GFL
	TR-150	Infors AG

thermocycler	Tpersonal	Biometra
	Tgradient	Biometra
thermomixer	Thermomixer 5436	Eppendorf
UV/Vis spectrophotometer	Lambda 2	Perkin Elmer
vortex	Vortex-Genie 2	Scientific Industries
water purification	Milli-Q System	Millipore

2.1.2 Chemicals and Materials

antibodies	anti-His (murine)	GE Healthcare
	anti-mouse HRP-conjugate (Fc-specific)	Sigma-Aldrich
	NeutrAvidin HRP-conjugate	Pierce
blotting materials	Gel Blotting Papers	Roth
	Roti-PVDF-membrane	Roth
chemicals	Bradford reagent	Sigma-Aldrich
	FAD	Fluka
	FMN	Fluka
	GelStar® Nucleic Acid Gel Stain	Biozym
	Magnesium protoporphyrin IX monomethyl ester	Frontier Scientific
	Mts-Atf-LC-Biotin Label Transfer Reagent	Pierce
enzymes	Creatin Phosphokinase	Sigma-Aldrich
	Phusion™ DNA polymerase	New England Biolabs
	PreScission™ Protease	GE Healthcare
	restriction enzymes	New England Biolabs
	Ribonuclease A	Sigma-Aldrich
	T4 DNA Ligase	Finnzymes
	Taq DNA polymerase	Biotherm
	Thrombin	Sigma-Aldrich

kits	QIAquick Gel Extraction Kit	Qiagen
	QIAquick PCR Purification Kit	Qiagen
	QuikChange® Site-Directed Mutagenesis Kit	Stratagene
	SuperSignal® West Pico Chemiluminescence Kit	Pierce
molecular weight standards	GeneRuler™ DNA Ladder Mix	Fermentas
	MassRuler™ DNA Ladder Mix	Fermentas
	Protein Molecular Weight Marker	Fermentas
	PageRuler™ Prestained Protein Ladder	Fermentas
	Molecular weight marker Kit	Sigma-Aldrich
PCR materials	nucleotides (dNTPs)	Fermentas
	Oligonucleotides	MWG Biotech, Biomers
other materials	Chelating Sepharose FF	GE Healthcare
	Filter Minisart SRP4	Sartorius
	glutathione sepharose 4 FF	GE Healthcare
	gravity flow column "Poly-Prep", 0.8 x 4 cm	BioRad
	Microcon® Centrifugal Filter Unit	Millipore
	Precision cuvettes 115F-QS	Hellma
	Slide-A-Lyzer® MINI dialysis units	Pierce
	sterile filter	Millipore, Sartorius
	Superdex 200 HR 10/30, HR 26/60	GE Healthcare

Chemicals and reagents not specifically listed here were purchased from the following manufacturers: GE Healthcare, Fluka, Macherey-Nagel, Merck, Riedel-de Haën, Roche, Roth, and Sigma-Aldrich.

2.2 Bacterial Strains, Plasmids and Primers

2.2.1 Bacterial Strains

All bacterial strains used in this work are listed in Table 1.

Tab. 1: Bacterial strains used in this work.

Strain	Genotype	Reference/Source
E. coli DH5α	F$^-$1$^-$*sup*E44Δ(*argF-lac*)U169 *φ*80d*lac*ZΔM15 *hsd*R17 *rec*A1 *end*A1 *gyr*A96 *thi*-1 *rel*A1	(Hanahan, 1983)
E. coli BL21(λDE3)	F$^-$ *ompT gal dcm lon hsdS$_B$*(r_B^- m_B^-) λ(DE3 [*lacI lac*UV5-T7 gene 1 *ind*1 *sam*7 *nin*5	(Studier *et al.*, 1990)
E. coli BL21CodonPlus™ (DE3)-RIL	F$^-$ *ompT hsdS*(r_B^- m_B^-) *dcm*$^+$ Tet^r *gal* λ (DE3) *endA Hte[argU ileY leuW* Cam^r*]*	Stratagene
Synechococcus elongatus PCC 7942	Wildtype strain	(Aldehni *et al.*, 2003)
Rhodobacter capsulatus	mutant CB1200 (Δ*bchF* Δ*bchZ*); accumulates chlorophyllide	(Fidai *et al.*, 1994)
Thermosynechococcus elongatus BP1	Wildtype strain	(Yamaoka *et al.*, 1978)
Chlorobaculum tepidum TSL	Wildtype strain	DSMZ (German Collection of Microorganisms and Cell Cultures)
Prochlorococcus marinus subsp. marinus CCMP1375	Wildtype strain	Pasteur Collection
Roseobacter denitrificans OCh 114	Wildtype strain	DSMZ (German Collection of Microorganisms and Cell Cultures)

2.2.2 Plasmids

All plasmids used in this work are listed in Table 2.

Tab. 2: Plasmids used in this work.

vector	description	Reference/Source
pET32a	*E. coli* expression vector for N-terminal protein fusion with thioredoxin/His/S-tag; T7 promoter; Amp^R	Novagen
pGEX-6P-1	*E. coli* expression vector for N-terminal protein fusion with GST-tag; P_{tac} promoter; Amp^R	GE Healthcare
pAM1580	Integration vector for recombination into the genome of *S. elongatus* PCC 7942; carrying the gene *luxAB* in the MCS	(Aldehni *et al*., 2003)
pGEX-CtNBL	Vector pGEX-6P-1 carrying the *C. tepidum bchNBL* operon in the *Bam*HI -*Not*I restriction sites of the MCS; ribosomal binding site for *E. coli* was implemented upstream of *bchB* and *bchL*	Stefanie Ganskow, diploma thesis, 2005
pGEX-CtL	Vector pGEX-6P-1 carrying the *C. tepidum bchL* gene in the *Bam*HI-*Not*I restriction sites of the MCS	Markus Bröcker, diploma thesis, 2006
pGEX-TeNB	pGEX-6P-1 carrying the *T. elongatus chlN* and *chlB* genes in the *Bam*HI-*Not*I restriction sites of the MCS; ribosomal binding site for *E. coli* was implemented upstream of *chlB*	Frank Uliczka, diploma thesis, 2007
pGEX-TeL	pGEX-6P-1 vector carrying the *T. elongatus chlL* gene in the *Bam*HI-*Xho*I restriction sites of the MCS	This work
pGEX-PmNB	pGEX-6P-1 vector carrying the *P. marinus chlN* and *chlB* genes in the *Eco*RI-*Not*I restriction sites of the MCS; ribosomal binding site for *E. coli* was implemented upstream of *chlB*	Frank Uliczka, diploma thesis, 2007
pGEX-PmL	pGEX-6P-1 vector carrying the *P. marinus chlL* gene in the *Bam*HI-*Sal*I restriction sites of the MCS	Frank Uliczka, diploma thesis, 2007
pET-CtYZ	Vector pET32a, carrying the *C. tepidum bchY* and *bchZ* genes in the *Bam*HI-*Not*I restriction sites of the MCS; ribosomal binding site for *E. coli* was implemented upstream of *bchZ*	This work
pET-CtX	Vector pET32a, carrying the *C. tepidum bchX* gene in the *Bam*HI-*Sal*I restriction sites of the MCS	This work
pET-RdYZ	Vector pET32a, carrying the *R. denitrificans bchY* and *bchZ* genes in the *Bam*HI-*Not*I restriction sites of the MCS; ribosomal binding site for *E. coli* was implemented upstream of *bchZ*	This work
pET-RdX	Vector pET32a, carrying the *R. denitrificans bchX* gene in the *Sac*I-*Xho*I restriction sites of the MCS	This work
pISC	pRK415 vector containing the *isc* gene cluster (*iscS, iscU, iscA*, *hscBA* and *fdx*); Tet^R	Takahashi *et al*, 1999

vector	description	Reference/Source
pAM1580-AcsF-His	pAM1580-derivative: *luxAB* gene was replaced by a C-terminal His_6-tagged variant of *acsF* (Gene ID: 3775270) from *S. elongatus* PCC 7942 *via Nhe*I-*Sac*II restriction sites	This work
pAM1580-His-AcsF-His	The sequence of an additional N-terminal His_6-tag was introduced in vector pAM1580-AcsF-His *via* site-directed mutagenesis	This work
pAM1580-His-AcsF	A stop codon was introduced ahead of the C-terminal His_6-tag in the vector pAM1580-His-AcsF-His *via* site-directed mutagenesis	This work
pET32-AcsF	Vector pET32a carrying the *S. elongatus* PCC 7942 *acsF* gene in the *Bam*HI-*Sal*I restriction sites of the MCS	This work

2.2.3 Primers

All primers used in this work are listed in Table 3. Primers were purchased from MWG Biotech AG or Biomers.

Tab. 3: Primers used in this work.
The implemented *E. coli* specific ribosomal binding site for *chlB* and *bchZ* and sequences encoding His-tags are underlined, restriction sites are shown in italics. Exchanged nucleotides for mutagenesis of *P. marinus* DPOR are in bold.

Primer name	Sequence (5'-3')
TechlN_for	ATGC*GGATCC*ATGACTGTCACTGCTCCC
TechlN_rev	ACGC*CTCGAG*TCAGTGGGCAACCAGTTTTTG
TechlB_for	ATGC*CTCGAG*AATTTCACACAGGAAACAGTATTCATGAAACTTGCCTACTG
TechlB_rev	GCTTATT*GCGGCCGC*TTAAGCCCCCACGGCTTC
TechlL_for	GCTA*GGATCC*GTGTCGCTCCATTACCG
TechlL_rev	GCAT*CTCGAG*TTAGACAGCGGCGAGTG
PmchlN_for	CAGC*GAATTC*ATGAGCGGCTCAACG
PmchlN_rev	GCC*GTCGAC*TTAAACAGCTTCTAGAG
PmchlB_for	GACG*GTCGAC*TCAATTTCACACAGGAAACAGTATTCATGGAACTAACACTTTGG
PmchlB_rev	GCTGTAT*GCGGCCGC*TCAAGCTCCGAAATGAGC
PmchlL_for	AGC*GGATCC*ATGACTACAACCTTAGC
PmchlL_rev	TACC*GTCGAC*ACCCTAGTCAAAACC
CtbchY_for	CTATA*GGATCC*ATGTGCCCCGCGTTCGG
CtbchY_rev	CTATT*CTCGAG*TCACGCCGACGGCATAAAATAC
CtbchZ_for	CTATA*CTCGAG*AATTTCACACAGGAAACAGTATTCATGGCAAAAACCATCCGGG
CtbchZ_rev	CTATT*GCGGCCGC*TCAGCCCAACTGTTGC

Primer name	Sequence (5'-3')
CtbchX_for	GA*GGATCC*ATGGCAACGAGGCGG
CtbchX_rev	CTA*GTCGAC*TTACAGTTCGAAGAAG
RdbchY_for	CTATA*GGATCC*ATGATCAAGGGTCACCCGC
RdbchY_rev	CTATA*CTCGAG*CTAAATCATCTCCTGCGCTTTG
RdbchZ_for	CTATA*CTCGAG*AATTTCACACAGGAAACAGTATTCATGTTAGTCACAGATC ATG
RdbchZ_rev	CTATT*GCGGCCGC*TCATGTCTGATCCTCCAAATC
RdbchX_for	GA*GAGCTC*ATGAAAGATGAGGTTCC
RdbchX_rev	GT*CTCGAG*TCACGCATCGTCATAG
PmChlN E66A	GCAATTCTTG**C**AGAAAGAGACTTGGC
PmChlN L70R	GAAGAAAGAGAC**CGA**GCTGGTTTAGC
PmChlN L70D	GAAGAAAGAGAC**GAC**GCTGGTTTAGC
PmChlN V107D	CTTGCCCGAGCGAAG**AT**ATAAAAATTG
PmChlN K109S	GCCCGAGCGAAGTAATAA**GC**ATTGATTTATC
PmChlB G66D	CCAGAGATCTAG**AC**GGAGACACTGC
PmChlB Q101G	GAATTAATT**GGC**GATCAACCAGGTTC
PmChlB Q101D	GAATTAATT**GAC**GATCAACCAGGTTC
PmChlL Y127S	CTGCGGGGGAT**C**TGTAACTGGGC
PmChlL Y127D	CTGCGGGGGA**G**ATGTAACTGGGC
acsFSe_for	AC*GGATCC*ATGGTTGATTCCCTC
acsFSe_rev	TCT*GTCGAC*TTAGCGAACCGCAGGC
s.e.acsfpromoter	CGC AT*G CTA GC*G CTT TCC TCG GCG ATG AGC G
s.e.acsfCtermhistag	CGT AGC *CCG CGG* TTA GTG ATG GTG ATG GTG ATG TTC GAG CGC TTG GCG AAC CGC AGG CTG G
forws.e.acsfNhistag	CAA CCA ACT CCC AGC ACA GCT ATG GGC CAT CAC CAT CAC CAT CAC AGC AGC GGC ATG GTT GAT TCC CTC CAA AAA CCC
revs.e.acsfNhistag	GGG TTT TTG GAG GGA ATC AAC CAT GCC GCT GCT GTG ATG GTG ATG GTG ATG GCC CAT AGC TGT GCT GGG AGT TGG TTG
s.e.acsfstopforw	GTT CGA GCG CTT AGC GAA CCG CAG
s.e.acsfstoprev	CTG CGG TTC GCT AAG CGC TCG AAC

2.3 Growth Media and Media Additives

2.3.1 Media

As a standard medium for growth of all bacterial strains, Luria Bertani (LB) medium (Sambrook *et al.*, 2001) was used unless indicated otherwise. For solid media, 1.5 % (w/v) agar-agar was added before sterilization.

LB medium	tryptone	10.0 g/l
	NaCl	10.0 g/l
	yeast extract	5.0 g/l

For cultivation of *S. elongatus* PCC 7942 modified BG11 medium (Rippka *et al.*, 1979) was used. The *R. capsulatus* mutant CB1200 for production of the substrate Chlide was grown in RCV 2/3 PY medium (Young *et al.*, 1989).

modified BG11 medium	$NaNO_3$	1.5 g/l
	K_2HPO_4 x $3H_2O$	40 mg/l
	$MgSO_4$ x $7H_2O$	75 mg/l
	$CaCl_2$ x $2H_2O$	36 mg/l
	sodium citrate	6 mg/l
	ferric (III) ammonium citrate	6 mg/l
	EDTA (disodium salt)	1 mg/l
	Na_2CO_3	40 mg/l
	trace elements 1	1 ml

Sodium citrate and ferric (III) ammonium citrate were prepared as combined stock solution, while all other components were prepared solely as 200x stock solutions.

trace elements 1	H_3BO_3	2.86 g/l
	$MnCl_2$ x $4H_2O$	1.81 g/l
	$ZnSO_4$ x $7H_2O$	222 mg/l
	Na_2MoO_4 x $2H_2O$	390 mg/l
	$CuSO_4$ x $5H_2O$	79 mg/l
	$Co(NO_3)_2$ x $6H_2O$	49 mg/l
RCV 2/3 PY	DL-malic acid	4 g/l
	$(NH_4)_2SO_4$	1 g/l
	KH_2PO_4	625 mg/l
	K_2HPO_4	938 mg/l
	$MgSO_4$ x $7H_2O$	120 mg/l
	$CaCl_2$ x $2H_2O$	75 mg/l
	EDTA (disodium salt)	20 mg/l
	thiamine hydrochloride	1 mg/l
	peptone from casein	2 g/l
	yeast extract	2 g/l
	trace elements 2	1 ml
	pH adjusted to 6.8	
trace elements 2	H_3BO_3	2.8 g/l
	$MnSO_4$ x H_2O	1.6 g/l
	$NaMoO_4$ x $2H_2O$	752 mg/l
	$ZnSO_4$ x $7H_2O$	240 mg/l
	$Cu(NO_3)_2$ x $3H_2O$	40 mg/l

2.3.2 Additives

Antibiotics and other additives were prepared as concentrated stock solutions, sterilized by filtration (pore width 0.2 µm) and added to the medium after autoclaving. The following concentrations were used:

Substance	Solvent	Concentration of stock solution	Final concentration
ampicillin	H_2O	100 mg/ml	100 µg/ml
tetracycline	ethanol 70 % (v/v)	10 mg/ml	10 µg/ml
spectinomycin	H_2O	10 mg/ml	10 µg/ml
chloramphenicol	ethanol 100 % (v/v)	34 mg/ml	34 µg/ml
ferric (III) citrate	H_2O	100 mM	1 mM
IPTG	H_2O	100 mM	50 µM – 400 µM

2.4 Microbiological Techniques

2.4.1 Sterilization

All media were vapour sterilized at 121 °C and 1 bar positive pressure for 20 min. Other substances and solutions were either vapour sterilized or if temperature sensitive – sterilized by filtration (pore width 0.2 µm).

2.4.2 Cultivation of Bacteria

2.4.2.1 Cultivation of *E. coli*

Cells for recombinant protein production were grown under vigorous aeration. Pre-cultures were inoculated from glycerol stocks or single colonies from a plate culture in 100 ml of LB medium containing the respective antibiotics and grown overnight at 37 °C and 200 rpm in baffled flasks. After inoculation with pre-culture (1:100), 500 ml cultures were grown at 37 °C until induction of protein production with indicated amounts of IPTG. Cultures were then incubated at 17 °C, 25 °C or 37 °C for 1 - 5 h or overnight.

2.4.2.2 Cultivation of *Rhodobacter capsulatus* mutant CB1200

The *R. capsulatus* mutant CB1200 for the production of the COR substrate Chlide was grown in RCV 2/3 PY medium containing spectinomycin (10 µg/ml). A pre-culture of 25 ml of the mutant was grown at 30 °C and 130 rpm in the dark for two days. 100 ml culture were inoculated with 5 ml of the pre-culture. Cultivation was performed as

described by Gough *et al.* (2007) at 32 °C and 130 rpm in the dark. Therefore, the culture volume was increased over a period of three days by increasing the culture volume 5 times each day to yield 3 l culture.

2.4.2.3 Cultivation of *Synechococcus elongatus* PCC 7942

S. elongatus PCC 7942 was cultivated in modified BG11 medium under continuous illumination (Lumilux de Lux daylight bulbs, 2 x 15 W, 40 cm distance) at 25 °C and 100 rpm. For plate cultures, bacteria were plated directly on solid modified BG11 medium and incubated under continuous illumination (Lumilux de Lux daylight bulbs, 2 x 15 W, 40 cm distance) at 25 °C. When required, antibiotics were added.

2.4.3 Determination of Cell Density

The cell density of liquid cultures was determined by measuring the optical density (OD) at a wavelength of 578 nm. For cell densities with an $OD_{578} \geq 0.6$ dilutions with the respective cultivation medium were prepared before measurement. An OD_{578} of 1 corresponds to approximately 1 x 10^9 cells/ml.

2.4.4 Storage of Bacteria

Strains were kept on agar plates at 4 °C for up to four weeks. For long term storage glycerol stocks were prepared. Therefore, an overnight culture was mixed with glycerol to yield a final concentration of 20 % (v/v) and kept at -80 °C.

2.5 Molecular Biological Techniques

2.5.1 Preparation of Plasmid DNA (Miniprep)

Cells of a 2 ml overnight culture were harvested by centrifugation (10 min, 7'000 x g). The sedimented cells were resuspended in 150 µl of GTE solution and incubated for 5 min at room temperature (RT). For cell lysis, 300 µl of NaOH/SDS were added. The sample was

carefully mixed by inverting the tube and incubated at RT for 2 min. 225 µl of NaAc were added and the sample was carefully mixed again. After centrifugation (25 min, 15'000 x g) the supernatant was mixed with 600 µl isopropanol in a fresh tube and centrifuged (10 min, 15'000 x g). The sedimented DNA was resuspended in 200 µl of TES solution containing 3 µl of RNase and incubated for 1 h at 37 °C. Following an extraction with 200 µl CPI and vigorous shaking, the DNA was centrifuged (3 min, 15'000 x g). The DNA in the upper phase was precipitated again by addition of 400 µl 100 % (v/v) ethanol and centrifuged (20 min, 15'000 x g). Finally, the DNA precipitate was dried and solubilized in 20 - 50 µl H_2O.

GTE solution	Tris-HCl, pH 8.0	25 mM
	EDTA (disodium salt)	10 mM
	glucose	50 mM
NaOH/SDS	NaOH	200 mM
	SDS	1 % (w/v)
NaAc	sodium acetate, pH 4.8	3 M
TES solution	Tris-HCl, pH 8.0	50 mM
	EDTA (disodium salt)	10 mM
	NaCl	150 mM
CPI	phenol	50 % (v/v)
	chloroform	49 % (v/v)
	isoamyl alcohol	1 % (v/v)
RNase	ribonuclease A in 50 % (w/v) glycerol	10 g/l

2.5.2 Determination of DNA Concentration

The concentration and purity of a DNA solution was determined by measuring the absorbance at 260 nm and additionally at 280 nm to account for protein impurities. For a pure DNA solution, an A_{260nm} of 1 corresponds to a concentration of 50 µg/ml dsDNA. The

quality of the DNA solution is deduced from the ratio of A_{260nm} to A_{280nm}. With A_{260nm}/A_{280nm} = 1.8 - 2.0, the DNA can be considered as pure.

2.5.3 Agarose Gel Electrophoresis

For the analytical separation of DNA-fragments agarose gels (1 % (w/v) agarose in TAE buffer) were prepared. DNA samples were mixed with DNA loading dye to facilitate loading and to indicate the progress of the samples in the gel. GeneRuler™ DNA Ladder Mix or MassRuler™ DNA Ladder Mix (MBI Fermentas) were used as DNA standards according to the manufacturer's instructions. Depending on the size of the gel, a voltage of 80 – 100 V was applied. The DNA fragments migrate towards the anode with a velocity that is proportional to the negative logarithm of their length. After electrophoresis, gels were incubated in an ethidium bromide solution for 30 min. The DNA was detected *via* its fluorescence under UV light (λ = 312 nm).

TAE buffer (pH 8.0)	Tris-acetate	40 mM
	EDTA (disodium salt), pH 8.0	1 mM
DNA loading dye	bromophenol blue	350 µM
	xylene cyanol FF	450 µM
	glycerol	50 % (w/v)
ethidium bromide solution	ethidium bromide	0.1 % (w/v)

2.5.4 Cloning of DNA

For characterization of DPOR and COR enzymes from different organisms, the corresponding genes were cloned into *E. coli* standard expression vector systems.
The DPOR genes *chlN*, *chlB* and *chlL* from *P. marinus* and *T. elongatus* were cloned into the vector pGEX-6P-1 (GE Healthcare). For this purpose, both genes *chlN* and *chlB* were cloned into the MCS of the vector with an implemented *E. coli* specific ribosomal binding site upstream of *chlB*. The *chlL* gene was cloned separately in a pGEX-6P-1 vector.

For the investigation of the COR enzyme, the corresponding genes *bchY*, *bchZ* and *bchX* from *C. tepidum* and *R. denitrificans* were cloned into the vector pET32a (Novagen). In analogy to DPOR, the genes *bchY* and *bchZ* of COR were cloned with a specific *E. coli* ribosomal binding site upstream of *bchZ*. The gene *bchX* was cloned separately into the MCS of the vector pET32a.

To study the oxygen-dependent cyclase, the *acsF* gene from *S. elongatus* PCC 7942 and the respective promoter region located in the 250 bp upstream region were cloned into the integration vector pAM1580 (Aldehni *et al.*, 2003). Moreover, the individual *acsF* gene was cloned into a pET32a vector for the recombinant protein production in *E. coli*.

2.5.4.1 Amplification of DNA by Polymerase Chain Reaction (PCR)

For amplification of DNA by polymerase chain reaction (PCR), oligonucleotide primers were designed carrying appropriate recognition sequences for restriction endonucleases. Some oligonucleotide primers additionally contained sequences coding for an *E. coli* specific ribosomal binding site. All oligonucleotides used in this study are listed in Table 3. PCR was performed in a total volume of 20 µl. After an initial DNA denaturation step (95 - 98 °C), a cycle consisting of denaturation, primer annealing (50 - 68 °C), and primer elongation (72 °C) was completed 30 times. The reactions were terminated by a final elongation period. The duration of the elongation step was chosen according to the length of the DNA fragment to be amplified and the polymerases employed.

Standard thermocycler program for the Phusion™ DNA polymerase:

5 min	98 °C	
30 sec	98 °C	30x
30 sec	X °C	
30 sec/kb	72 °C	
5 min	72 °C	

Standard thermocycler program for the *Taq* polymerase:

5 min	95 °C	
30 sec	95 °C	30 x
30 sec	X °C	
60 sec/kb	72 °C	
5 min	72 °C	

Amplification of DPOR genes

For amplification of DPOR genes from *P. marinus* and *T. elongatus* a gradient PCR with varying annealing temperatures and template amounts was carried out to determine the optimal PCR conditions. PCR was performed by using 4 µl 5x Phusion HF buffer, 200 µM of each dNTPs, 1 µM primer and 0.2 µl Phusion™ DNA polymerase (2 U/µl) in a total volume of 20 µl.

The genes of *P. marinus* and *C. tepidum* were amplified by a colony PCR. Therefore, a cell suspension in 200 µl H_2O was incubated at 95 °C for 10 min. For the subsequent PCR reaction 1 - 10 µl of this template was used. For the amplification of the genes from *T. elongatus* 1 to 100 ng of genomic DNA (kindly provided by Corinna Lüer) was used. For the *P. marinus* genes *chlN*, *chlB* and *chlL* annealing temperatures of 51 °C, 68 °C and 57 °C, respectively, for the corresponding genes from *T. elongatus* annealing temperatures of 65.9 °C for *chlN* and *chlB*, and 57 °C for *chlL* were used.

Amplification of COR genes

For the characterization of COR enzymes, corresponding genes from *C. tepidum* and *R. denitrificans* were amplified using a colony PCR as described above. To determine the optimal PCR conditions, a gradient PCR was performed with varying annealing temperatures and template amounts. PCR reactions were the same as described for amplification of DPOR genes before. For amplification of *bchY* and *bchZ* genes from *C. tepidum* and *R. denitrificans* an annealing temperature of 68 °C was employed, the gene *bchX* was amplified using an annealing temperature of 66 °C.

Amplification of cyclase gene *acsF*

S. elongatus acsF was amplified by colony PCR. For this purpose, 0.5 cm^2 cell material of a plate culture were suspended in 200 µl H_2O. After heating for 4 min to 95 °C, 10 µl were used for the PCR reaction. PCR was performed in a total reaction volume of 20 µl with 2 µl 10x PCR buffer, 200 µM of each dNTPs, 1 µM primer and 1 µl *Taq* polymerase (5 U/µl).

For the amplification of the *acsF* gene an annealing temperature of 60.5 °C was used.

2.5.4.2 Restriction of DNA

Restriction of DNA (vectors and PCR products) was carried out using restriction endonucleases purchased from New England Biolabs. Reaction buffers, concentrations of enzymes, DNA concentrations as well as incubation temperatures were chosen according to manufacturer's instructions. The restriction was allowed to proceed for 1 - 3 h according to enzyme-dependent conditions.

2.5.4.3 Purification of PCR Products

After amplification of DNA by PCR, the resulting PCR products were purified using the "QIAquick PCR Purification Kit" (Qiagen) according to the manufacturer's instructions.

Restriction enzymes were removed by agarose gel electrophoresis. The DNA was visualized using the GelStar® Nucleic Acid Gel Stain (Biozym) on a blue light detector (Flu-O-blu). The DNA fragment was then excized from the gel and purified using the "QIAquick Gel Extraction Kit" (Qiagen) according to manufacturer's instructions.

2.5.4.4 Ligation of DNA

Ligation of DNA was carried out using T4 DNA ligase (MBI Fermentas) according to the manufacturer's instructions. An amount of 25 - 50 ng vector DNA was mixed with insert DNA (insert to vector ratio with regard to molar concentrations ~ 5:1) in a final volume of 20 µl. Moreover, control reactions in the absence of insert or ligase were carried out. All reactions were incubated for 2 h at RT or at 17 °C overnight.

2.5.5 Site-directed Mutagenesis (Quik Change)

Single amino acids or even multiple amino acid residues of a protein of interest can be exchanged by inserting site-specific mutations into the DNA sequence of the corresponding gene. The QuikChange® Site-directed Mutagenesis Kit (Stratagene) was employed in this work for mutational analysis of DPOR subunits ChlN, ChlB and ChlL from *P. marinus*. Furthermore, site-directed mutagenesis was used to yield variants of the oxygen-dependent cyclase encoding N-, C-, as well as N- and C-terminal His-tagged fusions of the protein.

The method utilizes a dsDNA plasmid carrying the gene of interest and two synthetic oligonucleotide primers. The primers contain the desired mutation and are complementary to opposite strands of the vector. During PCR with the PfuTurbo DNA polymerase a mutated plasmid is generated. The PCR product is treated with *Dpn*I, an endonuclease specifically digesting partially methylated DNA, here the parental template DNA. This allows isolation of the newly *in vitro* synthesized unmethylated DNA of the mutated plasmid with which a suitable *E. coli* strain is subsequently transformed. The DNA is then ligated by the DNA ligase of *E. coli*.

PCR reactions with the QuikChange® site-directed mutagenesis kit were carried out according to the manufacturer's instructions. However, the volume of the PCR reaction was reduced to 25 µl. Competent *E. coli* DH5α cells were transformed with the mutated plasmids. Primers used for site-directed mutagenesis are listed in Table 3.

2.5.6 Transformation of *E. coli* by the $CaCl_2$-Method

An overnight culture of *E. coli* DH5α, BL21 (λDE3) or BL21 CodonPlus™ (DE3)-RIL cells was inoculated in a ratio of 1:100 and grown in 500 ml LB under aerobic conditions. The bacteria were incubated at 37 °C and 200 rpm in baffled flasks until the culture reached an OD_{578} of 0.6. Then, cells were harvested by centrifugation (6'000 x g, 10 min, 4 °C). After washing the cells three times with ice-cold $CaCl_2$ solution, cells were suspended in 10 ml $CaCl_2$ solution. The competent cells were either used directly for transformation or stored at -80 °C.

$CaCl_2$ solution	$CaCl_2$	60 mM
	glycerol	15 % (w/v)
	PIPES (pH 7.0)	10 mM

The $CaCl_2$ competent *E. coli* cells were transformed by heat shock. For this purpose, 1 µl of plasmid DNA (3 µg/µl) was mixed with 100 µl of competent *E. coli* cells and incubated on ice for 10 min. After heating the cells for 2 min to 42 °C, cells were incubated for 10 min on ice. To regenerate the transformed cells, they were incubated in 1 ml of LB medium at 37 °C for 1 h. The transformation volume was streaked out on a LB medium agar plate with appropriate antibiotics and incubated overnight at 37 °C.

2.5.7 Sequencing

The successful modification of DNA (cloning as well as site-directed mutagenesis) was confirmed by sequence determination of the respective DNA region based on the Sanger method (Sanger *et al.*, 1977). The sequencing reactions were conducted with an ABI PRISM^{TM} 310 Genetic Analyser (Applied Biosystems). The required PCR in the presence of fluorescence-labeled ddNTPs and the purification of the PCR product were carried out as described by the manufacturer. The analysis of all sequencing results was done using DNASTAR software package (GATC Biotech).

2.6 Protein Biochemical Methods

2.6.1 Recombinant Protein Production

2.6.1.1 Production of Dark-Operative Protochlorophyllide Oxidoreductase (DPOR)

For recombinant production of DPOR subunits BchN/ChlN, BchB/ChlB and BchL/ChlL in *E. coli*, 500 ml LB medium containing ampicillin (100 µg/ml), chloramphenicol (34 µg/ml) and 1 mM Fe(III) citrate were inoculated (ratio 1:100) with an overnight culture of *E. coli* BL21 CodonPlus® (DE3)-RIL carrying pGEX-CtNBL for *C. tepidum* $(BchNB)_2$, pGEX-TeNB for *T. elongatus* $(ChlNB)_2$, pGEX-PmNB for *P. marinus* $(ChlNB)_2$, pGEX-

CtL for *C. tepidum* $BchL_2$, pGEX-TeL for *T. elongatus* $ChlL_2$ and pGEX-PmL for *P. marinus* $ChlL_2$, respectively. Cultures were grown aerobically at 37 °C and 200 rpm to an OD_{578} of 0.5. Recombinant expression of DPOR genes was induced by the addition of IPTG to a final concentration of 50 µM. Incubation was continued at 160 rpm and 17 °C for the production of the *C. tepidum* and *T. elongatus* proteins and at 25 °C for the *P. marinus* proteins, respectively. After 16 h, cultures were supplemented with 1.7 mM dithionite and incubated for a further 2 h in an anaerobic chamber (Coy Laboratory Products) without agitation. Cells were harvested by centrifugation for 10 min at 4'000 x g and 4 °C. Cell sediments were stored at -20 °C.

2.6.1.2 Production of Chlorophyllide *a* Oxidoreductase (COR)

COR subunits BchY and BchZ were produced in BL21 CodonPlus® (DE3)-RIL carrying plasmids pET-CtYZ encoding *C. tepidum* $(BchYZ)_2$ or pET-RdYZ encoding *R. denitrificans* $(BchYZ)_2$. Subunit BchX was produced in *E. coli* BL21(λDE3) carrying the plasmid pISC for expression of genes of the *isc*-operon. The *isc*-operon contains the genes *iscS, iscU, iscA*, *hscBA* and *fdx* coding for proteins involved in the iron-sulfur cluster maturation. For production of *C. tepidum* $BchX_2$ the plasmid pET-CtX, for production of *R. denitrificans* $BchX_2$ the plasmid pET-RdX was used. Protein production of COR subunits was performed as described above for DPOR at 17 °C. For production of subunit $BchX_2$ cells were grown in LB medium containing ampicillin (100 µg/ml) and tetracycline (10 µg/ml) supplemented with 1 mM Fe(III) citrate and 1 mM cysteine and protein production was induced with 300 µM IPTG.

2.6.1.3 Production of Oxygen-Dependent Cyclase (AcsF)

S. elongatus mutants carrying genomically integrated His-tag versions of AcsF, were cultivated at 25 °C and 100 rpm under continuous illumination (Lumilux de Lux daylight bulbs, 2 x 15 W, 40 cm distance). Cultures were inoculated from plate cultures, incubated for 1 - 7 days and analyzed for production of AcsF by SDS-PAGE (section 2.7.2) and Western Blotting (section 2.7.3).

For production of AcsF in *E. coli*, cells were grown as described above. Thereby, LB medium containing ampicillin (100 µg/ml) was used and recombinant protein production was induced by addition of 50 µM or 400 µM IPTG. Incubation was continued at 17 °C, 25 °C and 37 °C for 1 - 5 h and overnight.

2.6.2 Disruption of Cells

For characterization of DPOR and COR enzymes, sedimented cells were suspended in lysis buffer and disrupted by a single passage through a French Press® (SLM Amino, Polytec) at 1000 p.s.i. under anaerobic conditions.

lysis buffer	HEPES/NaOH, pH 7.5	100 mM
	NaCl	150 mM
	$MgCl_2$	10 mM

For analysis of the oxygen-dependent cyclase, wildtype cells of *T. elongatus* were incubated in buffer (10 mM HEPES/NaOH pH 7.8, 20 mM TES, 11 mM $MgCl_2$) containing lysozyme (2 mg/ml) for 1 h at 37 °C. After sonication for 1 min (0.5 sec interval, amplitude 60 %, MS72), the resulting cellular extract was used for activity assays. Alternatively, *T. elongatus* cells were suspended in 100 mM TES, 50 mM HEPES/NaOH, 10 mM $MgCl_2$, 1 M glycerol, pH 7.7 containing 0.004 % (w/v) PMSF. Cells were disrupted by double passage through a French Press® at 900 p.s.i.. After centrifugation for 15 min (16'000 x g), the resulting "low speed" supernatant was used for activity assays.

2.6.3 Affinity Chromatography

The following procedures were performed in an anaerobic chamber under anaerobic conditions (95 % N_2, 5 % H_2, <1 ppm O_2) and buffers were saturated with N_2 prior to use. After cell disruption, the cellular extract was centrifuged for 1 h (110'000 x g, 4 °C). The resulting supernatant was loaded onto a gravity-flow column equilibrated with lysis buffer.

2.6.3.1 Affinity Chromatography of GST-Tagged Proteins

For purification of GST-tagged proteins, a Poly-Prep chromatography column (BioRad) was packed with 500 µl of glutathione sepharose 4FF (GE Healthcare). After applying the protein sample, the column was washed with 7 column volumes (C_V) of PBS buffer. The resin was incubated with elution buffer A containing 15 mM glutathione for 30 min, subsequently proteins were eluted using 3x 500 µl elution buffer A.

PBS buffer (pH 7.4)	NaCl	137 mM
	KCl	2.2 mM
	Na_2HPO_4 x $7H_2O$	10 mM
	KH_2PO_4	1.7 mM
	DTT	10 mM
elution buffer A	HEPES/NaOH, pH 7.5	100 mM
	NaCl	150 mM
	$MgCl_2$	10 mM
	DTT	10 mM
	glutathione	15 mM

2.6.3.2 Affinity Chromatography of His-tagged Proteins

For the purification of His-tagged proteins, Chelating Sepharose FF (GE Healthcare) was used. The material was first loaded with two C_V of 100 mM of $NiSO_4$ and washed with 5 C_V of H_2O. After ultracentrifugation of the disrupted cells, the supernatant was loaded onto 500 µl of nickel-loaded Chelating Sepharose FF equilibrated with lysis buffer. After extensive washing with washing buffer and pre-elution with buffer containing 30 mM imidazole, proteins were eluted with buffer containing 200 mM imidazole (elution buffer B).

washing buffer	HEPES/NaOH, pH 7.5	100 mM
	NaCl	500 mM
	$MgCl_2$	10 mM
pre-elution buffer	HEPES/NaOH, pH 7.5	100 mM
	NaCl	500 mM
	$MgCl_2$	10 mM
	imidazole	30 mM
elution buffer B	HEPES/NaOH, pH 7.5	100 mM
	NaCl	500 mM
	$MgCl_2$	10 mM
	imidazole	200 mM

2.6.3.3 Protease Digestion for Removal of Affinity Tags

Fusion tags of the purified recombinant proteins were eliminated using either the PreScission Protease site (for GST-tagged proteins) or the thrombin cleavage site (for His-tagged proteins). Therefore, proteins bound to the resin were incubated overnight with the corresponding protease in 800 µl - 1000 µl lysis buffer containing 10 mM DTT (for GST-tagged proteins) or 1.7 mM dithionite (for His-tagged proteins), with exception of subunit BchX which was incubated without reductant, at 17 °C under anaerobic conditions.

2.7 Protein Characterization

2.7.1 Determination of Protein Concentration

Concentrations of purified proteins were determined using the Bradford reagent (Sigma-Aldrich) according to the manufacturer's instructions. The assay is based on the colorimetric method developed by Bradford (1976). Bovine serum albumin was used as a standard.

For the quantification of GST-fusion proteins in cell-free extracts of *E. coli*, a GST detection module (GE Healthcare) was used.

2.7.2 Discontinuous SDS Polyacrylamide Gel Electrophoresis (SDS-PAGE)

Proteins were analyzed by discontinuous sodium dodecyl sulfate-polyacrylamide gel electrophoresis (SDS-PAGE) as described by Laemmli (1970) with modifications by Righetti *et al.* (1990) for discontinuous SDS-PAGE.

Protein samples were incubated for 10 min at 95 °C in SDS loading dye to denature the proteins. Samples were loaded onto gels which were run at 45 mA until the band of bromophenol blue dye reached the lower end of the gel. During electrophoresis, proteins were first focussed in the stacking gel and subsequently separated according to their relative molecular mass in the running gel. The size standard employed was the Protein Molecular Weight Marker (MBI Fermentas). For immunochemical detection of the proteins, the protein standard PageRuler^{TM} Prestained Protein Ladder (MBI Fermentas)

was used. Subsequently, gels were stained with Coomassie Brilliant Blue G-250 and destained until distinct protein bands were visible. For documentation, gels were scanned (ScanMakerX12USI; ScanWizard 5; Microtek) and then dried between two cellophane foils for storage.

acrylamide stock solution	acrylamide	30 % (w/v)
	N,N'-methylen bisacrylamide	0.8 % (w/v)
running gel (12 %)	acrylamide stock solution	2 ml
	1.5 M Tris-HCl, pH 8.8 with 0.4 % (w/v) SDS	1.25 ml
	H_2O_{deion}	1.75 ml
	10 % (w/v) APS	50 µl
	TEMED	5 µl
stacking gel (6 %)	acrylamide stock solution	0.5 ml
	0.5 M Tris-HCl pH 6.8 with 0.4 % (w/v) SDS	625 µl
	H_2O_{deion}	1.375 ml
	10 % (w/v) APS	25 µl
	TEMED	2.5 µl
electrophoresis buffer	Tris-HCl, pH 8.4	50 mM
	glycine	380 mM
	SDS	0.1 % (w/v)
SDS loading dye	Tris-HCl, pH 6.8	100 mM
	glycerol	40 % (v/v)
	β-mercaptoethanol	10 % (v/v)
	SDS	3.2 % (w/v)
	bromophenol blue	0.2 % (w/v)
staining solution	acetic acid	10 % (v/v)
	ethanol	25 % (v/v)
	Coomassie Brilliant Blue	0.25 % (w/v)

destaining solution	acetic acid	10 % (v/v)
	ethanol	30 % (v/v)

2.7.3 Immunochemical Detection of Proteins by Western Blot

For the immunochemical detection, electrophoretically separated proteins were transferred onto a polyvinylidene difluoride (PVDF - pore width 0.45 µm) membrane (Roti®; Roth) using a Trans Blot apparatus (semi dry transfer cell; BioRad). Therefore, the PVDF-membrane was activated in methanol for 15 min and then equilibrated in Towbin buffer. After SDS-PAGE, the unstained gel and two pieces of Whatman paper were equilibrated in Towbin buffer for 15 min. The proteins were blotted onto the membrane for 30 min at 10 V per gel using the semi dry method according to the manufacturer's instructions.
For detection of biotin-labeled DPOR subunits (section 2.7.9), the membrane was blocked overnight with blocking buffer A. Then, the membrane was incubated with NeutrAvidin antibody (1:35'000) conjugated with horseradish peroxidase (Pierce) for 1 h, washed three times for 5 min with washing solution A and transferred for 10 min in 0.8 % (w/v) NaCl solution. Afterwards, the detection of proteins was performed using a chemiluminescence reaction with luminol and peroxide solution (SuperSignal® West Pico Chemiluminescence Kit; Pierce) according to the manufacturer's instructions, followed by exposition to an X-ray film for 10 sec.
For the detection of the His-tagged AcsF protein, the membrane was blocked overnight in blocking buffer B, washed in PBS buffer and incubated for 1 h with murine anti-His antibody (1:4'000). After washing three times for 10 min in washing solution B, incubation with the secondary anti-mouse antibody (1:4'000) conjugated with horseradish peroxidase followed for 50 min. The membrane was washed in PBS-Tween for 10 min, then the chemiluminescence reaction was performed as described above with an exposure time of 30 min.

Towbin buffer	Tris-HCl, pH 8.5	25 mM
	glycine	192 mM

blocking buffer A	Tris-HCl, pH 7.5	20 mM
	NaCl	150 mM
	BSA	2 % (w/v)
washing solution A	Tris-HCl pH 7.5	20 mM
	NaCl	150 mM
	BSA	0.1 % (w/v)
	Triton X-100	0.1 % (v/v)
	SDS	0.05 % (w/v)
PBS (pH 7.4)	NaCl	137 mM
	KCl	2.2 mM
	Na_2HPO_4 x $7H_2O$	10 mM
	KH_2PO_4	1.7 mM
blocking buffer B	10x PBS	10 % (v/v)
	Tween 20	0.1 % (v/v)
	BSA	5 % (w/v)
washing solution B	10x PBS	10 % (v/v)
	Tween 20	0.1 % (v/v)
	BSA	0.5 % (w/v)

2.7.4 N-terminal Sequencing

Automated Edman degradation was used to confirm the identity of purified proteins and quantify protein subunits from Western Blots. Therefore, protein samples were separated by SDS-PAGE (section 2.7.2) and blotted onto a PVDF membrane using a semi dry Western Blot (section 2.7.3). Afterwards, transferred proteins were stained with Ponceau S and bands of interest were marked. N-terminal sequencing of the samples was performed by R. Getzlaff (HZI, Braunschweig) with a Sequence Analyzer ABI-494 (Applied Biosystems).

Ponceau S	Ponceau S	0.4 % (w/v)
	trichloracetic acid	368 mM
	sulfo salicylic acid	240 mM

2.7.5 Mass Spectroscopy

Chromatographically purified protein fractions were analyzed for the protein content by LC-MS/MS. This work was done by Dr. Manfred Nimtz at the HZI, Braunschweig.

2.7.6 Determination of Native Molecular Mass

Analytical gel permeation chromatography was performed using a Superdex 200 HR 26/60 or Superdex 200 HR 10/30 column (GE Healthcare) under anaerobic conditions. The columns were equilibrated with GPC buffer and calibrated with the following marker proteins: carbonic anhydrase (M_r ~29'000), bovine serum albumin (M_r ~66'000), alcohol dehydrogenase from yeast (M_r ~150'000) and β-amylase from sweet potato (M_r ~200'000) (Molecular weight marker Kit, Sigma-Aldrich). Then, 200 µl - 5 ml of the purified proteins (~1 - 5 mg/ml) after protease cleavage (section 2.6.3.3) were run under identical conditions at a flow rate of 0.7 ml/min (Superdex HR 10/30) or 1 ml/min (Superdex HR 26/60). Protein elution was monitored by measuring the absorbance at 280 nm.

GPC buffer	HEPES/NaOH, pH 7.5	100 mM
	NaCl	150 mM
	$MgCl_2$	10 mM

2.7.7 UV/Visible Light Absorption Spectroscopy

UV/visible light absorption spectra of recombinantly purified DPOR and COR subunits were recorded under anaerobic conditions in a rubber-sealed anaerobic cuvette using a V-550 spectrophotometer (Jasco). Spectra from 250 to 800 nm at a scan speed of 200 nm/min were monitored.

2.7.8 Determination of Iron and Sulfur Contents

The iron content of purified DPOR and COR subunits was measured colorimetrically with bathophenantroline following acid denaturation as described by Lovenberg *et al*. (1963). Bathophenantroline disulfonate forms a complex with Fe(II) ions. This complex can be detected photometrically at a wavelength of 340 nm. The iron content of the samples was determined *via* a calibration curve obtained from a series of dilutions of an iron standard (Merck).

To quantify the content of labile sulfur in proteins, the method of Beinert *et al*. (1983) using N,N-diemethyl-p-phenylendiamine (DMPD) in combination with $FeCl_3$ was applied. Determination of the sulfur content is performed by release of sulfur from the [Fe-S] cluster in form of sulfide by the addition of Zn-acetate solution (1% (w/v)) and 3 M NaOH. After acidification by 23 mM $FeCl_3$ in 1 M HCl, the sulfide reacts with DMPD forming methylene blue. This dye can then be detected photometrically at a wavelength of 670 nm.

2.7.9 Label Transfer Experiments

After preparative gel permeation chromatography, purified $ChlL_2$ protein from *P. marinus* was labeled with the trifunctional label transfer reagent Mts-Atf-LC-biotin biotin (2-{N2-[N6-(4-azido-2,3,5,6-tetrafluoro-benzoyl-6-aminocaproyl)-N6-(6-biotinamido-caproyl)-L-lysinyl-amido]}ethyl methanethio-sulfonate) (Pierce). Besides a biotin moiety, this reagent contains a sulfhydryl-specific methane-thiosulfonate (Mts) group which can form disulfide bonds with free sulfhydryl groups of the $ChlL_2$ protein. After exposure to UV light, the photoreactive tetrafluorophenyl azide (Atf) moiety of the crosslinker inserts into carbon hydrogen bonds and unsaturated carbon chains of the protein within a 21.8 Å distance. Upon addition of reducing agents the disulfide bond is cleaved and the biotin label is transferred to the interacting protein partner.

All procedures for the labeling experiments were performed at low concentrations of DTT (< 1 mM DTT) and under subdued light to prevent premature loss of the label and activation of the Atf moiety. Purified $ChlL_2$ from *P. marinus* was mixed with 5-fold molar excess of Mts-Atf-LC-biotin in a total reaction volume of 500 µl in phosphate-buffered saline (100 mM sodium phosphate, 150 mM NaCl, pH 7.4). After incubation for 1 h at 21 °C, the unbound reagent was removed by dialysis using Slide-A-Lyzer® MINI Dialysis

Units (Pierce). Label transfer experiments contained 25 µM of $(ChlNB)_2$ from *P. marinus* and 70 µM of the corresponding biotinylated $ChlL_2$ protein ($ChlL_2$-Mts-Atf-LC-biotin) in a volume of 100 µl phosphate-buffered saline. Assays further contained 2 mM ATP, an ATP-regenerating system consisting of 20 mM creatine phosphate and 10 units creatine phosphokinase and the DPOR substrate Pchlide at a concentration of 13 µM. Complex formation was initiated for 5 min at 21 °C. Then the crosslinking reaction was induced by exposure to UV light using a CAMAG UV lamp (365 nm; 2 x 8 W) for 30 min at a distance of 5 cm. Then 100 µl of SDS sample buffer (Sambrook *et al.*, 2001) containing the reducing agent DTT at a concentration of 100 mM were added. Thereby, the $ChlL_2$ protein was liberated from the crosslinked complex resulting in the transfer of the biotin label onto the $(ChlNB)_2$ protein. In control experiments, the $(ChlNB)_2$ complex or the $ChlL_2$ protein was omitted. Furthermore, negative controls were performed by substituting $(ChlNB)_2$ with bovine serum albumine. All samples were subsequently analyzed on a 12 % SDS-PAGE. Proteins were blotted onto a PVDF membrane using a Trans-Blot apparatus semi dry transfer cell (BioRad) according to manufacturer's instructions (section 2.7.3). Biotin-labeled proteins were detected by using a NeutrAvidin antibody conjugated with horseradish peroxidase (Pierce).

2.7.10 Electron Paramagnetic Resonance (EPR) Spectroscopy

Samples for EPR spectroscopy were prepared in an anaerobic chamber. Purified COR subunits were concentrated (10 mg/ml) using Microcon® Centrifugal Filter Units (Millipore; molecular weight cutoff 10'000). 100 µl of protein solution were supplemented with 2 µl of 1 M dithionite and incubated for 30 min. Proteins were finally transferred to quartz EPR tubes with 4 mm outer diameter and frozen in liquid nitrogen. Control samples contained protein fractions in the absence of a reducing agent.

The 9.5 GHz X-Band EPR spectra were recorded in collaboration with the group of Prof. Dr. Lendzian (TU Berlin) on a Bruker ESP300E spectrometer equipped with a rectangular microwave cavity in the TE_{102} mode. For temperature control at 10 K, the sample was kept in an Oxford ESR 900 helium flow cryostat with an Oxford ITC4 temperature controller. The microwave frequency was detected with an EIP frequency counter (Microwave Inc). Magnetic field was calibrated using a Li/LiF standard with known g-value of 2.002293 ± 0.000002 (Stesmans *et al.*, 1989). Simulations of the

experimental EPR spectra have been carried out with the program *EasySpin* (Stoll *et al.*, 2006)

2.7.11 Flavin Cofactor Analysis by HPLC

After analysis of purified $BchX_2$ protein by UV/visible absorption spectroscopy, the protein was precipitated by the addition of 5 % (v/v) perchloric acid and centrifuged at 10'000 x g for 10 min. The supernatant was analyzed using a HPLC-system 1500 series (Jasco) and an ODS Hypersil 250 x 4.6 mm column (Techlab). Separation of substances was performed using an isocratic mode and a flow rate of 0.5 ml/min at 30 °C. Flavins were detected by fluorescence measurements using an excitation wavelength of 430 nm and an emission wavelength of 525 nm. Flavin-adenin-dinucleotide (FAD) and flavin-mononucleotide (FMN) were used as standards.

mobile phase	acetonitrile		water		trifluoric acid		phosphoric acid
ratio (v/v/v/v)	14	:	84	:	1.5	:	0.09

2.8 Enzyme Activity Assays

2.8.1 DPOR Activity Assays

For determination of activity of the recombinantly produced DPOR enzymes, *in vitro* activity assays were performed. Functional DPOR enzymes from *C. tepidum*, *P. marinus* and *T. elongatus* were reconstituted by supplementing 100 pmol purified $(BchNB)_2$/$(ChlNB)_2$ complex with 200 pmol purified $BchL_2$/$ChlL_2$ protein, respectively, in a total volume of 125 µl in 100 mM HEPES/NaOH, pH 7.5, 150 mM NaCl and 10 mM $MgCl_2$. The assays contained 2 mM ATP, an ATP-regenerating system, consisting of 20 mM creatine phosphate and 10 units creatine phosphokinase, 10 mM DTT, 10 mM sodium dithionite as an electron donor and 13 µM of the substrate Pchlide.
Pchlide was isolated from the *bchL*-deficient *R. capsulatus* mutant strain ZY5 as described before (Bröcker *et al.*, 2008a, Fujita *et al.*, 2000). Samples were incubated under strict anaerobic conditions for 15 - 60 min at varying temperatures ranging from 20 - 50 °C in

the dark. Reactions were stopped by the addition of 500 µl acetone. After centrifugation for 30 min at 12'000 x g, the supernatant was analyzed by UV/visible absorption spectroscopy (section 2.7.7) using a V-550 spectrophotometer (Jasco). The DPOR reaction product Chlide shows a characteristic peak at 665 nm whereas the substrate possesses an absorption maximum at 626 nm. For the quantification of Pchlide and Chlide, extinction coefficients of $\varepsilon_{626} = 30.4\ mM^{-1}\ cm^{-1}$ for Pchlide and $\varepsilon_{665} = 74.9\ mM^{-1}\ cm^{-1}$ for Chlide were used (Fujita *et al.*, 2000, McFeeters *et al.*, 1971). The detection limit of the assay is at 15.75 nmol min^{-1} mg^{-1}.

All subsequent assays for the various DPOR systems were standardized at 35 °C allowing for the determination of specific activities under identical conditions. For this standard DPOR assay 100 pmol purified $(BchNB)_2/(ChlNB)_2$ was combined with 1 - 80 µl of a cell-free *E. coli* extract containing 0.05 - 300 pmol of the overproduced $BchL_2/ChlL_2$ protein, respectively. Obtained specific activities were set to 100 % and all other values were related to this. In all cases, assays were completed by control experiments in which the $BchL_2/ChlL_2$ protein, the $(BchNB)_2/(ChlNB)_2$ complex or alternatively the co-substrate ATP was omitted.

2.8.2 COR Activity Assays

2.8.2.1 Preparation of the Substrate Chlorophyllide *a*

For the production of the COR substrate, Chlide, the *R. capsulatus* mutant CB1200 was used. After cultivation (section 2.4.2.2) for three days in the dark, the slightly green 3 l culture was harvested by centrifugation (10 min, 4'000 x g) and subsequently freeze-dried. According to the protocol of Gough *et al*. (2007), 0.5 g of freeze-dried cells were extracted with 40 ml of acetone/H_2O/25 % NH_3 (80:20:1 (v/v/v)). The mixture was gently agitated for 2 min and centrifuged (5 min, 3'600 x g). After transfer of the supernatant to a new tube, carotinoids were extracted by the addition of 5 ml hexane and inverting 5 times. After phase separation, the acetone phase was evaporated and the obtained Chlide was suspended in 100 µl of DMSO, 30 mM Tricine/NaOH, pH 8.0 and stored at -20 °C until use.

2.8.2.2 Homologous COR Activity Assays

For the analysis of activity of the recombinantly produced COR enzymes from *C. tepidum* and *R. denitrificans*, *in vitro* activity assays under the conditions of the standard DPOR assay (section 2.8.1) using 10 µM Chlide as substrate were performed. COR enzymes were reconstituted by combining 100 pmol of purified $(BchYZ)_2$ with 1 - 50 µl of a cell-free *E. coli* extract containing 10 - 300 pmol of the overproduced $BchX_2$ proteins in a total volume of 125 µl, for 1 h at 35 °C in the dark. Reactions were stopped by the addition of 500 µl acetone, samples were centrifuged (30 min, 12'000 x g) and extracted with one volume of hexane to remove carotinoids. The lower acetone phase was analyzed by UV/visible absorption spectroscopy (section 2.7.7) using a V-550 spectrophotometer (Jasco) scanning from wavelength 600 nm to 800 nm. The COR reaction product Bchlide shows a peak at a wavelength of 734 nm while the substrate Chlide exhibits an absorption maximum at a wavelength of 665 nm. For the quantification of Chlide and Bchlide, extinction coefficients of $\varepsilon_{665} = 74.9\ mM^{-1}\ cm^{-1}$ for Chlide and $\varepsilon_{734} = 44.7\ mM^{-1}\ cm^{-1}$ for Bchlide were used (Nomata *et al.*, 2006b, McFeeters *et al.*, 1971). In all cases, assays were completed by control experiments in which the $BchX_2$ protein, the $(BchYZ)_2$ complex or alternatively the co-substrate ATP was omitted.

2.8.2.3 COR Activity Assays using Substrate Analogs

For the investigation of the substrate recognition of the COR enzyme, activity assays with substrate analogs (kindly provided by Prof. Dr. Scheer and Prof. Dr. Rüdiger, LMU Munich) were performed. Therefore, in the standard COR activity assay the natural substrate Chlide was replaced by the corresponding substrate analogs. Employed substrate analogs were Zn-bacteriopheophorbide *c* (Zn-BPheid *c;* $\varepsilon^* = 60\ mM^{-1}\ cm^{-1}$), Zn-3-Acetyl-pheophorbide *a* (Zn-3-Acetyl-Pheid *a*; $\varepsilon = 65.2\ mM^{-1}\ cm^{-1}$) (Smith *et al.*, 1966), Pyro-chlorophyllide *a* (Pyro-Chlide *a;* $\varepsilon^* = 65\ mM^{-1}\ cm^{-1}$), Zn-Pyro-pheophorbide *a* (Zn-Pyro-Pheid *a*; $\varepsilon = 69.2\ mM^{-1}\ cm^{-1}$) (Schmid *et al.*, 2002b), Zn-3^1-13^2-dihydroxy-pheophorbide *a* (Zn-3^1-13^2-di-OH-Pheid *a*; $\varepsilon^* = 65\ mM^{-1}\ cm^{-1}$), Zn-3-Formyl-methyl-pheophorbide *a* (Zn-3-Formyl-Me-Pheid *a;* $\varepsilon^* = 65\ mM^{-1}\ cm^{-1}$) and Zn-3-Formyl-Pyro-methyl-pheophorbide *a* (Zn-3-Formyl-Pyro-Me-Pheid *a*; $\varepsilon^* = 65.2\ mM^{-1}\ cm^{-1}$). Extinction coefficients of the substrate analogs are given in brackets, coefficients marked with an asterisk were estimated according to Klement *et al.* (1999). Detection of COR products was performed using UV/visible absorption spectroscopy (section 2.7.7). Obtained activities of the homologous COR systems were set to 100 % and all other values were related to this.

Based on the comparable values for the extinction coefficients of the substrate analogs, relative activities were estimated from the obtained absorption spectra.

2.8.2.4 COR Substrate Competition Assay

All substrate analogs showing no activity in the COR activity assays were tested for their ability to inhibit COR catalysis. Therefore, the COR activity assay was performed in the presence of 10 µM Chlide, additionally Chlide derivatives found not to sustain COR activity were supplemented at concentrations ranging from 5 - 20 µM. Product formation was monitored by UV/visible absorption spectroscopy (section 2.7.7).

2.8.3 Chimeric Activity Assays

For the elucidation of the potential evolution of the electron-transferring subunits of DPOR, COR and nitrogenase, studies with chimeric enzymes were performed. Therefore, the DPOR subcomplexes $(BchNB)_2$ or $(ChlNB)_2$ from *C. tepidum*, *P. marinus* and *T. elongatus* were combined with protein subunit $BchX_2$ of the COR enzyme from *C. tepidum* and *R. denitrificans.* For this type of experiments the standard DPOR assay (section 2.8.1) contained concentrations of 10 - 300 pmol of the $BchX_2$ protein instead of protein $BchL_2$/$ChlL_2$. Control experiments were performed in the absence of subunit $BchX_2$ and in the absence of $(BchNB)_2$/$(ChlNB)_2$, respectively.

Likewise, the purified nitrogenase subunit $NifH_2$ (Hu *et al.*, 2006, Bursey *et al.*, 1998) which was a kindly gift of Prof. Dr. Ribbe (University of California, Irvine, CA) was used for chimeric experiments with the corresponding DPOR subcomplexes $(BchNB)_2$/$(ChlNB)_2$ from *C. tepidum*, *P. marinus* and *T. elongatus*. For chimeric enzyme activities the modified standard DPOR assay containing 100 pmol $(BchNB)_2$/$(ChlNB)_2$ from *C. tepidum*, *P. marinus* or *T. elongatus,* respectively, was supplemented with purified $NifH_2$ at concentrations ranging from 100 - 2000 pmol in a total volume of 125 µl.

Activity of the chimeric enzymes was monitored by UV/visible absorption spectroscopy (section 2.7.7).

2.8.4 Activity Assays for the Oxygen-Dependent Cyclase (AcsF)

In order to analyze the activity of oxygen-dependent cyclase, an modified enzymatic assay according to Rzeznicka *et al*. (2005) was used. For this assay, 50 µg - 1 mg of a cellular extract of *T. elongatus* wildtype was incubated in assay buffer A supplemented with the substrate MME (15 µM), 5 mM NADPH and 14 µM $MgCl_2$. Assays were performed in a total reaction volume of 100 µl and incubated for 1 h at 35 °C - 55 °C under continuous agitation (300 rpm) in the dark. In control reactions the proposed cofactor NADPH, the substrate MME or the *T. elongatus* cellular extract was omitted. In an alternative control reaction *T. elongatus* cellular extract was incubated for 10 min at 95 °C. Reactions were stopped by mixing 80 µl of the sample with 750 µl acetone, 170 µl NH_4OH (0.12 M) and 300 µl hexane. After centrifugation (3 min, 10'000 x g), the lower phase was analyzed by fluorescence spectroscopy.

assay buffer A	HEPES/NaOH, pH 7.8	10 mM
	TES	20 mM
	$MgCl_2$	11 mM

An alternative cyclase assay according to Bollivar & Beale (1996) was performed in a reaction volume of 1 ml in assay buffer B. Assays containing 0.1 - 1 mg "low speed supernatant" which was obtained by centrifugation at 16'000 x g for 15 min, 15 µM MME and 5 mM NADPH were incubated for 1 h at 30 °C - 55 °C at 300 rpm in the dark. Reactions were stopped by addition of 3 ml chilled acetone. After centrifugation (45 sec, 15'000 x g), the supernatant was retained and the sediment was resuspended in 250 µl of 120 mM NH_4OH and then 1.5 ml of acetone was added with mixing. The suspension was centrifuged again, and the acetone supernatants were combined. The actone fraction was extracted twice with 5 and 2.5 ml of hexane, respectively. After adjusting the pH value of the sample to 6.8 using 120 mM maleic acid (pH 5.0), 1.7 ml saturated aequeous NaCl solution was added. This fraction was extracted with 3 ml of diethyl ether and analyzed by fluorescence spectroscopy.

Moreover, assay components were modified by using an NADPH-regenerating system consisting of 3 U of Glucose-6-P dehydrogenase and glucose-6-P and an ATP-regenerating system consisting of 20 mM creatine phosphate and 10 U of creatine phosphokinase. Additionally, assays containing magnesium protoporphyrin IX and the Magnesium

Protoporphyrin IX methyltransferase were performed for *in vitro* production of the cyclase substrate instead of the commercial available MME (Frontier Scientific).

assay buffer B	HEPES/NaOH, pH 7.7	50 mM
	TES	100 mM
	$MgCl_2$	10 mM
	DTT	5 mM

For analysis of reaction products by fluorescence spectroscopy, an emission scan from wavelength 500 - 700 nm with a scan speed of 200 nm/min using a LS50 B luminescence spectrometer (Perkin Elmer) was performed. Thereby, for the detection of the substrate, MME, an excitation wavelength of 420 nm was used whereas for the cyclase product, Pchlide, an excitation wavelength of 440 nm was chosen.

3 RESULTS AND DISCUSSION

In this thesis several enzymes of the (bacterio)chlorophyll pathway were characterized. First, the enzymes responsible for the D and B ring reduction of (bacterio)chlorophylls, DPOR and COR were investigated. Afterwards, analyses of chimeric enzymes consisting of DPOR, COR and nitrogenase were performed. Finally, the reaction of the oxygen-dependent cyclase important for the formation of the isocyclic ring of (bacterio)chlorophylls was studied.

3.1 The Dark-Operative Protochlorophyllide Oxidoreductase (DPOR)

3.1.1 Cloning, Production and Purification of DPOR from Different Organisms

An important regulatory step in (bacterio)chlorophyll biosynthesis is the reduction of ring D by the protochlorophyllide oxidoreductase. The nitrogenase-like multi-subunit enzyme DPOR catalyzes this reaction independent of light enabling the host organisms to green in the dark. Besides a detailed biochemical characterization of DPOR from different organisms, the elucidation of the transient interaction of the individual subunits of DPOR during catalysis was a central aim of this thesis.

For this purpose, the corresponding genes *bchN*, *bchB* and *bchL* from the green sulfur bacterium *C. tepidum* (Bröcker *et al.*, 2008a) and *chlN*, *chlB* and *chlL* from the prochlorophyte *P. marinus* and the cyanobacterium *T. elongatus* were cloned into standard *E. coli* expression vectors (pGEX-6P-1). The resulting constructs pGEX-CtNBL, pGEX-CtL, pGEX-PmNB, pGEX-PmL, pGEX-TeNB and pGEX-TeL, respectively, allow for the anaerobic purification of subunits BchN/ChlN and BchL/ChlL *via* a glutathione-S-transferase (GST) tag in an anaerobic chamber. Production of the corresponding proteins was performed in *E. coli* BL21 Codon Plus^{TM} (DE3)-RIL cells under aerobic conditions. The expression of the DPOR genes by addition of 50 µM IPTG resulted in production of significant amounts of the individual proteins from all three organisms. Due to the tight interaction of BchB/ChlB with GST-BchN/ChlN, subunit BchB/ChlB is co-purified during affinity chromatography. Such complex formation has been already described for the

DPOR enzyme from *R. capsulatus* (Fujita *et al.*, 2000), and analogously for the related nitrogenase subunits (May *et al.*, 1991).

The purification of the DPOR enzymes *via* affinity chromatography with a glutathione sepharose matrix was performed according to manufacturer's instructions. Proteins were eluted with buffer containing 15 mM glutathione. The purification of the proteins from *C. tepidum*, *P. marinus* and *T. elongatus* is summarized in Figure 12.

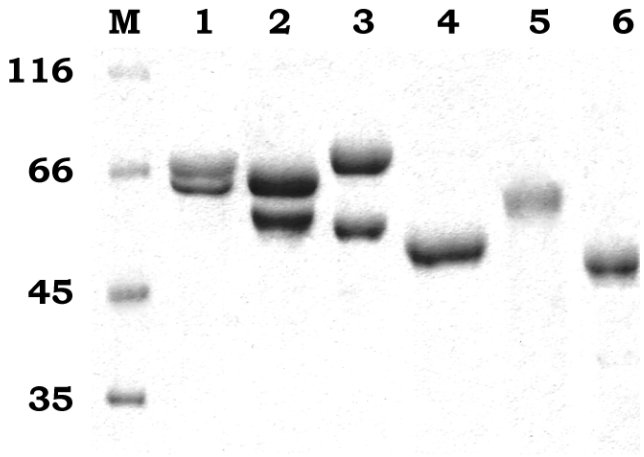

Fig. 12: SDS-PAGE analysis of purified recombinant DPOR subunits BchN/ChlN or BchB/ChlB and BchL/ChlL.
Proteins were produced recombinantly in *E. coli*, chromatographically purified, separated through 12 % SDS-PAGE, and visualized *via* Coomassie Brilliant Blue staining. *Lane M*, molecular mass marker; relative molecular masses (x 1000) are indicated. *Lane 1*, purified *C. tepidum* GST-BchN complexed with subunit BchB; *lane 2*, purified *P. marinus* GST-ChlN complexed with subunit ChlB; *lane 3*, purified *T. elongatus* GST-ChlN complexed with subunit ChlB; *lane 4*, purified *C. tepidum* GST-BchL protein; *lane 5*, purified *P. marinus* GST-ChlL protein; *lane 6*, purified *T. elongatus* GST-ChlL protein.

Affinity chromatography *via* glutathione sepharose resulted in apparently pure DPOR subunits for all of the organisms employed. Thereby, the observed relative molecular masses are in good agreement with the calculated molecular masses for the protein subunits BchN/ChlN and BchB/ChlB from *C. tepidum* (*lane 1*) (GST-BchN = 73.5 kDa, BchB = 58.9 kDa), *P. marinus* (*lane 2*) (GST-ChlN = 73 kDa, ChlB = 58.7 kDa), and from *T. elongatus* (*lane 3*) (GST-ChlN = 78.4 kDa, ChlB = 56.3 kDa). Purified GST-BchL or GST-ChlL proteins from *C. tepidum* (GST-BchL = 56.3 kDa), *P. marinus* (GST-ChlL = 59.2 kDa), and *T. elongatus* (GST-ChlL = 58 kDa) are presented in Figure 12, *lanes 4 - 6*. The integrity of all proteins was verified by N-terminal sequencing and mass spectrometry (data not shown). Thereby, subunit BchN/ChlN and BchB/ChlB were identified to be present in equimolar amounts.

3.1.2 Biochemical Characterization of DPOR from Different Organisms

The DPOR enzyme from *C. tepidum* has already been characterized in our laboratory (Bröcker *et al.*, 2008a). In the following, the biochemical features of the enzymes from the prochlorophyte *P. marinus* and the cyanobacterium *T. elongatus* were investigated.

3.1.2.1 Analytical Gel Permeation Chromatography of DPOR Subunits

To determine the oligomeric state of subunits ChlN/ChlB and ChlL from *P. marinus* and *T. elongatus*, an analytical gel permeation chromatography of the proteins under strict anaerobic conditions was performed. For this purpose, a calibration curve with marker proteins of known molecular masses was determined. The following elution diagrams (Fig. 13) were obtained for the protein subunits ChlN/ChlB from *P. marinus* (*A*) and *T. elongatus* (*B*) and ChlL from *P. marinus* (*C*):

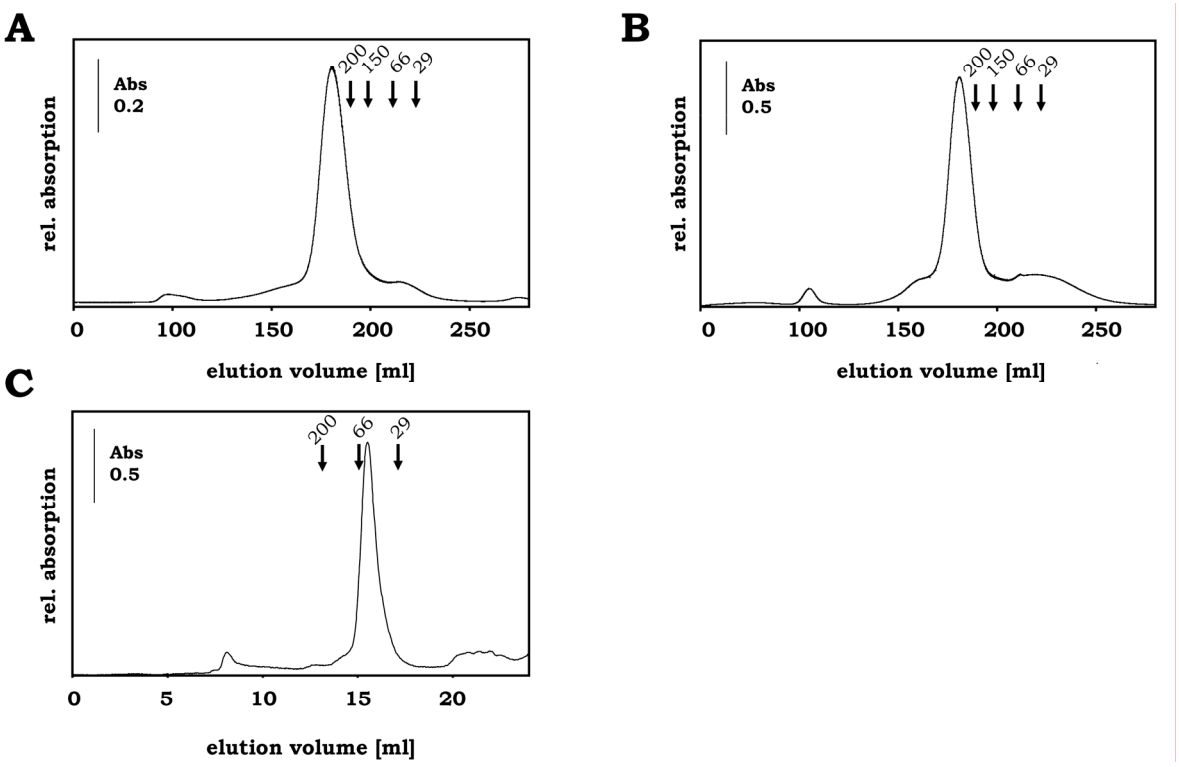

Fig. 13: Analytical gel permeation chromatography (GPC) analysis of purified ChlN/ChlB proteins from *P. marinus* (A) and *T. elongatus* (B) as well as ChlL protein from *P. marinus* (C).
Purified proteins at a concentration of ~ 5 mg/ml were loaded onto a Superdex 200 HR 26/60 (ChlN/ChlB proteins) or Superdex 200 HR 10/30 column (ChlL protein) (GE Healthcare) and eluted with 100 mM HEPES pH 7.5, 150 mM NaCl and 10 mM $MgCl_2$ at a flow rate of 1 ml/min. GPC was performed under strict anaerobic conditions by monitoring the absorbance at 280 nm. *A*, co-purified ChlN/ChlB complex after protease cleavage from *P. marinus* (20 mg); *B*, co-purified ChlN/ChlB complex after protease cleavage from *T. elongatus* (25 mg); *C*, purified $ChlL_2$ protein after protease cleavage from *P. marinus* (10 mg).

The analytical gel permeation chromatography after protease cleavage revealed a relative molecular mass of 210'000 for ChlN/ChlB from *P. marinus* (ChlN = 46'199 Da, ChlB = 58'729 Da) and *T. elongatus* (ChlN = 51'508 Da, ChlB = 56'317 Da) indicating a heterotetrameric composition for subunits ChlN and ChlB. These findings are consistent with the oligomeric states observed for the enzyme from *C. tepidum* and the homologous nitrogenase subunits NifD and NifK (Bröcker *et al*., 2008a, Tezcan *et al.*, 2005). Therefore, the complex was denoted as $(BchNB)_2$ for *C. tepidum* and $(ChlNB)_2$ for *P. marinus* and *T. elongatus*.

Analysis of the ChlL protein from *P. marinus* (Fig. 13, *C*) showed a relative molecular mass of 60'000 (ChlL = 33'493 Da) suggesting a homodimeric composition of this subunit which has also been shown for previously characterized DPOR enzymes (Bröcker *et al.*, 2008a, Fujita *et al.*, 2000) and the homologous nitrogenase system (Tezcan *et al.*, 2005). Therefore, the subunit BchL or ChlL was referred to as $BchL_2$ and $ChlL_2$, respectively. Due to very low protein yields, the determination of the native molecular mass of the ChlL protein from *T. elongatus* by gel permeation chromatography was not successful.

3.1.2.2 Analysis of Potential [Fe-S] Clusters in Subunits of DPOR

Elution fractions of co-purified $(ChlNB)_2$ proteins as well as $ChlL_2$ proteins were brownish in color indicative for the presence of a [Fe-S] cluster. To identify a potential [Fe-S] cluster, the purified protein fractions were subsequently analyzed by UV/Vis spectroscopy. The UV/visible absorption spectrum (Fig. 14) revealed an absorption maximum at a wavelength of 425 nm for the co-purified $(ChlNB)_2$ fractions from *P. marinus* and *T. elongatus* as well as for the $ChlL_2$ protein from *P. marinus* which is characteristic for [4Fe-4S] clusters.

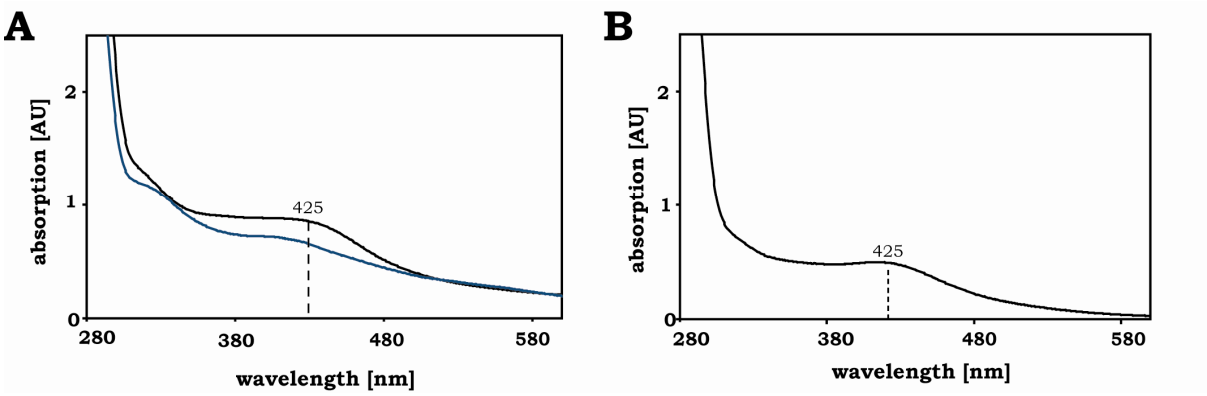

Fig. 14: UV/visible absorption spectra of purified $(ChlNB)_2$ complex and $ChlL_2$ from *P. marinus* (A) and purified $(ChlNB)_2$ complex from *T. elongatus* (B).
The spectra were recorded under anaerobic conditions and show an absorption maximum at 425 nm. *A*, absorption spectra of co-purified $(ChlNB)_2$ complex (*black* line, 50 µM) and $ChlL_2$ protein (*blue* line, 100 µM) from *P. marinus*; *B*, absorption spectra of co-purified $(ChlNB)_2$ complex (20 µM) from *T. elongatus*.

Amino acid sequence analysis of various DPOR enzymes revealed three highly conserved cysteine residues in subunits BchN/ChlN and one in subunit BchB/ChlB. For the corresponding subunits of the DPOR enzyme from *C. tepidum* three essential cysteine residues (Cys^{21}, Cys^{46}, and Cys^{103}) of the BchN subunit and Cys^{94} of subunit BchB were identified and proposed as ligands for a [4Fe-4S] cluster (Bröcker *et al.*, 2008a) which has also been characterized by EPR analysis (Bröcker *et al.*, 2008b, Nomata *et al.*, 2008). The obtained UV/visible absorption spectra of the $(ChlNB)_2$ complex from *P. marinus* and *T. elongatus* were in good agreement with the presence of a [4Fe-4S] cluster in these DPOR proteins. The determination of the iron and sulfur contents of the purified protein fractions yielded 7.7 mol of iron and 6.9 mol of sulfur per mol $(ChlNB)_2$ complex from *P. marinus* and 7.6 mol of iron per mol $(ChlNB)_2$ complex from *T. elongatus*. These values provide further evidence for the presence of two [4Fe-4S] clusters located on the $(ChlNB)_2$ tetramer.

Similarly, the $ChlL_2$ protein from *P. marinus* shows a peak at 425 nm typical for [4Fe-4S] clusters (Fig. 14, *A*). The $ChlL_2$ protein from *P. marinus* contained 3.6 mol of iron and 3.4 mol of sulfur per mol $ChlL_2$ suggesting one [4Fe-4S] cluster per dimer. However, the amounts of purified $ChlL_2$ protein from *T. elongatus* were to low for the reliable determination of iron and sulfur contents. Subunit $ChlL_2$ contains two highly conserved cysteine residues (Cys^{97} and Cys^{131}, *C. tepidum* numbering). For the $BchL_2$ protein from *R. capsulatus* it was already shown by EPR analysis that this subunit coordinates an intersubunit [4Fe-4S] cluster (Nomata *et al.*, 2006a).

Based on the characteristics of the absorption spectroscopy and the iron and sulfur content of the investigated enzymes, the same [Fe-S] cluster composition for the subunits from *P. marinus* and *T. elongatus* as described for previously characterized DPOR enzymes is assumed.

Altogether, the DPOR protein subunits from *P. marinus* and *T. elongatus* did not show any differences with respect to the oligomeric structure and [Fe-S] cluster composition when compared with the previously characterized enzymes from *C. tepidum* (Bröcker *et al.*, 2008a) and *R. capsulatus* (Fujita *et al.*, 2000), respectively.

3.1.3 Activity of Homologous DPOR Enzymes

The recombinantly produced DPOR subunits were tested for DPOR activity. For this purpose, the purified $(BchNB)_2$/$(ChlNB)_2$ complexes were combined with *E. coli* cell-free extract containing overproduced $BchL_2$/$ChlL_2$ protein. To determine specific activities of homologous DPOR enzymes from *C. tepidum*, *P. marinus* and *T. elongatus*, the assays were performed under identical conditions at pH 7.5 in the presence of 2 mM of ATP, an ATP-regenerating system, 10 mM of dithionite, 10 mM of $MgCl_2$ and 150 mM of NaCl at a temperature of 35 °C. An assay temperature of 35 °C was mandatory because the activity of the DPOR enzyme from *T. elongatus* decreased significantly when temperatures below 32 °C were used (data not shown). Furthermore, all procedures for the enzyme assays were performed under strictly anaerobic conditions. DPOR activity was detected by UV/visible absorption spectroscopy where the product Chlide has an absorption maximum at a wavelength of 665 nm whereas the substrate Pchlide shows a peak at 626 nm. In Figure 15, the obtained UV/visible absorption spectra for the DPOR systems from *C. tepidum* (*A*), *P. marinus* (*B*) and *T. elongatus* (*C*) are shown.

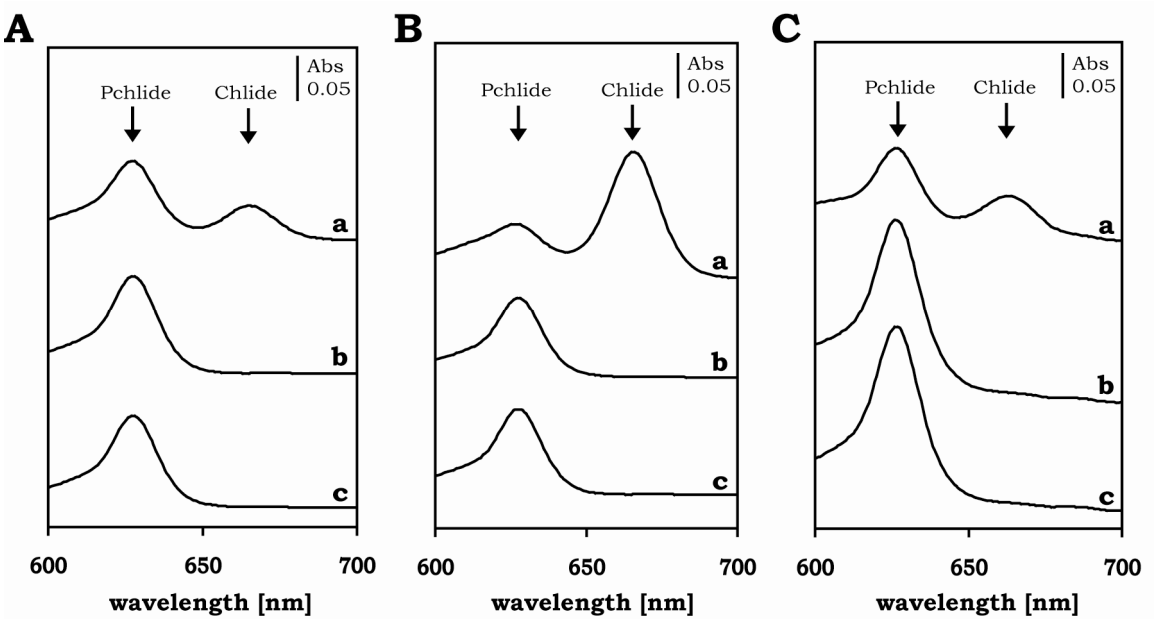

Fig. 15: UV/visible absorption spectra of the standard DPOR activity assay of homologous DPOR enzymes from *C. tepidum* (A), *P. marinus* (B) and *T. elongatus* (C).
Assays were performed as described in "Materials and Methods". After incubation of the assay for 1 h at 35 °C, pigments were extracted with acetone. Absorption maxima of the DPOR substrate Pchlide and the product Chlide are indicated by *arrows*. *A*, Activity of DPOR from *C. tepidum*. *Trace a*, DPOR assay containing 100 pmol of purified *C. tepidum* $(BchNB)_2$ and 200 pmol of *C. tepidum* $BchL_2$ protein; *traces b* and *c,* negative control without $(BchNB)_2$ (*b*) and without $BchL_2$ protein (*c*). *B*, Activity of DPOR from *P. marinus*. *Trace a*, DPOR assay containing 100 pmol of purified *P. marinus* $(ChlNB)_2$ and 150 pmol of *P. marinus* $ChlL_2$ protein; *traces b* and *c,* negative control without $(ChlNB)_2$ (*b*) and without $ChlL_2$ protein (*c*). *C*, Activity of DPOR from *T. elongatus*. *Trace a*, DPOR assay containing 100 pmol of purified *T. elongatus* $(ChlNB)_2$ and 200 pmol of *T. elongatus* $ChlL_2$ protein; *traces b* and *c,* negative control without $(ChlNB)_2$ (*b*) and without $ChlL_2$ protein (*c*).

DPOR activity was clearly detected for all three homologous DPOR systems (Fig. 15). Control experiments without $(BchNB)_2/(ChlNB)_2$ (*traces b*) or without $BchL_2/ChlL_2$ protein (*traces c*) show only the substrate Pchlide with an absorption maximum at 626 nm. Similarly, without the addition of ATP, no product formation was detectable (data not shown). However, incubation of $(BchNB)_2/(ChlNB)_2$ complex with $BchL_2/ChlL_2$ *(traces a*) resulted in the formation of Chlide with an absorption maximum at 665 nm.

Under the conditions employed, a specific DPOR activity of 163 pmol min^{-1} mg^{-1}, 847 pmol min^{-1} mg^{-1}, and 107 pmol min^{-1} mg^{-1} was obtained for the enzymes from *C. tepidum*, *P. marinus*, and *T. elongatus*, respectively.

Obviously, despite the significantly differing optimal growth temperatures for *C. tepidum* (48 °C), *P. marinus* (24 °C), and *T. elongatus* (55 °C) (Wahlund *et al.*, 1993, Nakamura *et al.*, 2002, Moore *et al.*, 1995), the employed DPOR standard assay ensures enzymatic activity for all three tested DPOR systems. Consequently, these standardized conditions enabled the following analysis of heterologous DPOR enzymes.

3.1.4 Activity of Heterologous DPOR Enzymes

In order to investigate the docking surface responsible for the transient interaction of subunits $(BchNB)_2$/$(ChlNB)_2$ and $BchL_2$/$ChlL_2$, an overall of six heterologous DPOR enzymes consisting of individual subunits from *C. tepidum*, *P. marinus* and *T. elongatus* were reconstituted using the conditions of the standard DPOR assay. Therefore, the relative activities of the homologous enzyme complexes were set to 100 % and all other values were related to that value. The ratio of $BchL_2$/$ChlL_2$ and $(BchNB)_2$/$(ChlNB)_2$ was optimized by altering the amount of $BchL_2$/$ChlL_2$ from 0.05 to 200 pmol using a constant amount of 100 pmol of $(BchNB)_2$/$(ChlNB)_2$. Figure 16 shows exemplarily an UV/visible absorption spectrum for a heterologous DPOR system consisting of *T. elongatus* $(ChlNB)_2$ in combination with *P. marinus* $ChlL_2$.

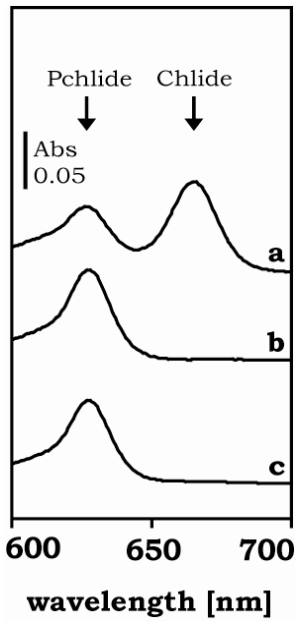

Fig. 16: UV/visible absorption spectra of a heterologous DPOR enzyme of *T. elongatus* $(ChlNB)_2$ in combination with *P. marinus* $ChlL_2$.
Assays were performed as described in "Materials and Methods". After incubation of the assay for 1 h at 35 °C, pigments were extracted with acetone. Absorption maxima of the DPOR substrate Pchlide and the product Chlide are indicated by *arrows*. *Trace a*, DPOR assay containing 100 pmol of purified *T. elongatus* $(ChlNB)_2$ and 50 pmol of *P. marinus* $ChlL_2$ protein; *traces b* and *c,* negative control without $(ChlNB)_2$ (*b*) and without $ChlL_2$ protein (*c*).

After incubation of both subunits, product formation for the heterologous DPOR system was clearly detectable (Fig. 16, *trace a*), whereas in assays without the addition of $(ChlNB)_2$ (*trace b*) or $ChlL_2$ (*trace c*) no Chlide formation was observed.

For five of six possible enzyme combinations, DPOR activity for the heterologous systems was observed. Table 4 summarizes the activities of the various chimeric enzymes.

Tab. 4: Enzymatic activities of heterologous DPOR systems.
Standard DPOR assays were performed for 1 h at 35 °C as described in "Materials and Methods". The relative enzymatic activity of the corresponding wildtype DPOR was set to 100 %, and all other values were related to this value.

	***C. tepidum* $BchL_2$**	***T. elongatus* $ChlL_2$**	***P. marinus* $ChlL_2$**
C. tepidum **$(BchNB)_2$**	100 %	30 %	100 %
T. elongatus **$(ChlNB)_2$**	50 %	100 %	100 %
P. marinus **$(ChlNB)_2$**	3 %	< 1 %	100 %

When $BchL_2$ from *C. tepidum* was combined with *P. marinus* $(ChlNB)_2$ and *T. elongatus* $(ChlNB)_2$ relative DPOR activities of 3 % and 50 %, respectively, were obtained. The chimeric DPOR system composed of two subunits from thermophilic organisms, *C. tepidum* $BchL_2$ and *T. elongatus* $(ChlNB)_2$, shows high activity. In contrast, chimeric activity of $BchL_2$ from the moderate thermophilic *C. tepidum* with $(ChlNB)_2$ from the mesophilic *P. marinus* was low (3 %) as one might expect due to the varying temperature optima. *T. elongatus* $ChlL_2$ in combination with *C. tepidum* $(BchNB)_2$ resulted in a significant DPOR activity of 30 %. Only the enzymatic activity for *T. elongatus* $ChlL_2$ in combination with *P. marinus* $(ChlNB)_2$ was below the detection limit of the employed assay (< 1 %). Again, the mentioned differing temperature optima of the organisms might be responsible for the absent activity. However, the combination of *P. marinus* $ChlL_2$ with $(BchNB)_2$ from *C. tepidum* or $(ChlNB)_2$ from *T. elongatus* even resulted in activity comparable to the wildtype DPOR from *P. marinus*. Obviously, $ChlL_2$ from *P. marinus* can perfectly substitute the $BchL_2$/$ChlL_2$ subunits from *C. tepidum* and *T. elongatus*.

Comparable results have also been described for nitrogenase components from different organisms. In *in vitro* assays significant activity for chimeric nitrogenase enzymes was obtained (Emerich *et al.*, 1978, Biggins *et al.*, 1971, Smith *et al.*, 1976, Kelly, 1969, Murphy *et al.*, 1971, Smith *et al.*, 1971, Eady *et al.*, 1974, Burris, 1971).

From the observed activities for the various chimeric DPOR enzymes, it was concluded that the docking face responsible for protein-protein-interaction and the subsequent electron transfer has been highly conserved during the evolution of the DPOR enzymes.

3.1.5 Label Transfer Experiments

To elucidate the protein-protein-interaction of $ChlL_2$ with $(ChlNB)_2$ from *P. marinus* in further detail, label transfer experiments were performed under anaerobic conditions. For this purpose, the trifunctional crosslinker Mts-Atf-LC-biotin (Pierce) was coupled chemically to the individual DPOR subunits from *P. marinus*. In addition to a biotin moiety, this reagent contains a sulfhydryl-specific methane thiosulfonate (Mts) group, which can form disulfide bonds with free sulfhydryl groups of the bait protein. Moreover, the crosslinker harbors a photoreactive tetrafluorophenyl azide (Atf) moiety which inserts into carbon hydrogen bonds and unsaturated carbon chains of the prey protein within a distance of 21.8 Å.

First, the reagent was linked to purified $ChlL_2$ protein from *P. marinus via* disulfide bonds (Fig. 17, *lane 1*). The labeled $ChlL_2$ protein was then incubated with the $(ChlNB)_2$ complex, and crosslinking of both protein subcomplexes was initiated by UV radiation. Afterwards, the covalent crosslinking was opened *via* reduction by the addition of DTT resulting in the transfer of the attached biotin label onto components of the $(ChlNB)_2$ complex. The transfer of the biotin label was visualized by Western Blot analysis using a horseradish peroxidase NeutrAvidin conjugate (Fig. 17).

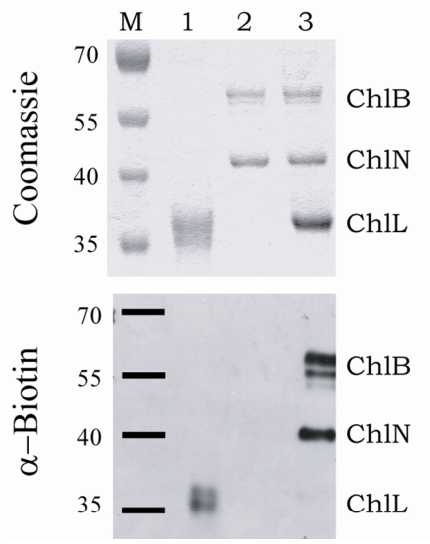

Fig. 17: Label transfer experiments with *P. marinus* DPOR.
Label transfer from subunit $ChlL_2$ from *P. marinus* to the corresponding $(ChlNB)_2$ complex from *P. marinus*. $ChlL_2$ was labeled as described in "Materials and Methods" and incubated with 25 µM $(ChlNB)_2$ followed by exposure to UV light to initiate crosslinking. Subsequent reduction resulted in the transfer of the biotin label onto subunits ChlN and ChlB. *Top panel*, SDS-PAGE after crosslinking and label transfer stained with Coomassie Brilliant Blue. *Bottom panel*, immunoblot of identical samples treated with a NeutrAvidin antibody conjugated with horseradish peroxidase. *Lane M*, molecular mass marker; relative molecular masses (x 1000) are indicated. *Lane 1*, $ChlL_2$ after labeling; *lane 2*, $(ChlNB)_2$ without the addition of labeled $ChlL_2$ protein; *lane 3*, label transfer onto $(ChlNB)_2$ after incubation of $(ChlNB)_2$ complex with labeled $ChlL_2$ protein.

As shown in Figure 17 (*lane 3*), efficient label transfer to the ChlN as well as to the ChlB subunit was obtained. Consequently, upon $ChlL_2$/$(ChlNB)_2$ interaction ChlN and ChlB, proteins are located in the operating range (21.8 Å) of the label transfer reagent localized on the ChlL subunit. From these results, an involvement of both subunits, ChlN and ChlB in the protein-protein-interaction with subunit $ChlL_2$ was concluded. However, all attempts to determine the amino acid position carrying the transferred biotin label by tandem mass spectrometry were not successful. Therefore, a mutagenesis strategy was employed to further characterize the protein-protein-interaction of DPOR.

3.1.6 Mutagenesis of DPOR Subunits from *P. marinus*

Due to the observed activity of heterologous DPOR enzymes, a high degree of sequence conservation for the docking surface was suggested. Furthermore, the results of the label transfer experiments indicated an involvement of both subunits, ChlN and ChlB, in the protein-protein-interaction with the $ChlL_2$ protein. Therefore, amino acid sequences of all three subunits were analyzed for highly conserved regions potentially located on the protein surface. The amino acids responsible for the dynamic interaction of the nitrogenase subunits (Fig. 18 - 20, highlighted in *gray*) have been studied in great detail based on the crystal structure of various ternary complexes of nitrogenase (Tezcan *et al.*, 2005, Schindelin *et al.*, 1997, Schmid *et al.*, 2002a, Roe *et al.*, 1997, Georgiadis *et al.*, 1992). Using a sequence alignment of the individual subunits of DPOR, nitrogenase and COR (Fig. 18 - 20), the related regions in the individual DPOR subunits were identified. For the individual species employed in the alignment, the presence (+) or absence (-) of DPOR, nitrogenase and COR is indicated. Analysis of the sequence alignments showed that the conserved amino acid regions essential for the protein-protein-interaction in nitrogenase were different, but also conserved in the individual DPOR subunits.
Based on these alignments, 10 amino acid residues of the individual subunits of *P. marinus* DPOR were exchanged, followed by a kinetic analysis of purified recombinant mutant DPOR proteins.

3.1.6.1 Mutant Proteins of DPOR Subunit ChlL

Recently the structure of the BchL protein of DPOR from *R. sphaeroides* was solved (Sarma *et al.*, 2008). In this study, amino acid sequence alignments in combination with structural comparisons revealed that only two residues involved in nitrogenase complex formation are also conserved in subunit BchL of DPOR. However, residues Tyr^{129}, Gln^{133}, Gln^{168}, and His^{169} of DPOR subunit BchL (*R. sphaeroides* numbering) have been found to substitute for residues Arg^{100}, Thr^{104}, Arg^{140}, and Glu^{141} (*A. vinelandii* numbering) at the docking face of NifH. Because of the different chemical properties of these amino acid residues, it was concluded that the docking faces of DPOR and nitrogenase differ significantly, mainly due to an altered charge distribution (Sarma *et al.*, 2008). To determine DPOR-specific amino acid residues involved in protein-protein-interaction, the conserved docking face of DPOR subunit $ChlL_2$ was analyzed for appropriate candidates. Based on the amino acid sequence alignment shown in Figure 18, and the structural analysis of the $BchL_2$ protein from *R. sphaeroides*, residue Tyr^{127} (representing Tyr^{129} in *R. sphaeroides*) was altered into a smaller residue carrying a net negative charge (Y127D) or into a distinctively smaller polar residue (Y127S).

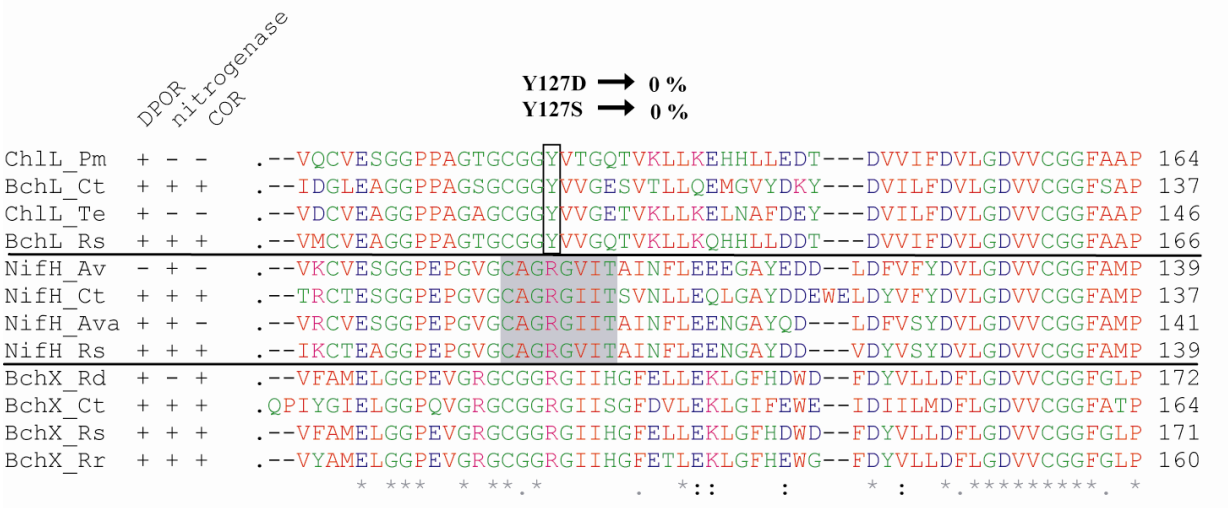

Fig. 18: Alignment of DPOR subunits BchL/ChlL with the corresponding subunits of nitrogenase and COR. DPOR activity of ChlL mutants are shown.
Amino acid sequence alignments of DPOR subunits from *P. marinus* (Pm), *C. tepidum* (Ct), *T. elongatus* (Te), and *R. sphaeroides* (Rs) with the corresponding nitrogenase subunits from *A. vinelandii* (Av), *C. tepidum*, *Anabaena variabilis* (Ava), and *R. sphaeroides* and with the corresponding COR subunits from *R. denitrificans* (Rd), *C. tepidum*, *R. sphaeroides*, and *Rhodospirillum rubrum* (Rr). A complete sequence alignment can be found in appendix A. For the individual species employed in the alignment, the presence (+) or absence (-) of DPOR, COR and nitrogenase is indicated. Sequence motifs responsible for the dynamic protein-protein-interaction of nitrogenase are highlighted in *gray*. Residues that are identical among the subunits of all three enzymes are indicated by an *asterisk*, conserved substitutions by a *colon*, and semiconserved substitutions by a *period*. The position of the DPOR amino acid mutagenized is marked by a *box*, and the activities of the respective mutant proteins are indicated.

Residue Tyr^{127} is found conserved in all BchL and ChlL proteins, whereas in the homologous nitrogenase system as well as in the COR enzymes an arginine at the identical position was observed. Neither of the mutant ChlL proteins, Y127D and Y127S, sustained detectable DPOR activity. From these data, in combination with the previously described three-dimensional structure of the $BchL_2$ protein from *R. sphaeroides*, it was concluded that Tyr^{127} is essential for DPOR catalysis. This surface-exposed residue might be directly involved in protein-protein-interaction and/or may be responsible for the intersubunit electron transfer.

3.1.6.2 Mutant Proteins of DPOR Subunit ChlN

Highly conserved DPOR regions, presumably located on the protein surface of the ChlN and ChlB subunits, were predicted by amino acid sequence alignments and analysis of the surface probability in combination with secondary structure predictions (Rost *et al.*, 2004). These analyses were hampered because the orthologous nitrogenase subunits NifD and NifK share an overall sequence identity of only ~15 %.

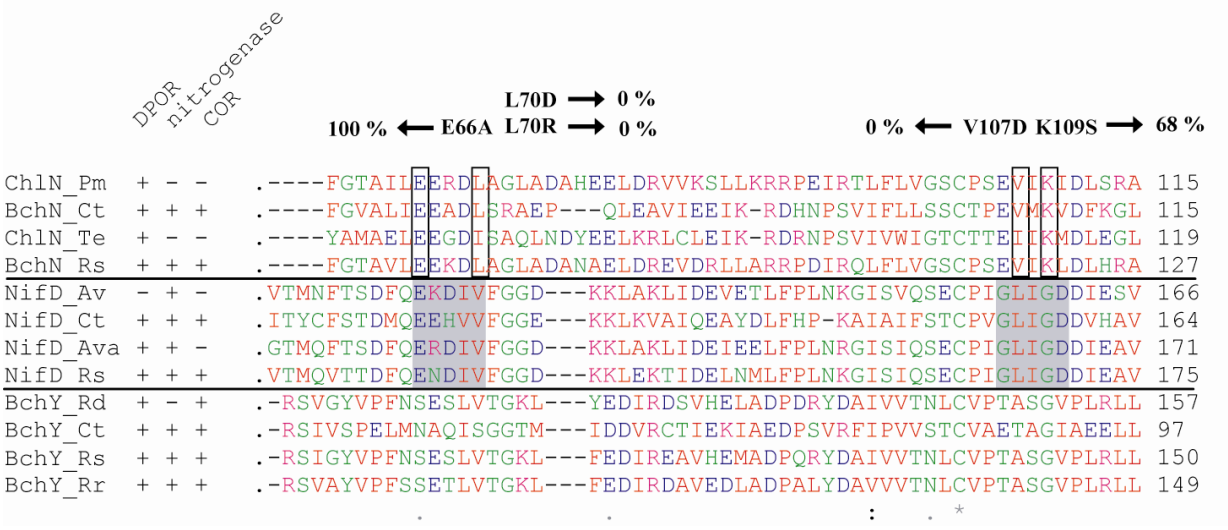

Fig. 19: Alignment of DPOR subunits BchN/ChlN with the corresponding subunits of nitrogenase and COR. DPOR activity of DPOR subunit ChlN mutants are shown.
Amino acid sequence alignments of DPOR subunits from *P. marinus* (Pm), *C. tepidum* (Ct), *T. elongatus* (Te), and *R. sphaeroides* (Rs) with the corresponding nitrogenase subunits from *A. vinelandii* (Av), *C. tepidum*, *Anabaena variabilis* (Ava), and *R. sphaeroides* and with the corresponding COR subunits from *R. denitrificans* (Rd), *C. tepidum*, *R. sphaeroides*, and *Rhodospirillum rubrum* (Rr). A complete sequence alignment can be found in appendix B. For the individual species employed in the alignment, the presence (+) or absence (-) of DPOR, COR and nitrogenase is indicated. Sequence motifs responsible for the dynamic protein-protein-interaction of nitrogenase are highlighted in *gray*. Residues that are identical among the subunits of all three enzymes are indicated by an *asterisk*, conserved substitutions by a *colon*, and semiconserved substitutions by a *period*. The positions of DPOR amino acids mutagenized are marked by *boxes*, and the activities of the respective mutant proteins are indicated.

Nevertheless, the amino acid sequence alignment in Figure 19 places the conserved surface exposed amino acid sequence EEXD(L/I)(A/S)X of DPOR subunit BchN (or ChlN) (residues 66 - 72 in *P. marinus*) alongside the sequence motif EX(D/H)(I/V)VFG (residues 120 - 124 in *A. vinelandii*) of nitrogenase. This motif of nitrogenase is known to be involved in $NifH_2$/$(NifDK)_2$ interaction (highlighted in *gray*). From this consideration, it was deduced that Glu^{66} as well as Leu^{70} might be involved in DPOR protein-protein-interaction. However, full DPOR activity was obtained for the mutant DPOR ChlN protein E66A from *P. marinus*. These data indicate that the highly conserved residue Glu^{66} is not essential for DPOR activity. In contrast, the DPOR subunit ChlN mutant L70D as well as mutant L70R failed to sustain detectable DPOR activity. Thus, mutation of Leu^{70} into the negatively charged residue Asp, as well as into the positively charged residue Arg, completely abolished DPOR activity.

A second conserved surface-exposed loop region of NifD, composed of GLIGDD (residues 157 - 162 in *A. vinelandii*), aligns with the conserved sequence motif E(V/I)(I/M)KXD of residues 106 - 111 in *P. marinus* DPOR subunit ChlN. DPOR mutant protein V107D did not show any detectable activity. Mutant K109S revealed a significantly decreased DPOR activity of 68 % when compared with the wildtype *P. marinus* enzyme. The results of these conservative alterations indicate that both residues are important for DPOR catalysis.

With respect to the postulated surface-exposed nature of the two identified loop regions, residues Leu^{70}, Val^{107}, and Lys^{109} are proposed to be located at the docking surface. This might also include a direct involvement in the electron transfer process.

3.1.6.3 Mutant Proteins of DPOR Subunit ChlB

Amino acid sequence alignments of DPOR subunit ChlB with the corresponding NifK protein revealed that the conserved loop regions at the nitrogenase docking surface do not have clearly defined counterparts in subunit BchB/ChlB of DPOR (Fig. 20).

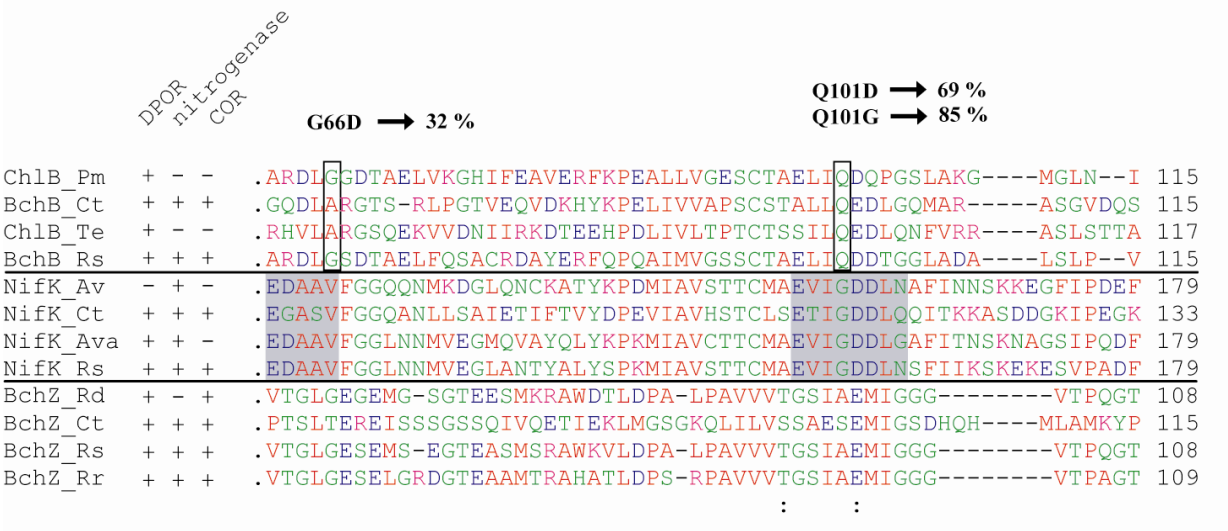

Fig. 20: Alignment of DPOR subunits BchB/ChlB with the corresponding subunits of nitrogenase and COR. DPOR activity of DPOR subunit ChlB mutants are shown.
Amino acid sequence alignments of DPOR subunits from *P. marinus* (Pm), *C. tepidum* (Ct), *T. elongatus* (Te), and *R. sphaeroides* (Rs) with the corresponding nitrogenase subunits from *A. vinelandii* (Av), *C. tepidum*, *Anabaena variabilis* (Ava), and *R. sphaeroides* and with the corresponding COR subunits from *R. denitrificans* (Rd), *C. tepidum*, *R. sphaeroides*, and *Rhodospirillum rubrum* (Rr). A complete sequence alignment can be found in appendix C. For the individual species employed in the alignment, the presence (+) or absence (-) of DPOR, COR and nitrogenase is indicated. Sequence motifs responsible for the dynamic protein-protein-interaction of nitrogenase are highlighted in *gray*. Residues that are identical among the subunits of all three enzymes are indicated by an *asterisk*, conserved substitutions by a *colon*, and semiconserved substitutions by a *period*. The positions of DPOR amino acids mutagenized are marked by *boxes*, and the activities of the respective mutant proteins are indicated.

However, the amino acid sequence L(G/A)XX(T/S) of *P. marinus* DPOR ChlB (residues 65 - 70) might be involved in the dynamic interaction of DPOR subunits. In this mutant enzyme study, the DPOR subunit ChlB variant G66D revealed an activity of only 32 % when compared to the wildtype enzyme. This result indicates that Gly^{66} is important for DPOR catalysis. As bioinformatic analyses indicate a high surface probability for Gly^{66}, it could be concluded that a steric effect, or alternatively an electrostatic repulsion of the interacting $ChlL_2$ subunit, is responsible for the observed reduction of DPOR activity. The results obtained are in agreement with a model in which Gly^{66} is part of the docking face of $(BchNB)_2/(ChlNB)_2$.

A second loop region, IQ(D/E)(Q/D) (residues 100 - 104), of subunit ChlB of *P. marinus* DPOR was aligned with a region of the corresponding nitrogenase NifK protein consisting of a highly conserved sequence signature, IGDDL (residues 160 - 164 in *A. vinelandii*). Because Gln^{101} was the only amino acid residue found to be conserved in all of the DPOR BchB/ChlB proteins analyzed, this residue was altered into a charged residue of a smaller size (Q101D). Moreover, Gln^{101} was changed into a Gly residue (Q101G). The DPOR ChlB mutant Q101D showed a reduced activity of 69 % compared to the wildtype enzyme.

For this mutation towards a smaller aspartate residue, a steric effect was excluded; however, repulsion of the carboxylate group might result in the observed reduced activity. The second mutation was of special interest, because Gln^{101} was found to align with the highly conserved Gly^{159} in the sequence of NifK from *A. vinelandii*. In ChlB mutant Q101G DPOR activity was partly restored as indicated by a relative activity of 85 % when compared with mutant Q101D. Mutant protein Q101G now shares the specific sequence signature IGD which is highly conserved among all nitrogenase sequences. This finding might reflect a common evolutionary origin of DPOR and nitrogenase enzymes because a glycine at position 101 is a good substitute for Gln^{101}. Based on these data, an involvement of residue Gln^{101} in DPOR protein-protein-interaction analogous to the nitrogenase system was concluded.

In summary, based on the results of the *P. marinus* mutant DPOR study, residues Leu^{70}, Val^{107}, and Lys^{109} of DPOR subunit ChlN, Gly^{66} and Gln^{101} of DPOR subunit ChlB and Tyr^{127} of DPOR subunit ChlL are postulated to be involved in the protein-protein-interaction of $ChlL_2$ with the $(ChlNB)_2$ complex. The aforementioned residues have a significantly different chemical character when compared with the related residues of nitrogenase.

These findings are in good agreement with the results of the recently published structure of the $BchL_2$ protein from *R. sphaeroides* (Sarma *et al.*, 2008) where a docking face with a distinctively varying distribution of charge was postulated.

3.2 The Chlorophyllide *a* Oxidoreductase (COR)

3.2.1 Cloning, Production and Purification of COR from Different Organisms

Another nitrogenase-like enzyme of the (bacterio)chlorophyll pathway, the chlorophyllide *a* oxidoreductase (COR), catalyzes the reduction of ring B which is unique to the synthesis of bacteriochlorophylls. Analogously to DPOR and nitrogenase, COR is a multi-subunit enzyme composed of three subunits, termed BchY, BchZ, and BchX. In this thesis, a detailed biochemical analysis of this enzyme was performed. Furthermore, studies with chimeric enzymes composed of nitrogenase, DPOR and COR were performed

(section 3.3). This might give indications for the potential evolution of nitrogenase-like enzymes and the electron-transferring subunit of these enzymes, respectively.

Therefore, the corresponding genes *bchY*, *bchZ,* and *bchX* genes from *C. tepidum* and *R. denitrificans* were cloned into a standard *E. coli* expression vector (pET32a). Analogously to the DPOR cloning strategy, the obtained constructs (pET-CtYZ, pET-RdYZ, pET-CtX and pET-RdX) allow for the anaerobic co-purification of subunits BchY and BchZ *via* a N-terminal thioredoxin/His/S-tag of BchY whereas subunit BchX was produced separately with a thioredoxin/His/S-tag. Expression of COR genes *bchY* and *bchZ* was induced in *E. coli* BL21 Codon Plus^{TM} (DE3)-RIL cells transformed with the corresponding plasmids under aerobic conditions by addition of 50 µM of IPTG. In contrast, the production of subunit BchX was performed in *E. coli* strain BL21 (λDE3) carrying the corresponding plasmids and harbouring an additional plasmid encoding the *isc*-operon. The *isc* operon encodes proteins responsible for the assembly of [Fe-S] clusters (Kriek *et al.*, 2003) and was used to ensure an optimal iron-sulfur cluster insertion in the potential [Fe-S] cluster containing BchX proteins. Gene expression of *bchX* was induced by addition of 300 µM of IPTG. Proteins were purified chromatographically under anaerobic conditions using nickel-chelating sepharose and an elution with buffer containing 250 mM of imidazole. The purification of the COR subunits from *C. tepidum* and *R. denitrificans* is shown in Figure 21.

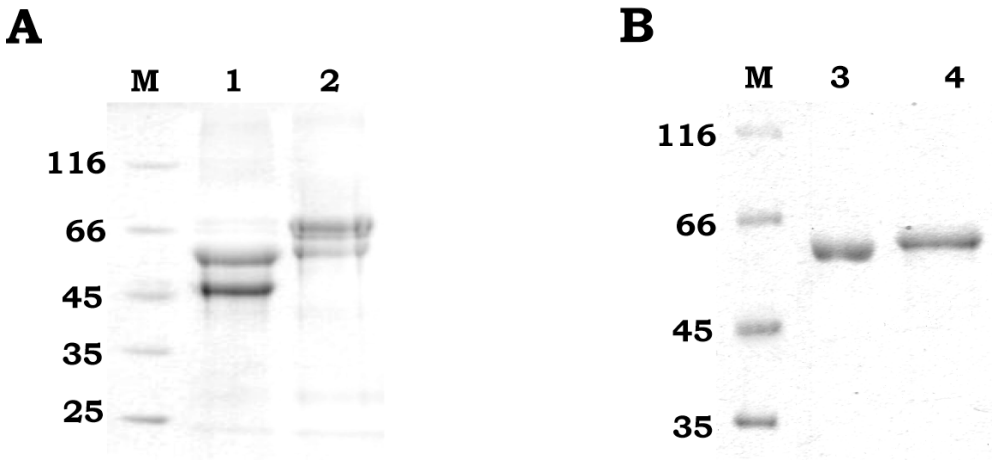

Fig. 21: SDS-PAGE analysis of purified COR subunits BchY, BchZ, and BchX from *C. tepidum* and *R. denitrificans*.
Proteins were produced recombinantly in *E. coli*, anaerobically purified by chromatography, separated through 12 % SDS-PAGE, and visualized *via* Coomassie Brilliant Blue staining. *Lane M*, molecular mass marker; relative molecular masses (x 1000) are indicated. *A*, purified subunits BchY and BchZ; *Lane 1*, purified *C. tepidum* Trx/His/S-BchY complexed with subunit BchZ; *lane 2*, purified *R. denitrificans* Trx/His/S-BchY complexed with subunit BchZ; *B*, purified BchX proteins; *lane 3*, purified *C. tepidum* Trx/His/S-BchX protein; *lane 4*, purified *R. denitrificans* Trx/His/S-BchX protein.

After affinity chromatography apparently pure COR subunits from *C. tepidum* and *R. denitrificans* were obtained. Obviously, subunit BchZ is co-purified with subunit BchY due to the tight interaction of both proteins which has been already observed for the related DPOR and nitrogenase subunits (Fujita *et al.*, 2000, May *et al.*, 1991). The relative molecular masses observed by SDS-PAGE analysis are in good agreement with the calculated molecular masses for the protein subunits BchY and BchZ from *C. tepidum* (*lane 1*) (Trx/His/S-BchY = 61 kDa, BchZ = 51.3 kDa) and from *R. denitrificans* (*lane 2*) (Trx/His/S-BchY = 71 kDa, BchZ = 53.2 kDa). Similarly, the corresponding bands for the BchX proteins from *C. tepidum* (*lane 3*) (Trx/His/S-BchX = 59.9 kDa) and *R. denitrificans* (*lane 4*) (Trx/His/S-BchX = 53.9 kDa) are consistent with the theoretical molecular masses of the proteins. The purified protein subunits of COR were subsequently analyzed for their biochemical properties.

3.2.2 Biochemical Characterization of COR from Different Organisms

3.2.2.1 Analytical Gel Permeation Chromatography of COR Subunits

For the determination of the native molecular mass, BchX as well as BchY/BchZ proteins from *C. tepidum* and *R. denitrificans* were liberated from the nickel-chelating column by thrombin cleavage and analyzed by gel permeation chromatography. The obtained elution profiles are shown in Figure 22.

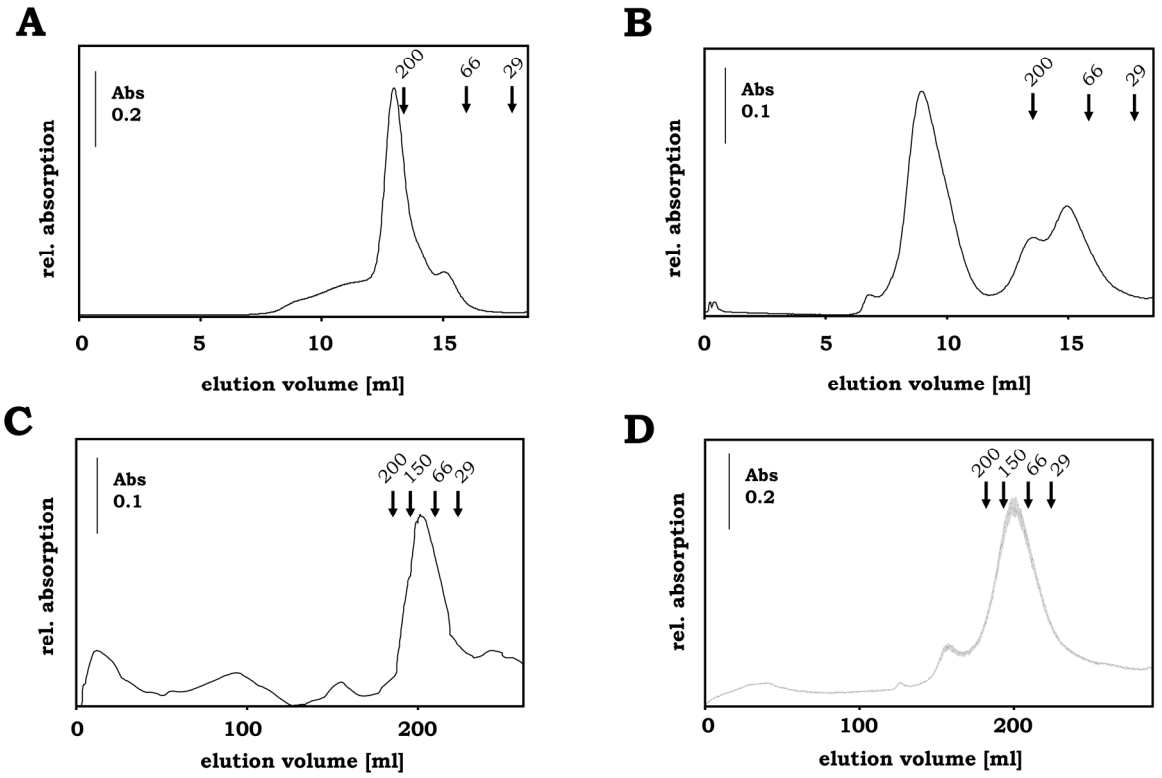

Fig. 22: Analytical gel permeation chromatography (GPC) analysis of co-purified BchY/BchZ proteins from *C. tepidum* (A) and *R. denitrificans* (B) as well as BchX proteins from *C. tepidum* (C) and *R. denitrificans* (D).
Purified proteins at a concentration of 1 - 5 mg/ml were loaded onto a Superdex 200 HR 10/30 (BchY/BchZ) or Superdex 200 HR 26/60 column (BchX) (GE Healthcare) and eluted with 100 mM HEPES pH 7.5, 150 mM NaCl and 10 mM $MgCl_2$ at a flow rate of 0.75 ml/min and 1 ml/min, respectively. GPC was performed under strict anaerobic conditions by monitoring the absorbance at 280 nm. *A*, Co-purified BchY/BchZ complex from *C. tepidum* after protease cleavage (5 mg); *B*, co-purified BchY/BchZ complex from *R. denitrificans* after protease cleavage (2 mg); *C*, purified BchX protein from *C. tepidum* after protease cleavage (10 mg); *D*, purified BchX protein from *R. denitrificans* after protease cleavage (10 mg).

The analytical gel permeation chromatography of the COR subunits BchY and BchZ (Fig. 22, *A* and *B*) revealed a relative molecular mass of 200'000 and 220'000, respectively for BchY/BchZ from *C. tepidum* (BchY = 47'300 Da, BchZ = 51'275 Da) and *R. denitrificans* (BchY = 56'900 Da, BchZ = 53'244 Da). These results in combination with the almost identical protein amounts obtained in SDS-PAGE analysis (Fig. 21) indicate a heterotetrameric complex architecture similar to the homologous DPOR subunits $(BchNB)_2$/$(ChlNB)_2$ as well as nitrogenase subunits NifD and NifK (Bröcker *et al.*, 2008b, Tezcan *et al.*, 2005). Therefore, the complex was denoted as $(BchYZ)_2$. The elution profile (Fig. 22, *B*) of the BchY/BchZ protein fraction from *R. denitrifcans* additionally shows a peak corresponding to dimeric subunit BchY. A slightly increased level for the overproduction of BchY when compared to the overproduction of BchZ results in the additional purification of $BchY_2$. A comparable co-purification of a homodimeric subunit has been observed for the related DPOR system from *P. marinus* (Bröcker *et al.*, 2008b).

Moreover, in the elution diagram of the BchY/BchZ protein from *R. denitrifcans* a significant absorption peak at ~ 9 ml elution volume was detected. SDS-PAGE analysis revealed the presence of proteins with native molecular masses > 100'000 which might indicate the presence of protein aggregates of BchY and BchZ in this elution fraction.
Analysis of the BchX protein (Fig. 22, *C* and *D*) showed a relative molecular mass of 95'000 and 85'000, respectively, for BchX from *C. tepidum* (BchX = 46'000 Da) and *R. denitrificans* (BchX = 39'800 Da) suggesting a homodimeric composition of this subunit. These findings are in good agreement with the subunit composition of the homologous DPOR and nitrogenase systems. Analogously to DPOR subunit $BchL_2$ (or $ChlL_2$) and nitrogenase $NifH_2$, the COR subunit BchX was denoted therefore as $BchX_2$.

3.2.2.2 Analysis of Potential [Fe-S] Clusters in the Different Subunits of COR

Concentrated elution fractions of co-purified $(BchYZ)_2$ and $BchX_2$ proteins were brownish in color suggesting the presence of a [Fe-S] cluster. Therefore, the purified proteins were analyzed by UV/visible absorption spectroscopy (Fig. 23).

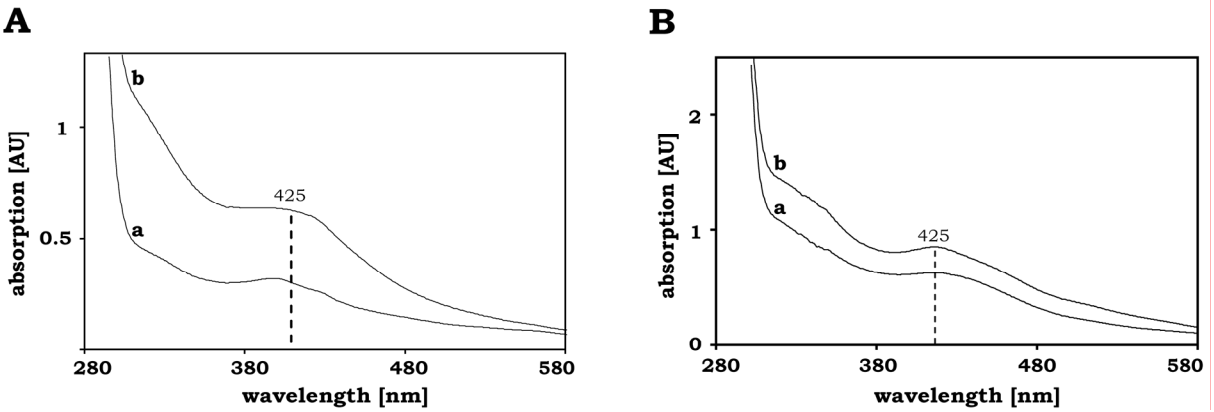

Fig. 23: UV/visible absorption spectra of purified BchY/BchZ proteins (A) and BchX proteins (B) from *C. tepidum* and *R. denitrificans*.
The UV/visible absorption spectra were recorded under anaerobic conditions with a protein concentration of 10 µM for $(BchYZ)_2$ and 150 µM for $BchX_2$ proteins and show an absorption maximum at 425 nm. *A*, absorption spectra of co-purified $(BchYZ)_2$ complex from *C. tepidum* (*trace a*) and *R. denitrificans* (*trace b*); *B*, absorption spectra of purified $BchX_2$ from *C. tepidum* (*trace a*) and *R. denitrificans* (*trace b*).

The UV/visible absorption spectra of COR subunits $(BchYZ)_2$ from *C. tepidum* and *R. denitrificans* (Fig. 23, *A*) show an absorption maximum at 425 nm characteristic for [4Fe-4S] clusters. Amino acid sequence alignments of subunits BchY and BchZ with the related subunits of DPOR revealed that all cysteinyl residues characterized as ligands for a catalytic [4Fe-4S] cluster in $(BchNB)_2$ and $(ChlNB)_2$ are also conserved in the corresponding COR subunits (compare appendices B and C). Therefore, it is assumed that

subunits $(BchYZ)_2$ form a [4Fe-4S] cluster as described for the DPOR subunits $(BchNB)_2$ and $(ChlNB)_2$.

Also for subunit $BchX_2$ (Fig. 23, *B*) from *C. tepidum* (*trace a*) as well as from *R. denitrificans* (*trace b*) an absorption maximum at 425 nm was observed. The determination of the iron content yielded 2.7 mol of iron per mol $BchX_2$ from *C. tepidum* and 3.4 mol of iron per mol of $BchX_2$ from *R. denitrificans* further suggesting the presence of a [4Fe-4S] cluster. Since residues Cys^{124} and Cys^{158} (*P. marinus* numbering) are found conserved in all sequences of BchX and BchL/ChlL proteins, it was concluded that the COR subunit BchX forms a redox-active intersubunit [4Fe-4S] cluster analogously as described for DPOR subunits BchL and ChlL.

Moreover, the [Fe-S] clusters present in subunit $BchX_2$ of COR were characterized by EPR analyses (Fig. 24).

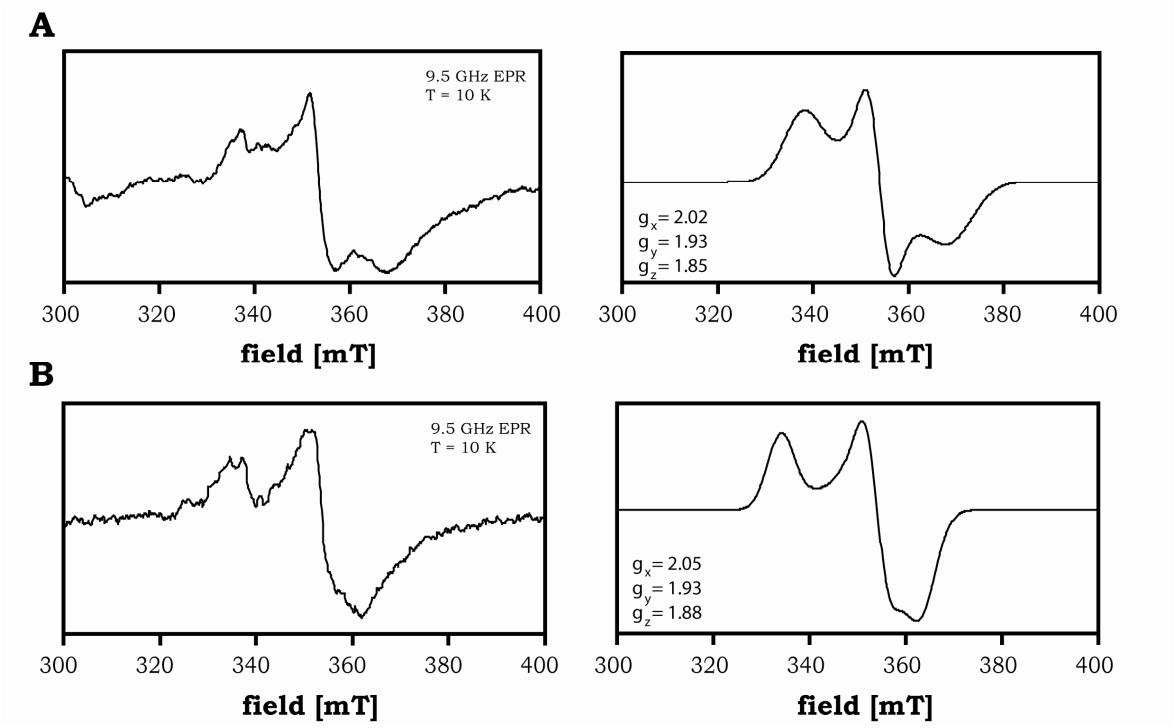

Fig. 24: EPR spectra of $BchX_2$ from *C. tepidum* (A) and *R. denitrificans* (B).
EPR spectra of $BchX_2$ proteins from *C. tepidum* (*A*) and *R. denitrificans* (*B*) after reduction with dithionite were recorded at 10 K and 9.5 GHz using a microwave power of 2.5 mW (modulation amplitude 1 mT, modulation frequency 12.5 kHz). The obtained EPR spectra are shown in the left panel, the corresponding simulated spectra and the principal values of the g-tensor are given in the right panel. Experimental spectra were accumulated from 32 measurements.

After reduction of the *C. tepidum* and *R. denitrificans* $BchX_2$ proteins with 20 mM dithionite, the EPR spectra exhibit signals with $g_x = 2.02$, $g_y = 1.93$, and $g_z = 1.85$ for $BchX_2$ from *C. tepidum* and with $g_x = 2.05$, $g_y = 1.93$, and $g_z = 1.88$ for $BchX_2$ from

R. denitrificans, respectively. These deduced g-values are characteristic for $[4Fe\text{-}4S]^{+1}$ clusters (Guigliarelli *et al.*, 1999, Hagen, 1992), and correlate well to the values obtained for the previously characterized DPOR $BchL_2/ChlL_2$ subunits from *R. capsulatus* and *P. marinus* (Fujita *et al.*, 2000, Bröcker *et al.*, 2008b). Thus, these findings provide further evidence for an identical cluster composition in $BchX_2$ of COR and the homologous $BchL_2/ChlL_2$ subunit of DPOR.

The obtained data concerning the [Fe-S] clusters of COR subunits $(BchYZ)_2$ and $BchX_2$ are in good agreement with recent EPR studies in which characteristic signals for a [4Fe-4S] cluster were obtained for the COR subunit $BchX_2$ as well as for subunit $(BchYZ)_2$ from *R. sphaeroides* (Kim *et al.*, 2008).

3.2.2.3 Analysis of a Potential Flavin Cofactor

In a recent study, a FMN cofactor for the COR subunit $BchX_2$ from *R. sphaeroides* using UV/visible absorption spectroscopy and HPLC analysis was described (Kim *et al.*, 2008). Therefore, $BchX_2$ subunits from *C. tepidum* and *R. denitrificans* were analyzed for a potential flavin cofactor. UV/visible absorption spectra revealed only peaks at 425 nm characteristic for [4Fe-4S] clusters (compare section 3.2.2.2) while no absorption maxima at 366 and 433 nm typical for the presence of flavin cofactors were detectable. For further analysis, the $BchX_2$ proteins were precipitated by addition of perchloric acid and the supernatant analyzed by UV/visible spectroscopy. Again, no signal for a covalently or non-covalently bound flavin cofactor such as FAD or FMN was found (data not shown). In order to clearly rule out a potential flavin cofactor, the supernatant of the precipitated $BchX_2$ proteins were analyzed by HPLC (Fig. 25).

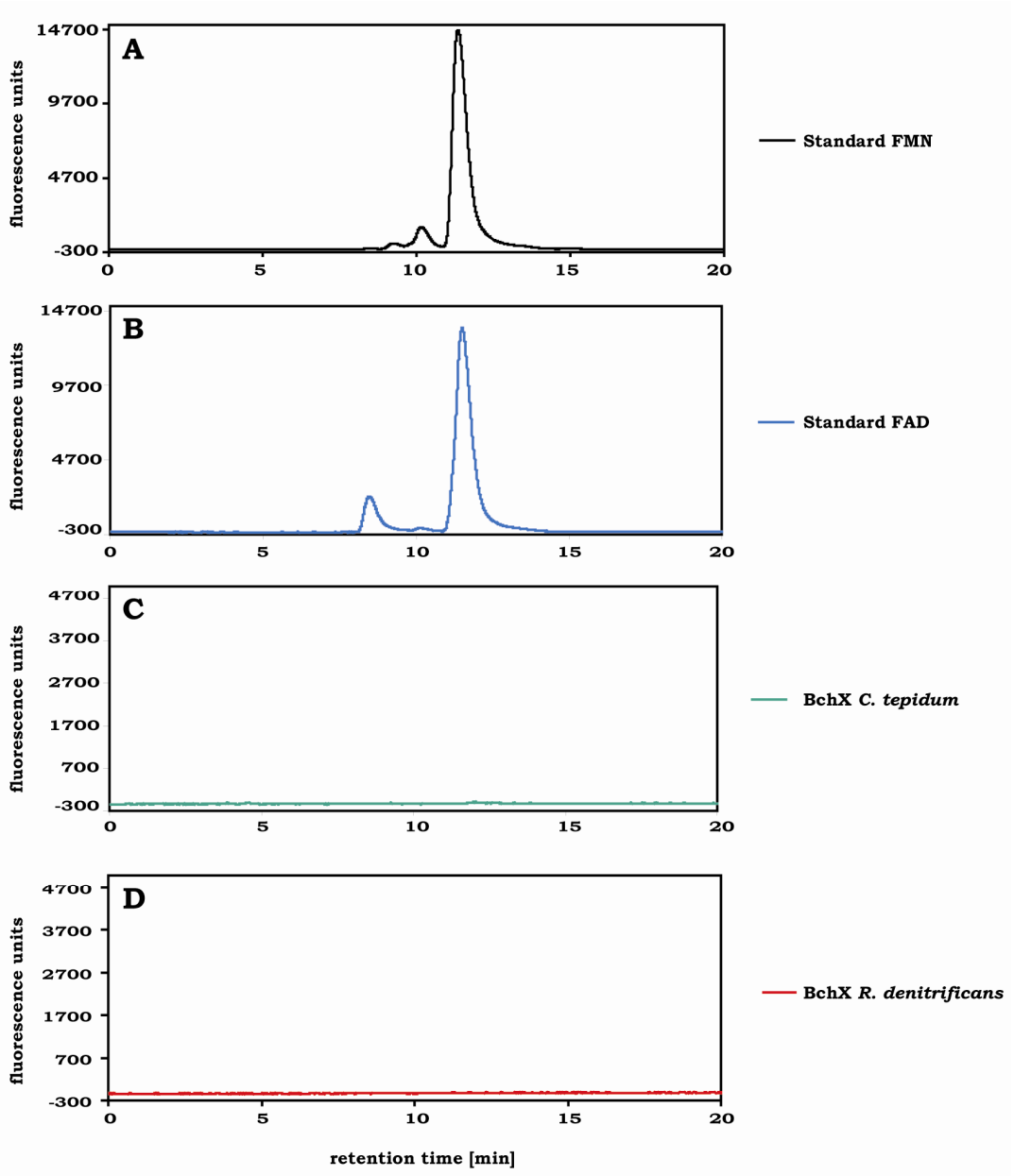

Fig. 25: HPLC analysis of a potential flavin cofactor in subunits $BchX_2$ from *C. tepidum* and *R. denitrificans*.
$BchX_2$ proteins were precipitated by the addition of 5 % (v/v) of perchloric acid. Fifty µl of the supernatant were injected on an ODS Hypersil 250 x 4.6 mm column. Flavins were detected by fluorescence (extinction: 430 nm; emission: 525 nm). Standards of FAD and FMN showed retention times of 8.6 and 11.7 minutes, respectively. No flavin cofactor was detectable in the $BchX_2$ fractions.

The corresponding flavin standards of FAD and FMN showed retention times of 8.6 min and 11.7 min, respectively (Fig. 25, *A* and *B*). The additional peak at 11.7 min for the FAD standard corresponds to FAD which was already converted to FMN due to the instability of the molecule. However, neither for the BchX protein from *C. tepidum* nor for the $BchX_2$ protein from *R. denitrificans* a peak for a flavin cofactor was observed in the HPLC analyses (Fig. 25, *C* and *D*).

These findings indicate that the $BchX_2$ subunits from *C. tepidum* and *R. denitrificans* do not contain a flavin cofactor as described for the enzyme from *R. sphaeroides* (Kim *et al.*, 2008).

To summarize, the $BchX_2$ subunits of COR show only the presence of a [4Fe-4S] cluster consistent with the cofactor composition of the previously characterized homologous DPOR systems.

3.2.3 Activity of the COR Enzyme

3.2.3.1 Production of Chlorophyllide *a*

For the production of the COR substrate, the *R. capsulatus* mutant CB1200 (Δ*bchF*-Δ*bchZ*) which accumulates Chlide was used. After cultivation of the mutant, Chlide was extracted from the freeze-dried cells by acetone, followed by extraction of carotinoids by hexane (Fig. 26, *A*) as described in "Materials and Methods". The extract was dissolved in DMSO and analyzed by UV/visible absorption and fluorescence spectroscopy (Fig. 26, *B* and *C*).

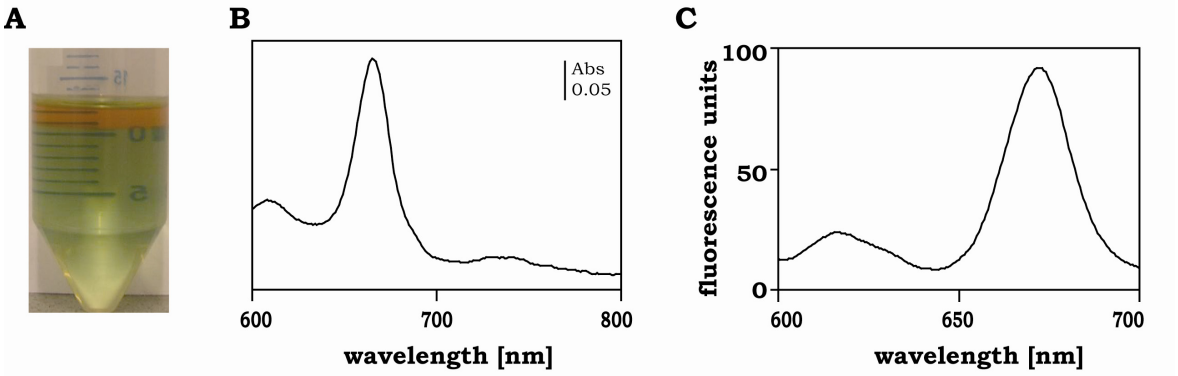

Fig. 26: Extraction of Chlide (A), UV/visible absorption spectrum (B) and fluorescence spectrum (C) for the extracted chlorophyllide *a* from the *R. capsulatus* mutant CB1200.
The COR substrate Chlide was extracted as described in "Materials and Methods". After extraction, the pigment was dissolved in DMSO. One µl of the extract was dissolved in acetone and analyzed by UV/visible absorption spectroscopy and fluorescence spectroscopy, respectively. For the fluorescence spectrum an emission scan from 500 - 700 nm was performed using an excitation wavelength of 428 nm.

The obtained UV/visible absorption spectrum (Fig. 26, *B*) shows a peak at 665 nm corresponding to the absorption maximum of Chlide. Besides this dominant absorption peak, an additional absorption maximum at ~ 610 nm can be observed which can be ascribed to low amounts of other tetrapyrroles in the extracted fraction. Additionally, the extracted substrate Chlide exhibits a minor additional absorption maximum at 735 nm.

In the fluorescence spectrum (Fig. 26, *C*) a peak at an emission wavelength of 670 nm characteristic for Chlide is detectable (Kotzabasis *et al.*, 1986). Consistent with the additional peak observed in the UV/visible absorption spectrum, this peak was also obtained in the fluorescence spectrum and ascribed to tetrapyrrole molecules which might have been co-purified by extraction.

By the extraction procedure for Chlide from the *R. capsulatus* mutant CB1200 concentrations up to 1.5 mM for Chlide were obtained which corresponds to a yield of 188 µg. The extracted Chlide was used as substrate in the following COR activity assays.

3.2.3.2 Activity of Homologous COR Enzymes

For further analysis of the COR enzyme, activity assays using the individual subunits from *C. tepidum* and *R. denitrificans* were performed. For this purpose, 100 pmol of the purified subcomplex $(BchYZ)_2$ was supplemented with a cell-free *E. coli* extract overproducing the $BchX_2$ protein. Analogously to the DPOR system, anaerobic conditions at pH 7.5 in the presence of 2 mM of ATP, an ATP-regenerating system, 10 mM of dithionite, 10 mM of $MgCl_2$ and 150 mM of NaCl at a temperature of 35 °C were employed for the assays.

Initial attempts to show COR activity were hampered since the precise ratio of subunit $BchX_2$ versus subunit $(BchYZ)_2$ was shown to be of importance for enzymatic activity. Furthermore, enzymatic activity was only detectable when the thioredoxin/His-tag was removed from the $(BchYZ)_2$ complex by thrombin cleavage. Nevertheless, COR activity was only observed for the COR system from *R. denitrificans*. All efforts to determine COR activity for the enzyme from *C. tepidum* failed. The activity was detected by UV/visible absorption spectroscopy where the substrate Chlide exhibits an absorption maximum at a wavelength of 665 nm whereas the product Bchlide absorbs at 735 nm. In Figure 27, the obtained UV/visible absorption spectra for the activity assay of the $(BchYZ)_2$ complex with $BchX_2$ subunit from *R. denitrificans* is illustrated.

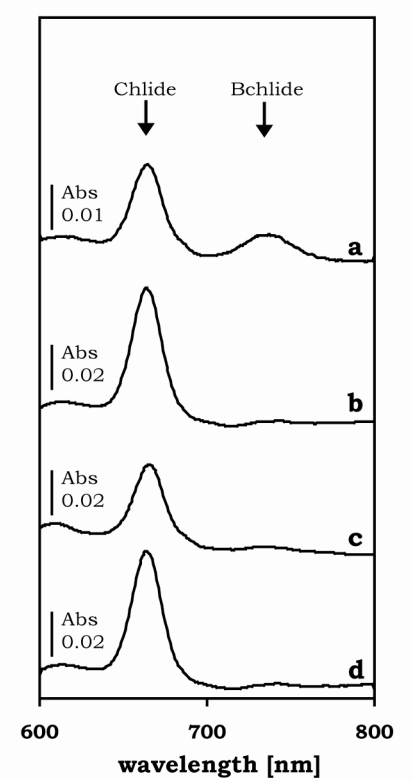

Fig. 27: UV/visible absorption spectra for the activity assay of the COR enzyme from *R. denitrificans*. Assays were performed as described in "Materials and Methods". After incubation of the assay for 1 h at 35 °C, pigments were extracted with acetone. Absorption maxima of the COR substrate Chlide and the product Bchlide are indicated by *arrows*. *Trace a*, COR assay containing 100 pmol of purified *R. denitrificans* $(BchYZ)_2$ and 20 pmol of *R. denitrificans* $BchX_2$; *traces b*, *c* and *d,* negative control without $(BchYZ)_2$ (*b*), without $BchX_2$ protein (*c*) and without ATP (*d*).

COR activity was detected by UV/visible absorption spectroscopy for the enzyme from *R. denitrificans* (Fig. 27). The incubation of $(BchYZ)_2$ complex with $BchX_2$ *(trace a*) from *R. denitrificans* resulted in significant formation of Bchlide with an absorption maximum at a wavelength of 735 nm. Spectra of control experiments without $(BchYZ)_2$ (*trace b*) or without $BchX_2$ protein (*trace c*) show only the characteristic peak of the substrate Chlide with an absorption maximum at a wavelength of 665 nm. Similarly, without the addition of ATP, no product formation was detectable *(trace d*). As mentioned before, the extracted substrate Chlide exhibits a minor absorption maximum at 735 nm as well which can be seen in all control reactions (*traces b*, *c* and *d*). Nevertheless, under the conditions of the employed assay, a specific activity of 42 pmol min^{-1} mg^{-1} for the COR enzyme from *R. denitrificans* was obtained.

3.2.3.3 Coupled DPOR/COR Activity Assay

DPOR and COR enzymes perform chemically almost identical reaction steps during (bacterio)chlorophyll biosynthesis. To partly reconstitute the (bacterio)chlorophyll biosynthetic pathway, a coupled DPOR/COR assay was performed. Conditions of this assay were identical as for the standard DPOR assay using Pchlide as substrate (13 µM) as well as the corresponding subunits from *P. marinus* DPOR. Additionally, the subunits of the COR enzymes from *C. tepidum* and *R. denitrificans* were included and incubated for 1 h at 35 °C. The resulting UV/visible absorption spectra for a coupled DPOR/COR assay using COR from *R. denitrificans* are shown in Figure 28.

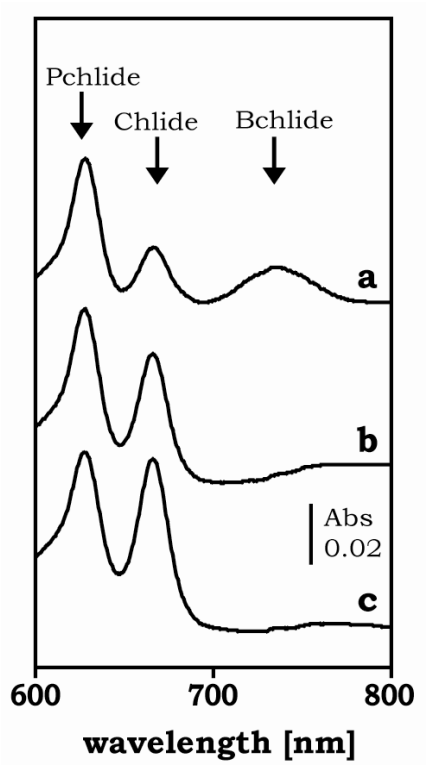

Fig. 28: UV/visible absorption spectra of a coupled DPOR/COR activity assay.
Assays were performed as described in "Materials and Methods" using DPOR from *P. marinus* and COR from *R. denitrificans*. After incubation of the assay for 1 h at 35 °C, pigments were extracted with acetone. Absorption maxima of the DPOR substrate Pchlide and the products of DPOR, Chlide, and COR, Bchlide, are indicated by *arrows*. *Trace a*, coupled DPOR/COR assay containing 200 pmol of *P. marinus* $(ChlNB)_2$ and 150 pmol of *P. marinus* $ChlL_2$ as well as 100 pmol of *R. denitrificans* $(BchYZ)_2$ and 20 pmol of *R. denitrificans* $BchX_2$; *traces b* and *c,* negative control without $(BchYZ)_2$ (*b*) and without $BchX_2$ protein (*c*).

This coupled activity assay clearly demonstrated activity for both enzymes. Besides the substrate peak of Pchlide with an absorption maximum at a wavelength of 626 nm, the product of the DPOR reaction yielded a peak at 665 nm corresponding to the formation of Chlide. Chlide is further converted to Bchlide by the COR enzyme showing an absorption at a wavelength of 735 nm. Thus, this part of the (bacterio)chlorophyll biosynthetic

pathway can be reconstituted *in vitro*. The observed activity for the *R. denitrificans* COR enzyme in the coupled assay yielded a higher specific activity (96 pmol min^{-1} mg^{-1}) than the activity observed for the COR enzyme alone (compare section 3.2.3.2). These findings might indicate a potential "metabolic channeling" mechanism of both enzymes which ensures efficient transfer of the substrates directly to the next enzyme of the pathway (Geck *et al.*, 1999, Massant *et al.*, 2002). Due to the phototoxicity of many tetrapyrroles as free compounds (Terry *et al.*, 2009), this "substrate channeling" mechanism would prevent the release of potential toxic chlorophyll radicals of the pathway within a cell. The mechanism of "substrate channeling" was already postulated for other enzymes of the tetrapyrrole and (bacterio)chlorophyll pathway (Moser *et al.*, 2001, Lüer *et al.*, 2005, Masoumi *et al.*, 2008).

All attempts to measure activity for the COR system from *C. tepidum* only resulted in the formation of Chlide (data not shown). One might speculate that the ratio of protein subunits $(BchYZ)_2$ and $BchX_2$ employed in the performed activity assays so far was not appropriate for detection of any activity of this enzyme. Further optimization is therefore necessary to obtain also activity for the COR enzyme from *C. tepidum*.

3.2.4 Substrate Recognition of COR

For the analysis of the substrate recognition of COR, activity assays using substrate analogs with different ring substituents were performed. The use of Zn-derivatives instead of the Mg-coordinating tetrapyrroles for analysis of the substrate specificity of enzymes in the (bacterio)chlorophyll pathway is well established (Helfrich *et al.*, 1994, Griffiths, 1980, Rüdiger *et al.*, 2005, Bröcker *et al.*, 2008b). The modified derivatives used in this study were kindly provided by Prof. Dr. Scheer and Prof. Dr. Rüdiger (LMU, Munich). All artificial substrates employed in the present study are illustrated in Figure 29.

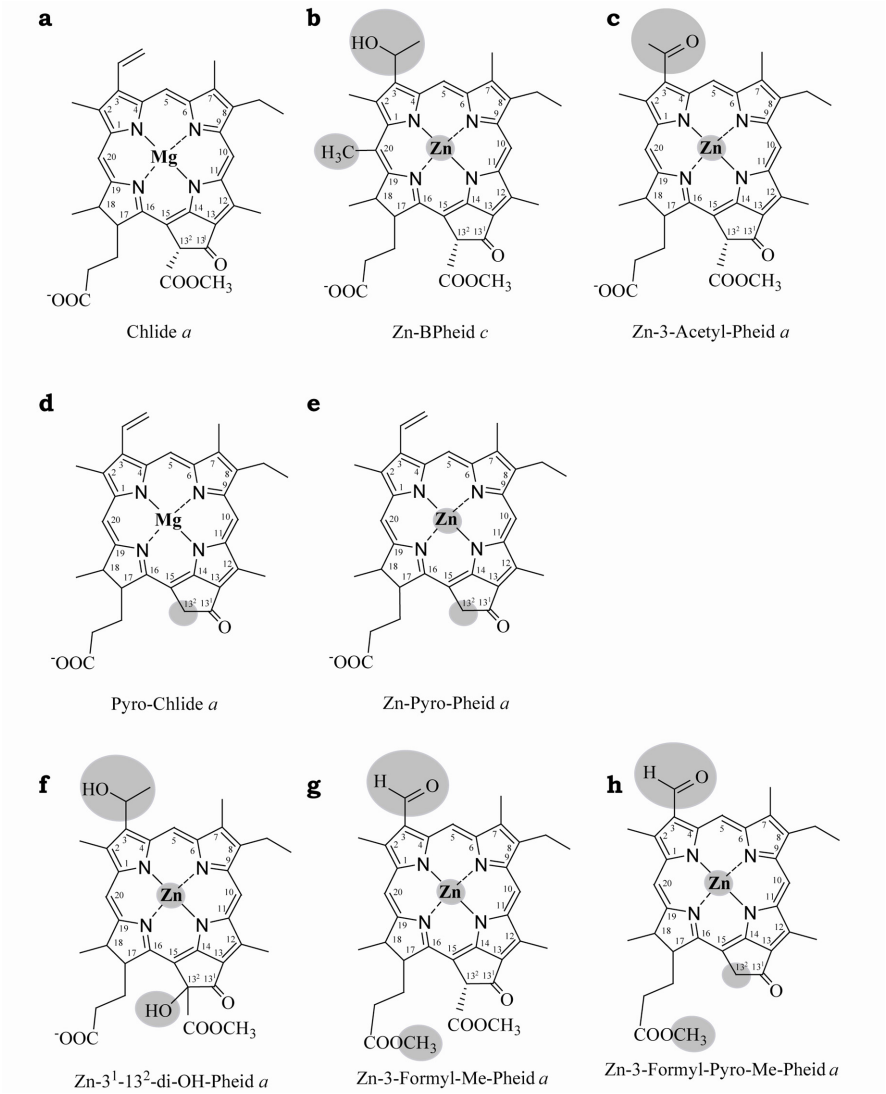

Fig. 29: Substrate Analogs for the analysis of COR substrate recognition.
a, the natural substrate of COR, Chlide. All other molecules (*b* - *h*) are substrate analogs with different modifications at the pyrrole ring system. Names are given below each molecule. Modifications compared with the natural substrate Chlide are highlighted in *gray*. BPheid = bacteriopheophorbide, Pheid = pheophorbide.

Seven substrate analogs were tested under conditions of the standard COR assay. The extinction coefficients of Zn-3-Acetyl-Pheid *a* (ε = 65.2 mM^{-1} cm^{-1}) and Zn-Pyro-Pheid *a* (ε = 69 mM^{-1} cm^{-1}) have been determined experimentally (Schmid *et al.*, 2002b, Smith *et al.*, 1966) while the extinction coefficients for all other substrate analogs were estimated according to Klement *et al*. (1999). Since all substrate analogs show comparable extinction coefficients in the range of 65 - 70 mM^{-1} cm^{-1} (section 2.8.2.3), activities were compared directly to each other from the absorption spectra of the activity assays. For this purpose, the relative activity of the wildtype *R. denitrificans* COR system with the natural substrate, Chlide, was set to 100 % and all other activities were related to that value. The obtained activities are shown in Figure 30.

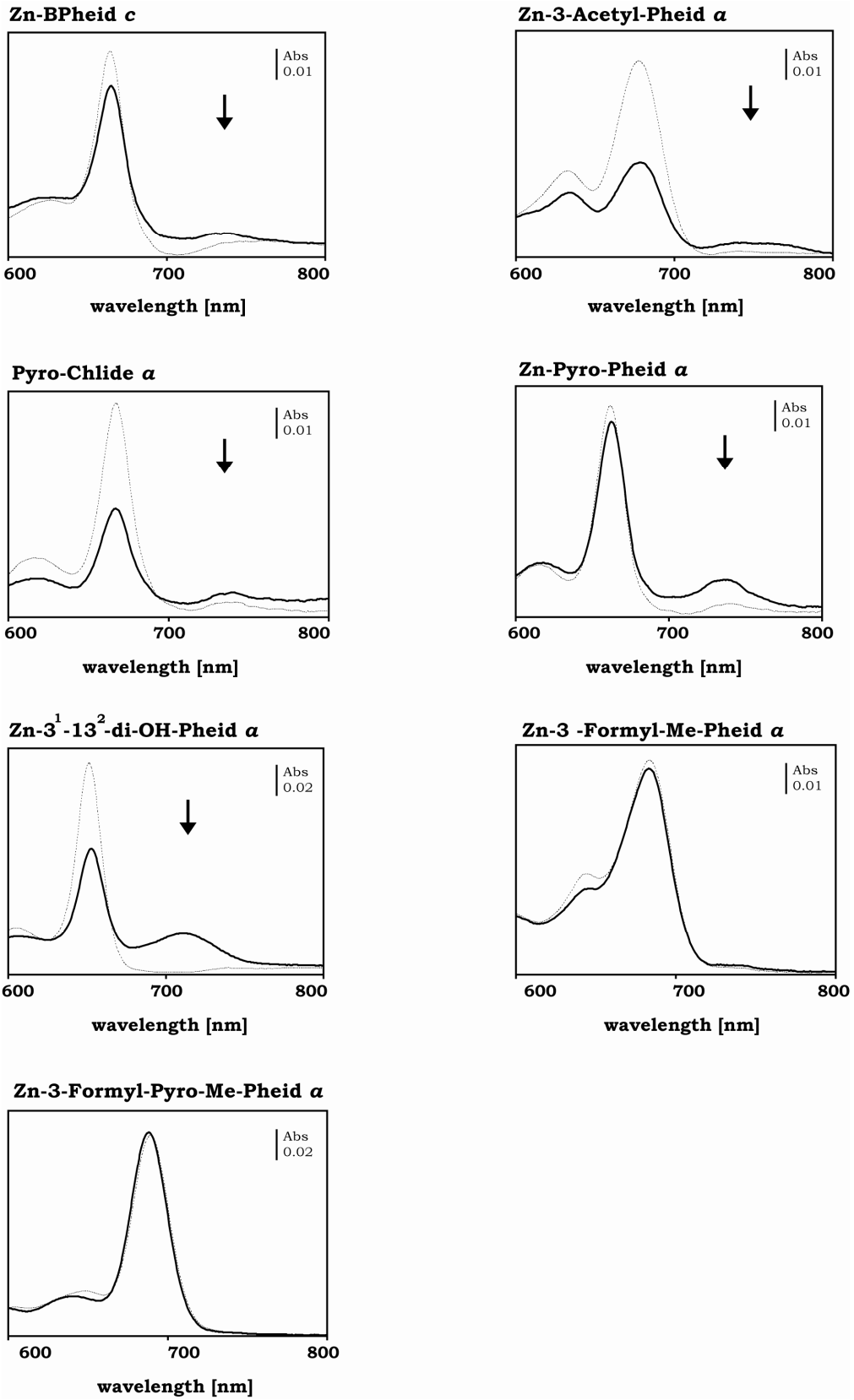

Fig. 30: UV/visible absorption spectra of COR activity assays using substrate analogs.
Assays were performed as described in "Materials and Methods" using COR from *R. denitrificans*. After incubation of the assay for 1 h at 35 °C, pigments were extracted with acetone. Absorption spectra of the negative controls are shown by *broken* lines, assays containing COR enzyme by *solid* lines. The *arrow* indicates the absorption maximum for the COR catalysis product for the corresponding substrate.

The obtained activities for the COR from *R. denitrificans* using substrate analogs are summarized in Table 5.

Tab. 5: Overview of COR substrate utilization.
COR assays were performed under the conditions of the COR standard assay. The relative enzymatic activity of the corresponding wildtype COR was set to 100 %, and all other values were related to this value.

No.	Tetrapyrrole	Modified pyrrole ring	λ_{Qy} [nm]	$\lambda_{product}$ [nm]	Relative activity [%]
a	Chlide *a*	wt	665	734	100
b	Zn-BPheid *c*	A	665	738	30
c	Zn-3-Acetyl-Pheid *a*	A	678	752	30
d	Pyro-Chlide *a*	E	667	738	30
e	Zn-Pyro-Pheid *a*	E	660	734	50
f	Zn-3^1-13^2-di-OH-Pheid *a*	A/E	650	715	100
g	Zn-3-Formyl-Me-Pheid *a*	A/D	684	-	< 1
h	Zn-3-Formyl-Pyro-Me-Pheid *a*	A/D/E	689	-	< 1

3.2.4.1 Substrate Analogs with Altered Substituents on Ring A

The substrate analog Zn-BPheid *c* (Fig. 29, *b*) carries a hydroxyl group at the $C3^1$ position of the tetrapyrrole structure and additionally a methyl group at the C20 position. Activity assays using this substrate analog showed a relative activity of 30 % when compared to the wildtype COR system of *R. denitrificans*. Obviously, modification on ring A as well as modification of the C20 position are tolerated by the COR enzyme and still allows for activity. This might indicate that the active site of COR enzymatic tolerates the additional hydroxyl group in the $C3^1$ position. Furthermore, the additional methyl group at the C20 position does not result in a steric conflict.

In the substrate analog Zn-3-Acetyl-Pheid *a* (Fig. 29, *c*), the vinyl group at the C3 position is replaced by an acetyl group. The obtained activity of 30 % for this substrate indicates that this modification on ring A still allows for DPOR activity. One might speculate that the carbonyl group of Zn-3-Acetyl-Pheid *a* might substitute for the vinyl group of the natural Chlide substrate.

3.2.4.2 Substrate Analogs with Altered Substituents on Ring E

Activity assays with Pyro-Chlide *a* (Fig. 29, *d*) as substrate yielded 30 %, the corresponding Zn-derivative Zn-Pyro-Pheid *a* (Fig. 29, *e*) resulted in 50 % activity when

compared to the natural substrate. In both molecules the methoxycarbonyl substituent at the $C13^2$ position is absent. These findings suggest that the presence of this substituent at the $C13^2$ position is not essential for COR activity. Furthermore, substitution of the central atom Mg^{2+} for Zn^{2+} does not impair enzyme activity. This observation is consistent with previously published studies which showed that Zn-derivatives are functional substrates for enzymes of the (bacterio)chlorophyll pathway (Bröcker *et al.*, 2008b, Klement *et al.*, 1999).

3.2.4.3 Substrate Analogs with Altered Substituents on Ring A and Ring E

The substrate analog Zn-3^1-13^2-di-OH-Pheid *a* (Fig. 29, *f*) carrying hydroxyl groups at $C3^1$ (ring A) and $C13^2$ (ring E) positions was tested for sustaining COR activity. Thereby, a relative activity of 100 % was observed when compared to the wildtype system. Again, a hydroxyl substituent in the $C3^1$ position of ring A does not impede substrate utilization. Furthermore, an additional hydroxyl group at the $C13^2$ position is also tolerated. The acceptance for a hydroxyl substituent at ring A was already shown by the obtained activity with Zn-Pheid *c* as substrate (section 3.2.4.1). This might indicate that substituents on position $C13^2$ are not determinants for substrate recognition. The high activity obtained by this substrate analog (100 %) was attributed to the higher solubility of this hydroxylated substrate. This might reduce the tendency to form dimers/aggregates (Brody, 1968) thereby resulting in a higher substrate concentration for the non-aggregated pigment. Alternatively, an electronic effect due to the sp^3-hybridization of $C13^2$ position was considered.

3.2.4.4 Substrate Analogs with Altered Substituents on Ring A and Ring D (and Ring E)

Using Zn-3-Formyl-Me-Pheid *a* (Fig. 29, *g*) as substrate in activity assays did not result in detectable COR activity. Besides a formyl group at C3 position (ring A), the substrate analog contains an additional methyl group at ring D. Both modifications might be responsible for the loss of activity.

Zn-3-Formyl-Pyro-Me-Pheid *a* (Fig. 29, *h*) was also tested as substrate for the COR enzyme from *R. denitrificans*. Analogously to the substrate analog Zn-3-Formyl-Me-Pheid *a*, this molecule contains identical modifications on ring A and D, respectively. Moreover, it lacks the methoxycarbonyl group at ring E. In the activity assay using this substrate, COR activity could not be shown. Again the formyl or methyl groups might be responsible for the absence of activity. Furthermore, the modification on ring E could also

account for the observed results. Nevertheless, based on the activities obtained with substrate analogs carrying comparable modifications on ring A and E (Zn-BPheid *c* (30 %), Zn-3-Acetyl-Pheid *a* (30 %) and Zn-Pyro-Pheid *a* (50 %)), it is reasonable to attribute the observed results for Zn-3-Formyl-Me-Pheid *a* and Zn-3-Formyl-Pyro-Me-Pheid *a* to the presence of the methyl group located on the carboxyethyl group of ring D.

3.2.4.5 Overall Substrate Recognition

Taken together, these findings imply a certain flexibility for the recognition of the Chlide substrate by the COR enzyme indicated by the observed activities with various substrate analogs tested.

Substitution of the central atom Mg^{2+} for Zn^{2+} is obviously accepted as indicated by the activities obtained with four Zn-analogs. Furthermore, modifications on ring A are tolerated by the COR enzyme. The replacement of the vinyl by a hydroxyl or an acetyl group (Zn-BPheid *c* and Zn-3-Acetyl-Pheid *a*), still allowed for enzymatic activity. In the literature, alternative pathways for bacteriochlorophyllide *a* formation have been suggested. The COR enzyme is proposed to reduce ring B of Chlide after the hydroxylation step of the C3 side chain. Alternatively, the B ring reduction is the initial catalytic step. However, based on the observed reduced activities (30 %) with substrate analogs carrying modifications on ring A (Zn-BPheid *c* and Zn-3-Acetyl-Pheid *a*), it is more likely that Chlide is the major substrate of COR when compared to 3^1-hydroxyethyl bacteriochlorophyllide *a*. Nevertheless, these results are in agreement with a branched pathway for the biosynthesis of bacteriochlorophylls in *R. denitrificans*. Such branching points for the biosynthesis of (bacterio)chlorophylls have been often described in the literature (Bollivar *et al.*, 1994, Kim *et al.*, 2008). However, this is one of the rare examples where direct evidence from biochemical experiments was obtained.

Substituents at ring E of the tetrapyrrole are also variable since removal of the methoxy carbonyl group (Pyro-Chlide *a* and Zn-Pyro-Pheid *a*) or an additional hydroxyl group (Zn-3^1-13^2-di-OH-Pheid *a*) resulted in significant COR activity. In contrast, the methyl group at the carboxyethyl group of ring D is not tolerated as indicated by the absent activities of the corresponding substrate analogs (Zn-3-Formyl-Me-Pheid *a* and Zn-3-Formyl-Pyro-Me-Pheid *a*).

3.2.5 Substrate Inhibition Assay

Moreover, the substrate analogs were tested for their competitive inhibition with the natural substrate Chlide. Therefore, standard activity assays using Chlide as substrate were performed in the presence of the two substrate analogs Zn-3-Formyl-Me-Pheid *a* and Zn-3-Formyl-Pyro-Me-Pheid *a* which are no substrates for COR catalysis. None of those substrate analogs was a competitive inhibitor of COR catalysis. This might indicate a steric hindrance due to the methyl group at the carboxyethyl group at ring D.

3.3 Chimeric Enyzmes Consisting of DPOR, COR and Nitrogenase

The individual subunits of the nitrogenase-like enzymes DPOR, COR, and nitrogenase show significant amino acid sequence identities. To gain insight into the evolution of these multi-subunit enzymes, the functional interaction of the electron-transferring subunits $BchX_2$ from various COR enzymes, and $NifH_2$ of nitrogenase from *A. vinelandii* with different DPOR $(BchNB)_2$/$(ChlNB)_2$ subunits was investigated. For this purpose, these proteins were recombinantly produced to generate various combinations of chimeric enzymes which were then functionally characterized.

3.3.1 Chimeric Enzymes of DPOR and Nitrogenase

In a recently published *in vitro* study, it was shown that the $BchL_2$ protein from *R. sphaeroides* is not able to serve as an electron donor for the MoFe protein from *A. vinelandii* (Sarma *et al.*, 2008). In the present thesis, the inverse experiment was performed. Under the conditions of the standard DPOR assay, the $BchL_2$ protein from *C. tepidum* and the $ChlL_2$ protein from *P. marinus* and *T. elongatus* were substituted by varying concentrations of $NifH_2$ from *A. vinelandii*, respectively. Under all of the conditions tested, no Chlide formation was detectable (data not shown). This experiment indicated that the docking surface of DPOR and nitrogenase have evolved significantly during evolution. These results are in good agreement with our sequence alignments (compare Fig. 18 - 20) and the analysis of the three-dimensional structure of the $BchL_2$ protein from *R. sphaeroides* (Sarma *et al.*, 2008).

3.3.2 Chimeric Enzymes of DPOR and COR

In a standard DPOR assay with $(BchNB)_2$ from *C. tepidum* and $(ChlNB)_2$ from *P. marinus* and *T. elongatus*, subunit $BchL_2$ or $ChlL_2$ was substituted by the $BchX_2$ subunit of COR from *C. tepidum* and *R. denitrificans*, respectively. Pchlide was used as substrate at a concentration of 13 µM in the presence of 2 mM of ATP, an ATP-regenerating system and with 10 mM of dithionite as reducing agent. For those experiments, 100 pmol of $(BchNB)_2$ or $(ChlNB)_2$ were supplemented with varying amounts of $BchX_2$ (10 - 300 pmol). The obtained UV/visible absorption spectra of the chimeric activity assay containing DPOR subcomplex $(BchNB)_2$ from *C. tepidum* and the COR subunit $BchX_2$ from *C. tepidum* are shown in Figure 31.

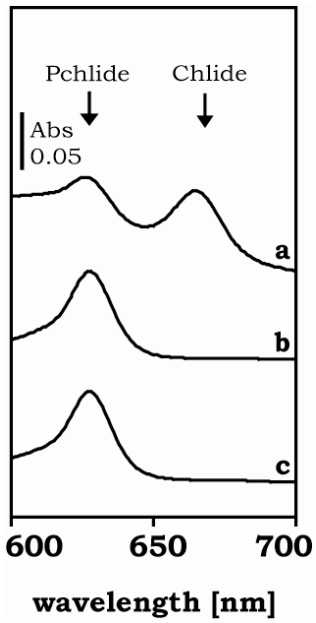

Fig. 31: UV/visible absorption spectra for chimeric enzyme consisting of DPOR and COR.
Assays were performed as described in "Materials and Methods". After incubation of the assay for 1 h at 35 °C, pigments were extracted with acetone. Absorption maxima of the DPOR substrate Pchlide and the product Chlide are indicated by *arrows*. *Trace a*, DPOR assay containing 100 pmol of purified *C. tepidum* $(BchNB)_2$ and 17 pmol of *C. tepidum* $BchX_2$ protein; *traces b* and *c,* negative control without $(BchNB)_2$ (*b*) and without $BchL_2$ protein (*c*).

In control experiments without $BchX_2$ or $(BchNB)_2$ no product formation was observed (Fig. 31, *traces b* and *c*). Furthermore, control experiments without the addition of ATP showed no Chlide formation (data not shown). However, in a standard assay containing 100 pmol of $(BchNB)_2$ from *C. tepidum* and 17 pmol of $BchX_2$ from *C. tepidum*, a chimeric activity of 90 % was observed when compared to the activity of the wildtype DPOR system (Fig. 31, *trace a*). When $(BchNB)_2$ from *C. tepidum* was supplemented with

20 pmol of $BchX_2$ from *R. denitrificans*, significant DPOR activity of 50 % was also observed.

The following Table (Tab. 6) summarizes the results of the chimeric enzymes consisting of DPOR, COR and nitrogenase.

Tab. 6: Chimeric Activity of DPOR subunit $(BchNB)_2$ or $(ChlNB)_2$ with subunit $NifH_2$ of nitrogenase and subunit $BchX_2$ of COR.
Standard DPOR assays were performed for 1 h at 35 °C as described in "Materials and Methods". The relative enzymatic activity of the corresponding wildtype DPOR was set to 100 %, and all other values were related to this value.

	***C. tepidum* $BchX_2$**	***R. denitrificans* $BchX_2$**	***A. vinelandii* $NifH_2$**
C. tepidum **$(BchNB)_2$**	90 %	50 %	< 1 %
T. elongatus **$(ChlNB)_2$**	< 1 %	< 1 %	< 1 %
P. marinus **$(ChlNB)_2$**	< 1 %	< 1 %	< 1 %

The BchX subunits employed share an overall sequence identity of 31 - 35 % when compared to the amino acid sequence of BchL or ChlL proteins. However, identical values were obtained when subunit BchX was compared with the NifH protein (compare appendix D) which failed to sustain DPOR activity. Furthermore, visual inspection of sequence alignments of BchX, BchL (or ChlL), and NifH proteins (compare Fig. 18) did not reveal any regions sharing a higher degree of sequence conservation for the BchX/BchL (or BchX/ChlL) couple compared to the BchX/NifH couple. This clearly becomes evident for the postulated docking region including Tyr^{127} in subunit BchL or ChlL. At this position, BchX and NifH proteins carry a highly conserved arginine residue, whereas a conserved tyrosine residue is found in all BchL and ChlL sequences. The observed chimeric activity of subunit $BchX_2$ of COR with subunit $(BchNB)_2$ of DPOR indicates that protein-protein-interaction and intersubunit electron-transfer is not dependent on highly conserved sequence motifs. Conservative mutations of amino acid residues located at the postulated docking face of $BchX_2$ still allow for the obtained chimeric activity.

3.3.3 Evolution of Electron-Donating Subunits $NifH_2$, $BchL_2$/$ChlL_2$ and $BchX_2$ from Nitrogenase, DPOR and COR

Subunits $NifH_2$, $BchL_2$ or $ChlL_2$, and $BchX_2$ are responsible for the ATP-dependent transfer of electrons onto the corresponding subunits $(NifDK)_2$, $(BchNB)_2$/$(ChlNB)_2$ and $(BchYZ)_2$, respectively (Burke *et al.*, 1993, Fujita *et al.*, 1993, Nomata *et al.*, 2006b). These heterotetrameric complexes are then required for accurate substrate recognition and reduction. The absence of activity for DPOR subunit $(BchNB)_2$ or $(ChlNB)_2$ with subunit $NifH_2$ of nitrogenase indicates that subunit $NifH_2$ and $BchL_2$ (or $ChlL_2$) have evolved significantly. In contrast, the chimeric activity of the DPOR subunit $(BchNB)_2$ in combination with subunit $BchX_2$ of COR suggests that the $BchX_2$ protein has evolved only sparingly from a common ancestor. Although highly conservative sequence mutations were introduced, the mode of protein-protein-interaction was preserved. Based on the presented results, Figure 32 shows a hypothetical model for the evolution of the electron-transferring subunits of nitrogenase, DPOR and COR.

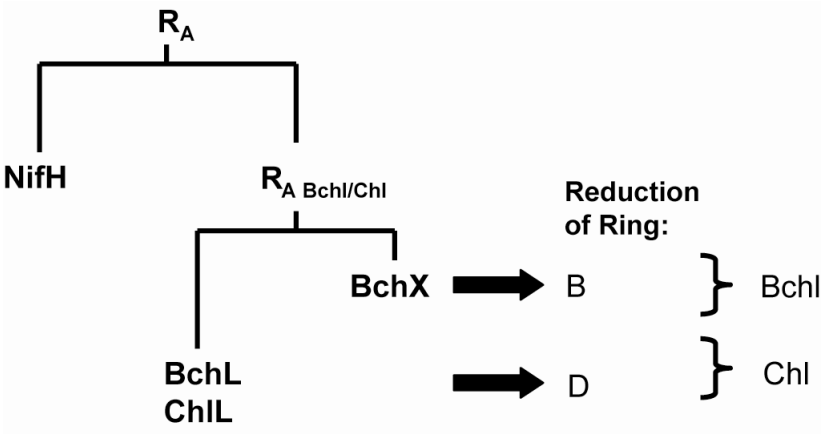

Fig. 32: Hypothetical model for the evolution of electron-transferring subunits of DPOR, COR, and nitrogenase.
An ancient reductase, R_A, gave rise to the nitrogenase branch (NifH) and a Chl/Bchl biosynthetic branch (BchX and BchL/ChlL). Current $BchX_2$ proteins of COR and $BchL_2$/$ChlL_2$ proteins of DPOR have evolved from the ancient reductase, $R_{A\ BChl/Chl}$. Bchl = bacteriochlorophyll, Chl = chlorophyll.

Gene duplication of an ancient reductase (R_A) gave rise to a nitrogenase (NifH) and a (bacterio)chlorophyll branch. This ancient reductase ($R_{A\ Bchl/Chl}$) of the Chl/Bchl path has thus evolved into the current $BchX_2$ and $BchL_2$ (or $ChlL_2$) proteins. This evolutionary process came along with the appearance of subunits $(BchNB)_2$ (or $(ChlNB)_2$) and $(BchYZ)_2$ responsible for the specific reduction of ring B and D, respectively.

3.4 The Oxygen-Dependent Cyclase (AcsF)

A further project in this thesis was the investigation of the isocyclic ring formation in (bacterio)chlorophylls which is catalyzed by the oxygen-dependent or the oxygen-independent cyclase. To date, this step of the (bacterio)chlorophyll biosynthetic pathway is only poorly understood. Based on the present-day knowledge, the oxygen-dependent enzyme is proposed to be composed of several subunits but only the membrane-associated subunit AcsF could be identified so far. The identification of other subunits is therefore of special interest to elucidate the reaction mechanism for the isocyclic ring formation in detail.

To identify further subunits of the cyclase, different strategies were pursued. For the co-purification of potential subunits, mutants of *S. elongatus* PCC 7942 were constructed carrying genome integrated His-tagged versions of AcsF. Moreover, the *acsF* gene from *S. elongatus* was cloned into expression vectors for the recombinant production of the corresponding His-tagged fusion protein in *E. coli*. Furthermore, attempts to establish an activity assay for the cyclase enzyme were performed.

3.4.1 Mutants of *Synechococcus elongatus* Encoding His-tagged Versions of AcsF

To characterize the oxygen-dependent cyclase in more detail, plasmids were constructed encoding N-, C-, or N- and C-terminal fusion proteins of *acsF* from *S. elongatus* PCC 7942. Therefore, the corresponding gene *acsF* including 250 bp of the upstream region was amplified to yield a PCR product containing the upstream promoter region. Additionally, the used oligonucleotides contained sequences coding His-tag sequences in the 3' or 5' region of the *acsF* gene. In cooperation with the group of Prof. Dr. Forchhammer at the Justus Liebig Universität Gießen the integration of the resulting vector constructs into the genome of *S. elongatus* PCC 7942 was performed.

All *S. elongatus* mutant strains were verified for integration of the *acsF* gene into genome by PCR. The expression of the modified *acsF* genes was analyzed by Western Blot using an antibody against the His-tag. The obtained autoradiogramm for a sample with N- and C-terminal tagged AcsF (His-AcsF-His) is shown in Figure 33.

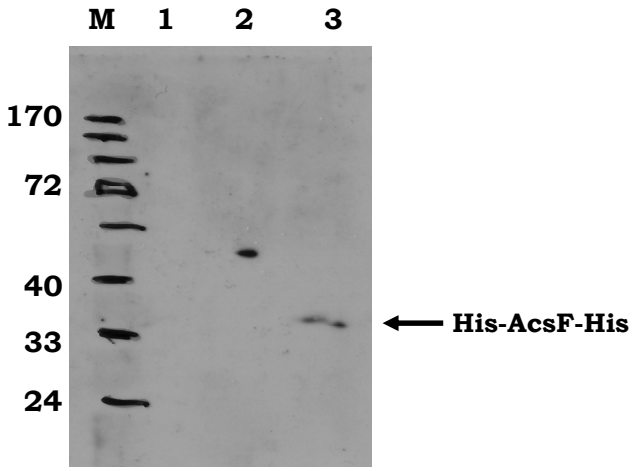

Fig. 33: Western Blot Analysis of His-tagged AcsF in *S. elongatus* mutants.
Proteins were separated by a 12 % SDS-PAGE and blotted onto a PVDF membrane. For detection of the proteins a primary anti-His antibody (murine) and an anti-mouse secondary antibody conjugated with the horseradish peroxidase was used. Bands were visualized by incubation of the membrane with the chemiluminescence substrate luminol. *Lane M*, molecular mass marker; relative molecular masses (x 1000) are indicated; *lane 1*, wildtype *S. elongatus* as negative control; *lane 2*, positive control (His-tagged GluTR; 4 ng); *lane 3*, *S. elongatus* mutant His-AcsF-His.

In the Western Blot production of His-tagged AcsF by the *S. elongatus* mutant after cultivation for two days was clearly detected (Fig 33, *arrow*). The observed protein band shows a slightly lower molecular mass as the theoretical molecular mass of *S. elongatus* AcsF (M_r 42'000) which has already been observed for recombinantly produced cyclase proteins in our laboratory before. Analogous results were also obtained for cultivation for two to six days for all three His-tag versions (data not shown). However, the amounts of produced protein are in the range of ~ 3 ng. All experiments did not result in detectable amounts of co-purified proteins. For co-purification of additional cyclase subunits higher amounts of the corresponding His-tagged protein are necessary.
Future experiments will concentrate on a cooperation with the group of Prof. Dr. Franco-Lara at the Technische Universität Braunschweig for the large-scale cultivation of the mutant strains in a fermenter.

3.4.2 Recombinant Production of AcsF from *Synechococcus elongatus* in *E. coli*

As an attempt to obtain larger quantities of the cyclase subunit AcsF for co-purification experiments, the corresponding gene *acsF* from *S. elongatus* PCC 7942 was cloned into a standard *E. coli* expression vector (pET32a). The resulting construct allows for production of the protein with a cleavable N-terminal thioredoxin/His/S-tag. *E. coli* BL21 (λDE3)

cells harbouring pET32a-AcsF were cultivated as described in section 2.6.1.3. Figure 34 shows the SDS-Gel of the intracellular proteins obtained by cultivation at 37 °C.

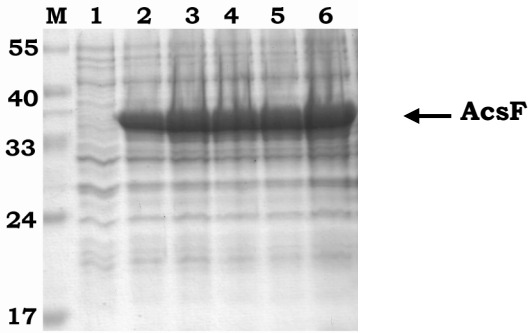

Fig. 34: SDS-PAGE analysis of *S. elongatus* AcsF production in *E. coli* at 37 °C.
Proteins were recombinantly produced in *E. coli* BL21 (λDE3) harbouring pET32a-AcsF as described in "Materials and Methods", separated through 12 % SDS-PAGE, and visualized *via* Coomassie Brilliant Blue staining. Recombinant protein production was induced by addition of 400 µM IPTG. *Lane M*, molecular mass marker; relative molecular masses (x 1000) are indicated. *Lane 1*, sample taken before induction of gene expression; *lane 2* - *lane 6*, samples taken 1 h, 2 h, 3 h, 4 h and 5 h after induction.

As shown in Figure 34, induction of gene expression resulted in high amounts of the AcsF protein (Fig. 34, *arrow*). However, the overproduced AcsF protein was found exclusively in the insoluble protein fraction. All attempts to recombinantly produce the soluble AcsF protein in *E. coli* failed. Based on these results it is not clear if it is possible to obtain a soluble AcsF protein in the absence of additional protein subunits.

3.4.3 Activity Assays with Cellular Extracts from *Thermosynechococcus elongatus*

The analysis of the cyclase reaction is strongly hampered since no reproducible activity assay for the enzyme is available. In the present study, a modified cyclase assay according to the description of Rzeznicka *et al.* (2005) was employed. The assay makes use of cellular extracts from wildtype *T. elongatus* BP-1 in the presence of commercially available MME (Frontier Scientific) as substrate. After extraction of the tetrapyrrole compounds, assays were analyzed by fluorescence spectroscopy (Fig. 35).

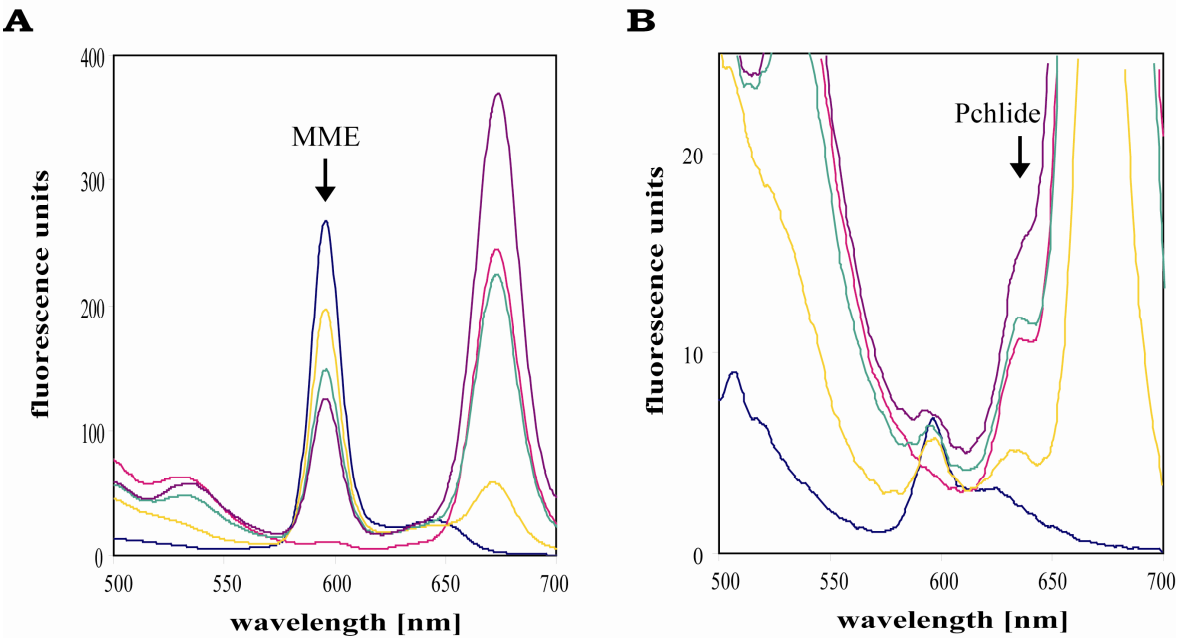

Fig. 35: Fluorescence spectra of cyclase activity assays according to Rzeznicka *et al.* (2005) using *T. elongatus* wildtype cell extract.
Assays were performed as described in "Materials and Methods". After incubation of the assay for 1 h at 55 °C, tetrapyrroles were extracted by addition of acetone, ammonia and hexane. The resulting supernatants were analyzed by fluorescence spectroscopy using an emission scan from 500 to 700 nm wavelength. For detection of MME (*A*) an excitation wavelength of 420 nm, for detection of Pchlide (*B*) an excitation wavelength of 440 nm was used. Emission maxima of MME and Pchlide are indicated by *arrows*.

- control without cell extract
- control without MME
- 100 µg *T. elongatus* cell extract
- 500 µg *T. elongatus* cell extract
- 700 µg *T. elongatus* cell extract

In the fluorescence spectrum (Fig. 35), the concentration of MME (595 nm, Fig. 35 *A*; *arrow*) and the concentration of chlorophylls (680 nm) correlates with the employed amount of *T. elongatus* cellular extract. However, the high amount of chlorophylls in the *T. elongatus* wildtype cells clearly impairs the detection of the product of the cyclase reaction (Fig. 35, *B*). No distinct separation of Pchlide from chlorophylls with the employed extraction protocol was obtained.

Therefore, another modified cyclase assay according to Bollivar & Beale (1996) was used. This protocol makes use of an alternative extraction method to reduce the chlorophyll background. The following fluorescence spectra were obtained with this method (Fig. 36).

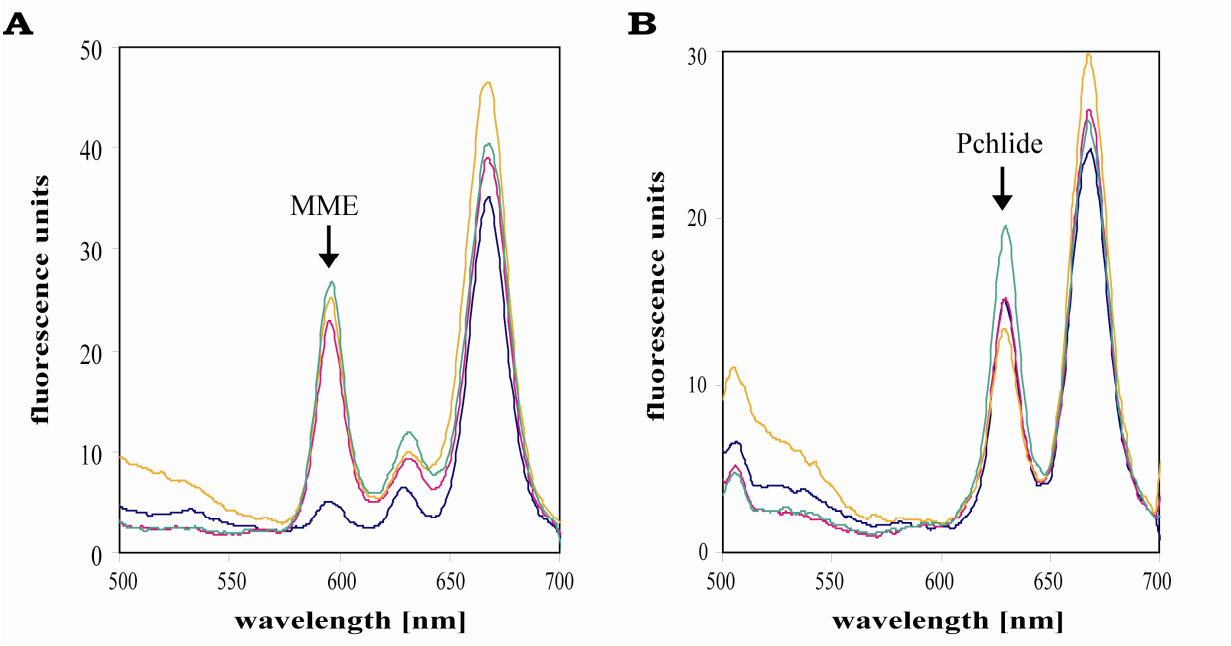

Fig. 36: Fluorescence spectra of cyclase activity assays according to Bollivar & Beale (1996) using *T. elongatus* wildtype cell extract.
Assays were performed as described in "Materials and Methods". After incubation of the assay using 500 µg *T. elongatus* cellular extract for 1 h at 30 °C, tetrapyrroles were extracted by addition of acetone, ammonia, hexane and diethyl ether. The resulting supernatants were analyzed by fluorescence spectroscopy performing an emission scan from 500 to 700 nm wavelength. For detection of MME (*A*) an excitation wavelength of 420 nm, for detection of Pchlide (*B*) an excitation wavelength of 440 nm was used. Emission maxima of MME and Pchlide are indicated by *arrows*.

- control *T. elongatus* cell extract, without incubation
- *T. elongatus* cell extract
- *T. elongatus* cell extract, 10 min at 95 °C
- *T. elongatus* cell extract without NADPH

In the obtained spectra (Fig. 36) a clear reduction of the amount of co-purified chlorophylls was observed which results in a distinct emission peak for Pchlide (Fig. 33 *B*; *arrow*). However, the observed emission peak at a wavelength of 635 nm corresponds to the endogenous cyclase activity of the *T. elongatus* wildtype cells since control reactions (without incubation) yielded the same fluorescence spectrum. Moreover, control reactions without the addition of the postulated cofactor, NADPH, or control reactions containing cellular extract after heat-inactivation (10 min, 95 °C) also resulted in an almost identical fluorescence spectrum.

Modifications of the assay using an NADPH-regenerating and an ATP-regenerating systems, different temperatures (30 °C - 55°C) as well as substrate which was produced *in vitro* by the magnesium protoporphyrin IX methyltransferase resulted in no detectable cyclase activity. It was hypothesized that the employed extraction method not only removes the amount of the co-purified chlorophylls but also removes significant amounts of the Pchlide molecule.

From these results, it was speculated that the oxygen-dependent cyclase enzyme might require special conditions not found in the assays performed. Future experiments with a focus on the specific isolation of the Pchlide reaction product have to be performed.

4 SUMMARY

Dark-operative protochlorophyllide oxidoreductase (DPOR) and chlorophyllide *a* oxidoreductase (COR) catalyze the stereospecific reduction of ring D and ring B during (bacterio)chlorophyll biosynthesis, respectively. Both enzymes show significant homology to the well-characterized nitrogenase complex, and are similarily composed of three protein subunits, namely BchN/ChlN, BchB/ChlB and BchL/ChlL (DPOR) and BchY, BchZ and BchX (COR), respectively.

In this study, the DPOR enzymes of various organisms were biochemically characterized in detail. Catalytic activity of chimeric DPOR enzymes composed of subunits from different organisms (*C. tepidum*, *P. marinus* and *T. elongatus*) indicated a conserved interaction surface for protein-protein-interaction. The involvement of both subunits, ChlN and ChlB, in the interaction with the $ChlL_2$ protein was shown. Important amino acid residues for catalysis and protein-protein-interaction of DPOR were identified.

A second part of this study focused on the biochemical analysis of the COR enzyme from different organisms. Based on the activity of COR with substrate analogs, a flexibility in substrate recognition was deduced. While ring A and ring E composition revealed a degree of flexibility for COR catalysis, substituents on ring D were found specific for substrate recognition.

To elucidate the potential evolution of the electron-transferring subunits of nitrogenase and nitrogenase-like enzymes, chimeric enzymes of DPOR, COR and nitrogenase were generated and investigated. While the failure to detect enzymatic activity for the chimeric enzyme of DPOR and nitrogenase indicates that both enzymes evolved significantly, the observed catalytic activity for the chimeric enzyme consisting of DPOR and COR suggests that subunits $BchX_2$ and $BchL_2$/$ChlL_2$ have evolved only sparingly from a common ancestor.

Overall, obtained results provided significant new insights into the mechanistic basis of enzyme catalysis and evolution for the formation of (bacterio)chlorophylls.

5 OUTLOOK

As outlined above, a detailed biochemically characterization of DPOR and COR as well as investigation of protein-protein-interaction surface of DPOR subunits was performed in this study. The following questions have to be addressed in future experiments:

- determination of the three-dimensional structure of DPOR and COR
- trapping the ternary protein complex of DPOR and COR
- analysis of kinetic parameters of COR

Concerning the oxygen-dependent cyclase, further studies have to be carried out for the characterization of the enzyme:

- identification of new subunits by transposon mutagenesis
- establishment of a robust activity assay

6 REFERENCES

Aldehni, M., Sauer, J., Spielhaupter, C., Schmid, R. and Forchhammer, K. (2003). Signal transduction protein P(II) is required for NtcA-regulated gene expression during nitrogen deprivation in the cyanobacterium *Synechococcus elongatus* strain PCC 7942. *J Bacteriol* **185,** 2582-2591.

Baker, M.E. (1994). Protochlorophyllide reductase is homologous to human carbonyl reductase and pig 20 beta-hydroxysteroid dehydrogenase. *Biochem J* **300,** 605-607.

Battersby, A.R. (2000) Tetrapyrroles: the pigments of life, pp. 507-526.

Beale, S.I. (1999). Enzymes of chlorophyll biosynthesis. *Photosynthetic Research* **60,** 43-73.

Beinert, H. (1983). Semi-micro methods for analysis of labile sulfide and of labile sulfide plus sulfane sulfur in unusually stable iron-sulfur proteins. *Anal Biochem* **131,** 373-378.

Biggins, D.R., Kelly, M. and Postgate, J.R. (1971). Resolution of nitrogenase of *Mycobacterium flavum* 30l into two components and cross reaction with nitrogenase components from other bacteria. *Eur J Biochem* **20,** 140-143.

Blankenship, R.E. and Hartman, H. (1998). The origin and evolution of oxygenic photosynthesis. *Trends Biochem Sci* **23,** 94-97.

Bollivar, D.W. (2006). Recent advances in chlorophyll biosynthesis. *Photosynth Res* **90,** 173-194.

Bollivar, D.W. and Beale, S.I. (1996). The Chlorophyll Biosynthetic Enzyme Mg-Protoporphyrin IX Monomethyl Ester (Oxidative) Cyclase (Characterization and Partial Purification from *Chlamydomonas reinhardtii* and *Synechocystis* sp. PCC 6803). *Plant Physiol* **112,** 105-114.

Bollivar, D.W., Suzuki, J.Y., Beatty, J.T., Dobrowolski, J.M. and Bauer, C.E. (1994). Directed mutational analysis of bacteriochlorophyll *a* biosynthesis in *Rhodobacter capsulatus*. *J Mol Biol* **237,** 622-640.

Bradford, M.M. (1976). A rapid and sensitive method for the quantitation of microgram quantities of protein utilizing the principle of protein-dye binding. *Anal Biochem* **72,** 248-254.

Bröcker, M.J. (2006). Charakterisierung der lichtunabhänigen Protochlorophyllid Oxidoreduktase aus *Chlorobium tepidum*. Diplomarbeit. Technische Universität Braunschweig.

Bröcker, M.J., Virus, S., Ganskow, S., Heathcote, P., Heinz, D.W., Schubert, W.D., Jahn, D. and Moser, J. (2008a). ATP-driven reduction by dark-operative protochlorophyllide oxidoreductase from *Chlorobium tepidum* mechanistically resembles nitrogenase catalysis. *J Biol Chem* **283,** 10559-10567.

Bröcker, M.J., Wätzlich, D., Uliczka, F., Virus, S., Saggu, M., Lendzian, F.,Scheer, H., Rüdiger, W., Moser, J. and Jahn, D. (2008b). Substrate Recognition of Nitrogenase-like Dark Operative Protochlorophyllide Oxidoreductase from *Prochlorococcus marinus*. *J Biol Chem* **283,** 29873-29881.

Brody, S.S. (1968). Low-temperature fluorescence excitation spectra for long-wavelength emission as a function of greening in *Euglena gracilis* and chlorophyll *a* concentration *in vitro*: a mathematical model to describe both systems. *Biophys J* **8,** 210-230.

Burke, D.H., Hearst, J.E. and Sidow, A. (1993). Early evolution of photosynthesis: clues from nitrogenase and chlorophyll iron proteins. *Proc Natl Acad Sci U S A* **90,** 7134-7138.

Burris, R.H. (1971) Chemistry and Biochemistry of Nitrogen Fixation. Plenum Press London, pp. 105 - 160.

Bursey, E.H. and Burgess, B.K. (1998). The role of methionine 156 in cross-subunit nucleotide interactions in the iron protein of nitrogenase. *J Biol Chem* **273,** 29678-29685.

Chereskin, B.M., Wong, Y.S. and Castelfranco, P.A. (1982). *In Vitro* Synthesis of the Chlorophyll Isocyclic Ring : Transformation of Magnesium-Protoporphyrin IX and Magnesium-Protoporphyrin IX Monomethyl Ester into Magnesium-2,4-Divinyl Pheoporphyrin A(5). *Plant Physiol* **70,** 987-993.

Chew, A.G. and Bryant, D.A. (2007). Chlorophyll biosynthesis in bacteria: the origins of structural and functional diversity. *Annu Rev Microbiol* **61,** 113-129.

Dailey, H.A. (2002). Terminal steps of haem biosynthesis. *Biochem Soc Trans* **30,** 590-595.

Dean, D.R., Bolin, J.T. and Zheng, L. (1993). Nitrogenase metalloclusters: structures, organization, and synthesis. *J Bacteriol* **175,** 6737-6744.

Eady, R.R. and Postgate, J.R. (1974). Nitrogenase. *Nature* **249,** 805-810.

Emerich, D.W. and Burris, R.H. (1978). Complementary functioning of the component proteins of nitrogenase from several bacteria. *J Bacteriol* **134,** 936-943.

Fidai, S., Hinchigeri, S.B., Borgford, T.J. and Richards, W.R. (1994). Identification of the PufQ protein in membranes of *Rhodobacter capsulatus*. *J Bacteriol* **176,** 7244-7251.

Frankenberg, N., Moser, J. and Jahn, D. (2003). Bacterial heme biosynthesis and its biotechnological application. *Appl Microbiol Biotechnol* **63,** 115-127.

Fujita, Y. (1996). Protochlorophyllide reduction: a key step in the greening of plants. *Plant Cell Physiol* **37,** 411-421.

Fujita, Y. and Bauer, C.E. (2000). Reconstitution of light-independent protochlorophyllide reductase from purified Bchl and BchN-BchB subunits. *In vitro* confirmation of nitrogenase-like features of a bacteriochlorophyll biosynthesis enzyme. *J Biol Chem* **275,** 23583-23588.

Fujita, Y., Matsumoto, H., Takahashi, Y. and Matsubara, H. (1993). Identification of a *nifDK*-like gene (ORF467) involved in the biosynthesis of chlorophyll in the cyanobacterium *Plectonema boryanum*. *Plant Cell Physiol* **34,** 305-314.

Ganskow, S. (2006). Heterologe Expression und Charakterisierung der lichtunabhängigen Protochlorophyllid Oxidoreductase aus *Chlorobium tepidum*. Diplomarbeit. Technische Universität Braunschweig.

Geck, M.K. and Kirsch, J.F. (1999). A novel, definitive test for substrate channeling illustrated with the aspartate aminotransferase/malate dehydrogenase system. *Biochemistry* **38,** 8032-8037.

Georgiadis, M.M., Komiya, H., Chakrabarti, P., Woo, D., Kornuc, J.J. and Rees, D.C. (1992). Crystallographic structure of the nitrogenase iron protein from *Azotobacter vinelandii*. *Science* **257,** 1653-1659.

Gough, S.P., Petersen, B.O. and Duus, J.O. (2000). Anaerobic chlorophyll isocyclic ring formation in *Rhodobacter capsulatus* requires a cobalamin cofactor. *Proc Natl Acad Sci U S A* **97,** 6908-6913.

Gough, S.P., Rzeznicka, K., Peterson Wulff, R., Francisco Jda, C., Hansson, A., Jensen, P.E. and Hansson, M. (2007). A new method for isolating physiologically active Mg-protoporphyrin monomethyl ester, the substrate of the cyclase enzyme of the chlorophyll biosynthetic pathway. *Plant Physiol Biochem* **45,** 932-936.

Griffiths, W.T. (1980). Substrate-specificity studies on protochlorophyllide reductase in barley (*Hordeum vulgare*) etioplast membranes. *Biochem J* **186,** 267-278.

Grimm, B., Porra, R.J., Rüdiger, W. and Scheer, H. (2006) Chlorophylls and Bacteriochlorophylls: Advances in Photosynthesis and Respiration, Vol. 25, Springer.

Guigliarelli, B. and Bertrand, P. (1999) Advances in Inorganic Chemistry, pp. 421-497.

Hagen, W.R. (1992) Advances in Inorganic Chemistry: EPR-spectroscopy of iron-sulfur proteins, pp. 165-222.

Hanahan, D. (1983). Studies on transformation of *Escherichia coli* with plasmids. *J Mol Biol* **166,** 557-580.

Helfrich, M., Schoch, S., Lempert, U., Cmiel, E. and Rüdiger, W. (1994). Chlorophyll synthetase cannot synthesize chlorophyll *a*'. *Eur J Biochem* **219,** 267-275.

Heyes, D.J., Kruk, J. and Hunter, C.N. (2006). Spectroscopic and kinetic characterization of the light-dependent enzyme protochlorophyllide oxidoreductase (POR) using monovinyl and divinyl substrates. *Biochem J* **394,** 243-248.

Hu, Y., Corbett, M.C., Fay, A.W., Webber, J.A., Hodgson, K.O., Hedman, B. and Ribbe, M.W. (2006). Nitrogenase Fe protein: A molybdate/homocitrate insertase. *Proc Natl Acad Sci U S A* **103,** 17125-17130.

Kelly, M. (1969). Comparisons and cross reactions of nitrogenase from *Klebsiella pneumoniae*, *Azotobacter chroococcum* and *Bacillus polymyxa*. *Biochim Biophys Acta* **191,** 527-540.

Kim, E.J., Kim, J.S., Lee, I.H., Rhee, H.J. and Lee, J.K. (2008). Superoxide generation by chlorophyllide *a* reductase of *Rhodobacter sphaeroides*. *J Biol Chem* **283,** 3718-3730.

Klement, H., Helfrich, M., Oster, U., Schoch, S. and Rüdiger, W. (1999). Pigment-free NADPH:protochlorophyllide oxidoreductase from *Avena sativa* L. Purification and substrate specificity. *Eur J Biochem* **265,** 862-874.

Kotzabasis, K. and Senger, H. (1986). Novel Chlorophyllides in Pigment Mutant C-2A' of *Scenedesmus obliquus*. *Naturwissenschaften* **73,** 681-682.

Kriek, M., Peters, L., Takahashi, Y. and Roach, P.L. (2003). Effect of iron-sulfur cluster assembly proteins on the expression of *Escherichia coli* lipoic acid synthase. *Protein Expr Purif* **28,** 241-245.

Laemmli, U.K. (1970). Cleavage of structural proteins during the assembly of the head of bacteriophage T4. *Nature* **227,** 680-685.

Lovenberg, W., Buchanan, B.B. and Rabinowitz, J.C. (1963). Studies on the Chemical Nature of Clostridial Ferredoxin. *J Biol Chem* **238,** 3899-3913.

Lüer, C., Schauer, S., Möbius, K., Schulze, J., Schubert, W.D., Heinz, D.W., Jahn, D. and Moser, J. (2005). Complex formation between glutamyl-tRNA reductase and glutamate-1-semialdehyde 2,1-aminomutase in *Escherichia coli* during the initial reactions of porphyrin biosynthesis. *J Biol Chem* **280,** 18568-18572.

Masoumi, A., Heinemann, I.U., Rohde, M., Koch, M., Jahn, M. and Jahn, D. (2008). Complex formation between protoporphyrinogen IX oxidase and ferrochelatase during haem biosynthesis in *Thermosynechococcus elongatus*. *Microbiology* **154,** 3707-3714.

Massant, J., Verstreken, P., Durbecq, V., Kholti, A., Legrain, C., Beeckmans, S., Cornelis, P. and Glansdorff, N. (2002). Metabolic channeling of carbamoyl phosphate, a thermolabile intermediate: evidence for physical interaction between carbamate kinase-like carbamoyl-phosphate synthetase and ornithine carbamoyltransferase from the hyperthermophile *Pyrococcus furiosus*. *J Biol Chem* **277,** 18517-18522.

Matsumoto, F., Obayashi, T., Sasaki-Sekimoto, Y., Ohta, H., Takamiya, K. and Masuda, T. (2004). Gene expression profiling of the tetrapyrrole metabolic pathway in *Arabidopsis* with a mini-array system. *Plant Physiol* **135,** 2379-2391.

May, H.D., Dean, D.R. and Newton, W.E. (1991). Altered nitrogenase MoFe proteins from *Azotobacter vinelandii*. Analysis of MoFe proteins having amino acid substitutions for the conserved cysteine residues within the beta-subunit. *Biochem J* **277,** 457-464.

McFeeters, R.F., Chichester, C.O. and Whitaker, J.R. (1971). Purification and Properties of Chlorophyllase from *Ailanthus altissima* (Tree-of-Heaven). *Plant Physiol* **47,** 609-618.

Milgrom, L.R. (1997) The Colours of Life. An Introduction to the Chemistry of Porphyrins and Related Compounds; Oxford University Press.

Moore, L.R., Goericke, R. and Chisholm, S.W. (1995). Comparative physiology of *Synechococcus* and *Prochlorococcus*: influence of light and temperature on growth, pigments, fluorescence and absorptive properties. *Mar. Ecol. Prog. Ser.* **116,** 259-275.

Moser, J., Schubert, W.D., Beier, V., Bringemeier, I., Jahn, D. and Heinz, D.W. (2001). V-shaped structure of glutamyl-tRNA reductase, the first enzyme of tRNA-dependent tetrapyrrole biosynthesis. *Embo J* **20,** 6583-6590.

Murphy, P.M. and Koch, B.L. (1971). Compatibility of the components of nitrogenase from soybean bacteroids and free-living nitrogen-fixing bacteria. *Biochim Biophys Acta* **253,** 295-297.

Nagata, N., Tanaka, R., Satoh, S. and Tanaka, A. (2005). Identification of a vinyl reductase gene for chlorophyll synthesis in *Arabidopsis thaliana* and implications for the evolution of *Prochlorococcus* species. *Plant Cell* **17,** 233-240.

Nakamura, Y., Kaneko, T., Sato, S., Ikeuchi, M., Katoh, H., Sasamoto, S., Watanabe, A., Iriguchi, M., Kawashima, K., Kimura, T., Kishida, Y., Kiyokawa, C., Kohara, M., Matsumoto, M., Matsuno, A., Nakazaki, N., Shimpo, S., Sugimoto, M., Takeuchi, C., Yamada, M. and Tabata, S. (2002). Complete genome structure of the thermophilic cyanobacterium *Thermosynechococcus elongatus* BP-1. *DNA Res* **9,** 123-130.

Nasrulhaq-Boyce, A., Griffiths, W.T. and Jones, O.T. (1987). The use of continuous assays to characterize the oxidative cyclase that synthesizes the chlorophyll isocyclic ring. *Biochem J* **243,** 23-29.

Nomata, J., Kitashima, M., Inoue, K. and Fujita, Y. (2006a). Nitrogenase Fe protein-like Fe-S cluster is conserved in L-protein (BchL) of dark-operative protochlorophyllide reductase from *Rhodobacter capsulatus*. *FEBS Lett* **580,** 6151-6154.

Nomata, J., Mizoguchi, T., Tamiaki, H. and Fujita, Y. (2006b). A second nitrogenase-like enzyme for bacteriochlorophyll biosynthesis: reconstitution of chlorophyllide *a* reductase with purified X-protein (BchX) and YZ-protein (BchY-BchZ) from *Rhodobacter capsulatus*. *J Biol Chem* **281,** 15021-15028.

Nomata, J., Ogawa, T., Kitashima, M., Inoue, K. and Fujita, Y. (2008). NB-protein (BchN-BchB) of dark-operative protochlorophyllide reductase is the catalytic component containing oxygen-tolerant Fe-S clusters. *FEBS Lett* **582,** 1346-1350.

Nomata, J., Swem, L.R., Bauer, C.E. and Fujita, Y. (2005). Overexpression and characterization of dark-operative protochlorophyllide reductase from *Rhodobacter capsulatus*. *Biochim Biophys Acta* **1708,** 229-237.

Ouchane, S., Steunou, A.S., Picaud, M. and Astier, C. (2004). Aerobic and anaerobic Mg-protoporphyrin monomethyl ester cyclases in purple bacteria: a strategy adopted to bypass the repressive oxygen control system. *J Biol Chem* **279,** 6385-6394.

Parham, R. and Rebeiz, C.A. (1995). Chloroplast biogenesis 72: a [4-vinyl]chlorophyllide *a* reductase assay using divinyl chlorophyllide *a* as an exogenous substrate. *Anal Biochem* **231,** 164-169.

Peters, J.W., Fisher, K. and Dean, D.R. (1995). Nitrogenase structure and function: a biochemical-genetic perspective. *Annu Rev Microbiol* **49,** 335-366.

Pinta, V., Picaud, M., Reiss-Husson, F. and Astier, C. (2002). *Rubrivivax gelatinosus acsF* (previously orf358) codes for a conserved, putative binuclear-iron-cluster-containing protein involved in aerobic oxidative cyclization of Mg-protoporphyrin IX monomethylester. *J Bacteriol* **184,** 746-753.

Porra, R.J., Schafer, W., Katheder, I. and Scheer, H. (1995). The derivation of the oxygen atoms of the 13(1)-oxo and 3-acetyl groups of bacteriochlorophyll *a* from water in *Rhodobacter sphaeroides* cells adapting from respiratory to photosynthetic conditions: evidence for an anaerobic pathway for the formation of isocyclic ring E. *FEBS Lett* **371,** 21-24.

Raymond, J., Zhaxybayeva, O., Gogarten, J.P., Gerdes, S.Y. and Blankenship, R.E. (2002). Whole-genome analysis of photosynthetic prokaryotes. *Science* **298,** 1616-1620.

Rees, D.C., Akif Tezcan, F., Haynes, C.A., Walton, M.Y., Andrade, S., Einsle, O. and Howard, J.B. (2005). Structural basis of biological nitrogen fixation. *Philos Transact A Math Phys Eng Sci* **363,** 971-984; discussion 1035-1040.

Righetti, P., Gianazza, E., Gelfi, C. and Chairi, M. (1990) Gel electrophoresis of proteins: a practical approach. 2nd edition, Oxford University Press.

Rippka, R., Desrulles, J., Waterbury, J.B., Herdman, M. and Stanier, R.Y. (1979). Genetic assignments, strain histories and properties of pure cultures of cyanobacteria. *J. Gen. Microbiol.* **111,** 1-61.

Roe, S.M., Gormal, C., Smith, B.E., Baker, P., Rice, D., Card, G. and Lindley, P. (1997). Crystallization and preliminary X-ray studies of nitrogenase component 1 (the MoFe protein) from *Klebsiella pneumoniae*. *Acta Crystallogr D Biol Crystallogr* **53,** 227-228.

Rost, B., Yachdav, G. and Liu, J. (2004). The PredictProtein server. *Nucleic Acids Res* **32,** W321-326.

Rüdiger, W., Bohm, S., Helfrich, M., Schulz, S. and Schoch, S. (2005). Enzymes of the last steps of chlorophyll biosynthesis: modification of the substrate structure helps to understand the topology of the active centers. *Biochemistry* **44,** 10864-10872.

Rzeznicka, K., Walker, C.J., Westergren, T., Kannangara, C.G., von Wettstein, D., Merchant, S., Gough, S.P. and Hansson, M. (2005). *Xantha-l* encodes a membrane subunit of the aerobic Mg-protoporphyrin IX monomethyl ester cyclase involved in chlorophyll biosynthesis. *Proc Natl Acad Sci U S A* **102,** 5886-5891.

Sambrook, J. and Russell, D.W. (2001) Molecular Cloning: A laboratory Manual Cold Spring Harbor, Cold Spring Harbor Laboratory Press.

Sanger, F., Nicklen, S. and Coulson, A.R. (1977). DNA sequencing with chain-terminating inhibitors. *Proc Natl Acad Sci U S A* **74,** 5463-5467.

Sarma, R., Barney, B.M., Hamilton, T.L., Jones, A., Seefeldt, L.C. and Peters, J.W. (2008). Crystal Structure of the L Protein of *Rhodobacter sphaeroides* Light-Independent Protochlorophyllide Reductase with MgADP Bound: A Homologue of the Nitrogenase Fe Protein. *Biochemistry* **47**, 13004-13015.

Schindelin, H., Kisker, C., Schlessman, J.L., Howard, J.B. and Rees, D.C. (1997). Structure of ADP x AIF4(-)-stabilized nitrogenase complex and its implications for signal transduction. *Nature* **387,** 370-376.

Schmid, B., Einsle, O., Chiu, H.J., Willing, A., Yoshida, M., Howard, J.B. and Rees, D.C. (2002a). Biochemical and structural characterization of the cross-linked complex of nitrogenase: comparison to the ADP-AlF4(-)-stabilized structure. *Biochemistry* **41,** 15557-15565.

Schmid, H.C., Rassadina, V., Oster, U., Schoch, S. and Rüdiger, W. (2002b). Pre-loading of chlorophyll synthase with tetraprenyl diphosphate is an obligatory step in chlorophyll biosynthesis. *Biol Chem* **383,** 1769-1778.

Shepherd, M. and Hunter, C.N. (2004). Transient kinetics of the reaction catalysed by magnesium protoporphyrin IX methyltransferase. *Biochem J* **382,** 1009-1013.

Smith, B.E., Thorneley, R.N., Eady, R.R. and Mortenson, L.E. (1976). Nitrogenases from *Klebsiella pneumoniae* and *Clostridium pasteurianum*. Kinetic investigations of cross-reactions as a probe of the enzyme mechanism. *Biochem J* **157,** 439-447.

Smith, J. and Calvin, M. (1966). Studies on the chemical and photochemical oxidation of bacteriochlorophyll. *Lawrence Berkeley National Laboratory*.

Smith, R.V., Telfer, A. and Evans, M.C. (1971). Complementary functioning of nitrogenase components from a blue-green alga and a photosynthetic bacterium. *J Bacteriol* **107,** 574-575.

Stesmans, A. and Van Gorp, G. (1989). Observation of the localized Si dangling-bond Pb defect at the Si/Si3N4 interface. *Phys Rev B Condens Matter* **39,** 2864-2867.

Stoll, S. and Schweiger, A. (2006). EasySpin, a comprehensive software package for spectral simulation and analysis in EPR. *J Magn Reson* **178,** 42-55.

Studier, F.W., Rosenberg, A.H., Dunn, J.J. and Dubendorff, J.W. (1990). Use of T7 RNA polymerase to direct expression of cloned genes. *Methods Enzymol* **185,** 60-89.

Suzuki, J.Y., Bollivar, D.W. and Bauer, C.E. (1997). Genetic analysis of chlorophyll biosynthesis. *Annu Rev Genet* **31,** 61-89.

Takahashi, Y. and Nakamura, M. (1999). Functional assignment of the ORF2-*iscS*-*iscU*-*iscA*-*hscB*-*hscA*-*fdx*-ORF3 gene cluster involved in the assembly of Fe-S clusters in *Escherichia coli*. *J Biochem* **126,** 917-926.

Terry, M. and Smith, A.G. (2009). Tetrapyrroles: Birth, Life and Death: Regulation of Tetrapyrrole Synthesis in Higher Plants. Springer

Tezcan, F.A., Kaiser, J.T., Mustafi, D., Walton, M.Y., Howard, J.B. and Rees, D.C. (2005). Nitrogenase complexes: multiple docking sites for a nucleotide switch protein. *Science* **309,** 1377-1380.

Townley, H.E., Sessions, R.B., Clarke, A.R., Dafforn, T.R. and Griffiths, W.T. (2001). Protochlorophyllide oxidoreductase: a homology model examined by site-directed mutagenesis. *Proteins* **44,** 329-335.

Uliczka, F. (2007). Überproduktion und Charakterisierung der lichtunabhängigen Protochlorophyllid Oxidoreduktase aus *Thermosynechococcus elongatus* und *Prochlorococcus marinus*. Diplomarbeit. Technische Universität Braunschweig.

Viney, J., Davison, P.A., Hunter, C.N. and Reid, J.D. (2007). Direct measurement of metal-ion chelation in the active site of the AAA+ ATPase magnesium chelatase. *Biochemistry* **46,** 12788-12794.

Wahlund, T.M. and Madigan, M.T. (1993). Nitrogen fixation by the thermophilic green sulfur bacterium *Chlorobium tepidum*. *J Bacteriol* **175,** 474-478.

Walker, C.J., Mansfield, K.E., Rezzano, I.N., Hanamoto, C.M., Smith, K.M. and Castelfranco, P.A. (1988). The magnesium-protoporphyrin IX (oxidative) cyclase system. Studies on the mechanism and specificity of the reaction sequence. *Biochem J* **255,** 685-692.

Wherland, S., Burgess, B.K., Stiefel, E.I. and Newton, W.E. (1981). Nitrogenase reactivity: effects of component ratio on electron flow and distribution during nitrogen fixation. *Biochemistry* **20,** 5132-5140.

Wilks, H.M. and Timko, M.P. (1995). A light-dependent complementation system for analysis of NADPH:protochlorophyllide oxidoreductase: identification and mutagenesis of two conserved residues that are essential for enzyme activity. *Proc Natl Acad Sci U S A* **92,** 724-728.

Willows, R.D. (2003). Biosynthesis of chlorophylls from protoporphyrin IX. *Nat Prod Rep* **20,** 327-341.

Wong, Y.S., Castelfranco, P.A., Goff, D.A. and Smith, K.M. (1985). Intermediates in the Formation of the Chlorophyll Isocyclic Ring. *Plant Physiol* **79,** 725-729.

Xiong, J. (2006). Photosynthesis: what color was its origin? *Genome Biol* **7,** 245.

Yamaoka, T., Satoh, K. and Katoh, S. (1978). Photosynthetic activities of a thermophilic blue-green alga. *Plant Cell Physiol.* **19,** 943-954.

Young, D.A., Bauer, C.E., Williams, J.C. and Marrs, B.L. (1989). Genetic evidence for superoperonal organization of genes for photosynthetic pigments and pigment-binding proteins in *Rhodobacter capsulatus*. *Mol Gen Genet* **218,** 1-12.

7 APPENDICES

Appendix A

Alignment Subunit ChlL

```
ChlL_Pm         ----MTT---TLANRPDGEGSVQVKLDPKVNIEEGALVIAVYGKGGIGKSTTSSNLSAAF 53
BchL_Ct         ----------------------------------MSLVLAVYGKGGIGKSTTSANISAAL 26
ChlL_Te         -------------------------MSLHYRGGKVNVKLAVYGKGGIGKSTTSCNISVAL 35
BchL_Rs         ----MSPKDLTIPTGADGEGSVQVHLD-EADKITGAKVFAVYGKGGIGKSTTSSNLSAAF 55
NifH_Av         ------------------------------MA---MRQCAIYGKGGIGKSTTTQNLVAAL 27
NifH_Ct         ----------------------------------MRKVAIYGKGGIGKSTTTQNTVAGL 25
NifH_Ava        ------------------------------MTDENIRQIAFYGKGGIGKSTTSQNTLAAM 30
NifH_Rs         ------------------------------MG--KLRQIAFYGKGGIGKSTTSQNTLAAL 28
BchX_Rd         MKDEVPNLKDFDKRLRDEAQAEPTLEVPQGEPASKTQIIAIYGKGGIGKSFTLANLSHMM 60
BchX_Ct         ------------MATRRANTFQPATRPT--EYLMAPRTIAIYGKGGIGKSFTTTNLSATF 46
BchX_Rs         -MTDAPELKAFDQRLRDEAAEEPTLEVPQGEPKKKTQVIAIYGKGGIGKSFTLANLSYMM 59
BchX_Rr         ----------MSAPLRDVAAITPAPLAS--TAKKETQVIAIYGKGGIGKSFTLANLSYMM 48

ChlL_Pm         SKLGKKVLQIGCDPKHDSTFTLTH-KMVPTVIDILEEVDFHSEELRPQDFMFEGFNG--- 109
BchL_Ct         ALKGAKVLQIGCDPKHDSTFPITG-KLQKTVIEALEEVDFHHEELSPEDIVETGFAG--- 82
ChlL_Te         ARRGKKVLQIGCDPKHDSTFTLTG-FLIPTIIDTLQAKDYHYEDVWPEDVIYKGYGG--- 91
BchL_Rs         SILGKRVLQIGCDPKHDSTFTLTG-SLVPTVIDVLKDVDFHPEELRPEDFVFEGFNG--- 111
NifH_Av         AEMGKKVMIVGCDPKADSTRLILH-SKAQNTIMEMAAEAGTVEDLELEDVLKAGYGG--- 83
NifH_Ct         AEAGKKVMVVGCDPKADSTRLLLG-GLQQKTVLDTLREEG--EEVELEDIIKEGYRN--- 79
NifH_Ava        AEMGQRIMIVGCDPKADSTRLMLH-AKAQTTVLHLAAERGAVEDLELHEVMLTGFRG--- 86
NifH_Rs         VEMGQKILIVGCDPKADSTRLILN-TKLQDTVLHLAAEAGSVEDLELEDVVKIGYKG--- 84
BchX_Rd         AEQGKRVLLIGCDPKSDTTSLLFGGKACPTIIETSTRKKLAGEEVKIGDVCFKRGG---- 116
BchX_Ct         AMMNKRVLQLGCDPKHDSTTSLFGGISLPTVTEVFAEKNAKNEQVQISDIVFRRDIPGFP 106
BchX_Rs         AQIGKRVLLIGCDPKSDTTSLLFGGKACPTIIETSARKKLAGEEVQIGDVCFKRDG---- 115
BchX_Rr         AQKGKRVLLIGCDPKSDTTSLLFGGRACPTIIETSSARKLAGEDLGIGDVCFKRDG---- 104

ChlL_Pm         --VQCVESGGPPAGTGCGGYVTGQTVKLLKEHHLLEDT---DVVIFDVLGDVVCGGFAAP 164
BchL_Ct         --IDGLEAGGPPAGSGCGGYVVGESVTLLQEMGVYDKY---DVILFDVLGDVVCGGFSAP 137
ChlL_Te         --VDCVEAGGPPAGAGCGGYVVGETVKLLKELNAFDEY---DVILFDVLGDVVCGGFAAP 146
BchL_Rs         --VMCVEAGGPPAGTGCGGYVVGQTVKLLKQHHLLDDT---DVVIFDVLGDVVCGGFAAP 166
NifH_Av         --VKCVESGGPEPGVGCAGRGVITAINFLEEEGAYEDD--LDFVFYDVLGDVVCGGFAMP 139
NifH_Ct         --TRCTESGGPEPGVGCAGRGIITSVNLLEQLGAYDDEWELDYVFYDVLGDVVCGGFAMP 137
NifH_Ava        --VRCVESGGPEPGVGCAGRGIITAINFLEENGAYQD---LDFVSYDVLGDVVCGGFAMP 141
NifH_Rs         --IKCTEAGGPEPGVGCAGRGVITAINFLEENGAYDD---VDYVSYDVLGDVVCGGFAMP 139
BchX_Rd         --VFAMELGGPEVGRGCGGRGIIHGFELLEKLGFHDWD--FDYVLLDFLGDVVCGGFGLP 172
BchX_Ct         QPIYGIELGGPQVGRGCGGRGIISGFDVLEKLGIFEWE--IDIILMDFLGDVVCGGFATP 164
BchX_Rs         --VFAMELGGPEVGRGCGGRGIIHGFELLEKLGFHDWD--FDYVLLDFLGDVVCGGFGLP 171
BchX_Rr         --VYAMELGGPEVGRGCGGRGIIHGFETLEKLGFHEWG--FDYVLLDFLGDVVCGGFGLP 160
                            *  .                          *

ChlL_Pm         LQH--ANYCLIVTANDFDSIFAMNRIVAAINAKAKNYK-VRLGGVIAN-----RSAELDQ 216
BchL_Ct         LNY--ADYAVIIATNDFDSIFAANRLCMAIQQKSVRYK-VQLAGIVANRVDYTKGGGTNM 194
ChlL_Te         LNY--ADYCLIVTDNGFDALFAANRIAASVREKARTHP-LRLAGLIGN-----RTNKRDL 198
BchL_Rs         LQH--ADQAVVVTANDFDSIYAMNRIIAAVQAKSKNYK-VRLAGCVAN-----RSRATDE 218
NifH_Av         IRENKAQEIYIVCSGEMMAMYAANNISKGIVKYANSGS-VRLGGLICN--SRNTDREDEL 196
NifH_Ct         IRDGKAEEIYIVCSGEMMAMYAANNICKGILKYADAGG-VRLGGLICN--SRKVDNEREM 194
NifH_Ava        IREGKAQEIYIVTSGEMMAMYAANNIARGILKYAHSGG-VRLGGLICN--SRKTDREAEL 198
NifH_Rs         IRENKAQEIYIVMSGEMMALYAANNIAKGILKYANSGG-VRLGGLICN--ERKTDRELEL 196
BchX_Rd         IARDMAQKVILVASNDLQSLYVANNVCSAVEYFRKLGGNVGVAGLVIN-----KDDGTGE 227
BchX_Ct         LARSLSEEVLLVTSNDRQSIFTSNNICQANNYFRTIGGRSRLLGLIVN-----RDDGSGM 219
BchX_Rs         IARDMAQKVILVGSNDLQSLYVTNNVCSAVEYFRKLGGNVGVAGLVIN-----KDDGTGE 226
BchX_Rr         IARDLCQKVIVVGSNDLQSLYVVNNVCSAVTYFRKMGGNVGVAGMVIN-----KDDGTGE 215
                  . .
```

```
ChlL_Pm         IEKFNEKTGLKTMAHFRNVDAIRRSRLKKCTIFEMDPEEEGVLEVQNEYLSLAKKMIDNV 276
BchL_Ct         LDQFAEQVGTRLLAKVPYHELIRKSRFAGKTLFAMDPNEPELAECLAPYNEIADQILS-E 253
ChlL_Te         IEKYVEAVPMPILEVLPLIEDIRVSRVKGKTLFEMAESDPSLNDVCDYYLNIADQILARP 258
BchL_Rs         VDRFCKETNFRRLAHMPDLDAIRRSRLKKKTLFEMD-EDQDVLAARAEYIRLAESLWRGL 277
NifH_Av         IIALANKLGTQMIHFVPRDNVVQRAEIRRMTVIEYDPKAKQADEYRALARKVVDNK-LLV 255
NifH_Ct         IEELARRLGTQMIHFVPRDNFVQRAEINRKTVIDFDPTHPQADEYRALAKKIDENK-MFV 253
NifH_Ava        IENLAERLNTQMIHFVPRDNIVQHAELRRMTVNEYAPDSNQGQEYRALAKKIINND-KLT 257
NifH_Rs         AEALAARLGCKMIHFVPRDNIVQHAELRRETVIQYAPESKQAQEYRELARKIHENSGKGV 256
BchX_Rd         AAAFAEAVDIPVLASIPQDDDLR--KKSANYQIVGTQESQWGDLFAMLGDNVA--VAPPQ 283
BchX_Ct         AENYAKAAGINVLMKVPYNLQAR--DMDDSFDFA-IKLPEVGEPFKKLATDILNNAITPC 276
BchX_Rs         AKAFAEAADIPILATIPADEDLR--RKSANYQIVGIPGTQWGPLFEGLAHAVG--EAPPI 282
BchX_Rr         AQAFAAKAGLPVLASIPADEDLR--RKSAAYQIVGRPGSPWGPLFEQLAINVG--EAPPL 271

ChlL_Pm         EPLE--AEPLKDRE-----------IFDLLG-FD-------------------------- 296
BchL_Ct         KPIASVPKPIGDRE-----------IFDIVGGWQ------------------------- 276
ChlL_Te         EGVV--PKDVPDRD-----------LFALLSDFYLNPQGSERSLAAV------------ 292
BchL_Rs         DPID--PHSLPDRD-----------IFELLG-FD-------------------------- 297
NifH_Av         IPNPITMDELEELL-----------MEFGIMEVEDE--SIVGKTAEEV------------ 290
NifH_Ct         IPKPLEIDELESLL-----------IEFGIAN---------------------------- 274
NifH_Ava        IPTPIEMDELEALL-----------IEYGILDDDSKHAEIIGKPAEATK----------- 295
NifH_Rs         IPTPITMEELEEML-----------MDFGIMQSEEDRLAAIAA-AEA------------ 291
BchX_Rd         RPTPLDQDGLLGLF-----------DASETG---GDYVLVPATDVDMR------------ 317
BchX_Ct         EASGLDFKDFVRLFGDVSEELPAAATADELFKRKGETAADPEAHDPERQQLLACIEKLPE 336
BchX_Rs         RPKPLSQDGLLDLF-----------TPEAIG---ADFKLEPATDADMR------------ 316
BchX_Rr         QPTPLDQDSLLGLF-----------SGDEVG---RDVVLEPATPEDMR------------ 305

ChlL_Pm         ---------------------------------------------
BchL_Ct         ---------------------------------------------
ChlL_Te         ---------------------------------------------
BchL_Rs         ---------------------------------------------
NifH_Av         ---------------------------------------------
NifH_Ct         ---------------------------------------------
NifH_Ava        ---------------------------------------------
NifH_Rs         ---------------------------------------------
BchX_Rd         ------------GKNAEPKPSLEVVYDDA-------------------- 334
BchX_Ct         PEREIYTLHEIEGKSPEQIAGLKGIGEQEVKAHIARARKAMRKLFFEL 384
BchX_Rs         ------------GKNAAAKKSLEVIYDDA-------------------- 333
BchX_Rr         ------------GGAVVEKASLEVVYDSV-------------------- 322
```

Appendix B

Alignment Subunit ChlN

```
ChlN_Pm         ----------------------------------------------------M---------SG 3
BchN_Ct         ----------------------------------------------MMPVS---------SD 7
ChlN_Te         ----------------------------------------------MTVTA---------PN 7
BchN_Rs         -----------------------------------MSLDLPPPPARGC---------RS 15
NifD_Av         -------MTGMSREEVESLIQEVLEVYPEKARKDRNKHLAVNDPAVTQS------KKCII 47
NifD_Ct         ------MEAKVLIPDPSKIKEELINKYPAKVAKKRSKSIVVNDPEIVPE---------VQ 45
NifD_Ava        MSPTESLNETTPVVDKKELIQDVLQAYPEKSRKRREKHLNVYE---EGK----SDCG-VK 52
NifD_Rs         ----MAKDIADSAETNMKLIEEVLAAYPDKARKKRAKHLNVAAPVAEAEPGLQSKCDNVK 56
BchY_Rd         ---MIKGHPHGDVSRVASDAPADAMGCHSGAD-MAEAARNAGQSELLDK---------FK 47
BchY_Ct         ------------------------------------------------------------
BchY_Rs         ----MSQTPGG------APMAPEAMGCHSTAD-MAAAASAAGNGELMER---------FK 40
BChY_Rr         ----MTELPAE--------AAQVVAGCHVGSDAMRRSAEVAGNGAVLAR---------YA 39


ChlN_Pm         STLLK-ETGPREVFCGLTSIVWLHRR-MPDAFFLVVGSRTCAHLIQSAAGVMIFAEPR-- 59
BchN_Ct         CQILK-EDNVTHSFCGLACVGWLYQK-IKDSFFLILGTHTCAHFLQNALGMMIFAKPR-- 63
ChlN_Te         ALNFECETGNYHTFCPISCVAWLYQK-IEDSFFLVIGTKTCGYFLQNAMGVMIFAEPR-- 64
BchN_Rs         TEVLK-ERGQREVFCGLTGIIWLHRK-MQDAFFLVVGSRTCAHLLQSAAGVMIFAEPR-- 71
NifD_Av          SNKKSQPGLMTIRGCAYAGSKGVVWGPIKDMIHISHGPVGCGQYSRAGRRN-YYIGTTGV 106
NifD_Ct         ANVRTVPGIITQRGCAYAGCKGVVLGPTRDIVNIVHGPIGCSFYAWLTRRNQTRPETPEH 105
NifD_Ava        SNIKSVPGTMTTRGCAYAGSKGVVWGPIKDMIHISHGPVGCGYYSWSGRRN-YYIGTTGI 111
NifD_Rs         SNIKSVPGVMTIRGCAYAGSKGVVWGPVKDMLHISHGPVGCGHYSWSQRRN-YYTGTTGV 115
BchY_Rd         ADYPVGPHDKPQSMCPAFGSLRVGLR-MKRVATVLSGSACCVYGLTFVS---HFYGAR-- 101
BchY_Ct         -------------MCPAFGGLRVLMR-IDGAQVCMAADQGCLYGLTFVS---HFYAAR-- 41
BchY_Rs         ADYPVGPHDKPQSMCPAFGSLRTGLR-MRRVGTIISGSACCTYGLSFVS---HFYGAR-- 94
BchY_Rr         ADYPAGPHDQPQSMCPAFGSLRVGLR-MRRTATVLSGSACCVYGLTFVS---HFYGAK-- 93
                                *                       .   *           .

ChlN_Pm         AEPRFGTAILEERDLAGLADAHEELDRVVKSLLKRRPEIRTLFLVGSCPSEVIKIDLSRA 115
BchN_Ct         AKPRFGVALIEEADLSRAEP---QLEAVIEEIK-RDHNPSVIFLLSSCTPEVMKVDFKGL 115
ChlN_Te         AEPRYAMAELEEGDISAQLNDYEELKRLCLEIK-RDRNPSVIVWIGTCTTEIIKMDLEGL 119
BchN_Rs         AEPRFGTAVLEEKDLAGLADANAELDREVDRLLARRPDIRQLFLVGSCPSEVIKLDLHRA 127
NifD_Av         VTMNFTSDFQEKDIVFGGD---KKLAKLIDEVETLFPLNKGISVQSECPIGLIGDDIESV 166
NifD_Ct         ITYCFSTDMQEEHVVFGGE---KKLKVAIQEAYDLFHP-KAIAIFSTCPVGLIGDDVHAV 164
NifD_Ava        GTMQFTSDFQERDIVFGGD---KKLAKLIDEIEELFPLNRGISIQSECPIGLIGDDIEAV 171
NifD_Rs         VTMQVTTDFQENDIVFGGD---KKLEKTIDELNMLFPLNKGISIQSECPIGLIGDDIEAV 175
BchY_Rd         ----RSVGYVPFNSESLVTGKLYEDIRDSVHELADPDRYDAIVVTNLCVPTASGVPLRLL 157
BchY_Ct         ----RSIVSPELMNAQISGGTMIDDVRCTIEKIAEDPSVRFIPVVSTCVAETAGIAEELL 97
BchY_Rs         ----RSIGYVPFNSESLVTGKLFEDIREAVHEMADPQRYDAIVVTNLCVPTASGVPLRLL 150
BchY_Rr         ----RSVAYVPFSSETLVTGKLFEDIRDAVEDLADPALYDAVVVTNLCVPTASGVPLRLL 149
                        *                                               .

ChlN_Pm         AERLSSQFNGQVRILNYSGSGIETTFTQGEDGALKALVPLMPSSQE-------------- 161
BchN_Ct         AHHLSTDK---TPVLFVPASGLVFNFTQAEDSVLQALVPFCPEAPA-------------- 158
ChlN_Te         APKLEAEIG--IPIVVARANGLDYAFTQGEDTVLAAMAARCPTSTAISDPEERNPIQRLL 177
BchN_Rs         AERLSAHHGPAVRVYNFSGSGIETTFTQGEDACLASIVPTLPATEA-------------- 173
NifD_Av         SKVKGAELSKT-IVPVRCEGFRGVSQSLGHHIANDAVRDWVLGKRDEDT-----TFA---- 217
NifD_Ct         AREMKEKLGDCNVFGFSCEGYRGVSQSAGHHIANNGVFKHMVGNNNEVK------------ 213
NifD_Ava        AKKKTKDTGKT-VVPVRCEGFRGVSQSLGHHIANDTIRDWVFPKADKAKKEGTLGFE---- 227
NifD_Rs         SKKKAKDIGKR-VVPVRCEGFRGVSQSLGHHIANDMIRDWVLEAGEGAR----AGYE---- 227
BchY_Rd         PKEINGVRIVGIDVPGFGVP----THAEAKDVLAGAMLNYARAEAMAGPVAAPVGGK---- 210
BchY_Ct         PKRVGNADVLLVRLPAFQIR----THPEAKDVAVSSLVKRFG----------AFGEP---- 140
BchY_Rs         PSEINGVRIVGIDVPGFGVP----THAEAKDVLAGAMLKYARSEIEAGPVQAPVSGR---- 203
BchY_Rr         PKAINGVRIIGIDVPGFGVP----THAEAKDILSGAMLAYARGEAEQGPVQAPRGGP---- 202
                .           .           . ...     :
```

```
ChlN_Pm         ----EQ---------------LLLAGTLAN-PVEDRLKTIFNRLGIQKVESFPPRESTKL 201
BchN_Ct         --GEKK---------------VVFVGSVND-ITADDLRTEAEQLGIPVGGFLPESRFDKL 200
ChlN_Te         NFGKKKEEVQAQSSQYHPHPPLVLFGSLPD-PVVTQLTLELKKQGIKVSGWLPAKRYTEL 236
BchN_Rs         ----RE---------------LLLVGALPD-VVEDQAVSLLTQLGIGPVRCLPAHHAAEA 213
NifD_Av         -STPYD---------------VAIIGDYNIGGDAWSSRILLEEMGLRCVAQWSGDGSISE 261
NifD_Ct         -PGKFK---------------LNLLGEYNIGGDAFEIERLLEKCGITLVASFSGNSTVGA 257
NifD_Ava        -PGPYD---------------VAIIGDYNIGGDAWSSRILLEEIGLRVVAQWSGDGTLHE 271
NifD_Rs         -PGPYD---------------VNIIGDYNIGGDAWSSRILLEEIGLNVIAQWSGDATIAE 271
BchY_Rd         --SARP---------------TVAMLGEMFP-ADPMMIGQMLAPMGLAAGPVLPCREWREL 253
BchY_Ct         --KKGK---------------TLVVLGEIFP-VDAMMIGGVLQKIGVESVITLPGADLDDY 183
BchY_Rs         --SDRP---------------TVALLGEMFP-ADPVMIGALLAPLGLAAGPVVPCRDWREL 246
BchY_Rr         --ASRP---------------TITLLGEMFP-ADPMGIGAMLDPLGLAVGPVVPVGEWRQL 245
                                     : . *                 *:      .

ChlN_Pm         PAIGPGTKVLLAQPYLTD-TARELKD-RGAEILQAPFPLGVEGSQLWIEAAANAF--KIK 257
BchN_Ct         PAIGPDTVLAPIQPYLSR-VCSRLNRERGSQVLTSLFPFGPDGTKTFWEDLAAMF--GIK 257
ChlN_Te         PVIDEGYYVAGVNPFLSR-TATTLIRRRKCQLITAPFPIGPDGTRTWIEQICATF--GIQ 293
BchN_Rs         PGVGPNTVFALVQPFLGD-THGALTR-RGARHIAAPFPFGEEGTTLWLKAIADEF--GVS 269
NifD_Av         IELTPKVKLNLVHCYRSMNYISRHMEEKYGIPWMEYNFFGPTKTIESLRAIAAKF-DESI 320
NifD_Ct         IENAHTADLNVIMCHRSINYMGDMMETKYGIPWMKVNFVGAESTAKSLRKIAEYFGDEEL 317
NifD_Ava        MMLTPSVKLNLVHCYRSMNYIARHMEETYGIPWLEYNFFGPTQIAKSLREIAAKF-DETI 330
NifD_Rs         MERAPAAKLNLIHCYRSMSYICRHMEENHGVPWMEYNFFGPSQIAASLRAIAAKF-DDRI 330
BchY_Rd         YAALDCAVVAAIHPFYVD-TVREFKA--AGRPVVGSAPVGYDGTAAWLKAIGETH--GVS 308
BchY_Ct         VQAGRASACAVLHPFYER-TAALFES--AGVKIVGGNPIGANATGQWIERIGEAL--DLD 238
BchY_Rs         YAALDSGVAAAIHPFYTA-SVREFQA--AGRAIVGSAPVGHDGTAAWLAAIGEAY--GIA 301
BchY_Rr         YAALDCAAVAAIHPFYTA-SLREFAA--AGRTAVGSAPVGRDGTAAWLAAIGEAC--GIA 300
                              .                 .*

ChlN_Pm         KTLVDATLEPLITRAHKALKPYVEQLSGKKLFLLPESQLEIPLARFLSNECGMKLIEVGV 317
BchN_Ct         VD-----LSDRAEAAWEKIKPQTDLLKGKKIFLTADTMMELPLARFLKN-AGAEVVECSS 311
ChlN_Te         PQG----LAEREAETWQKLSDYLELVRGKSVFFMGDNLLEISLARFLIR-CGMRVLEIGI 348
BchN_Rs         ADTFEAVTAAPRARARKAVAAASEGLRGKSVFFLPDSQLEPSLARFLTRECGMSAVEVGT 329
NifD_Av         QKKCEEVIAKYKPEWEAVVAKYRPRLEGKRVMLYIGGLRPRHVIGAYED-LGMEVVGTGY 379
NifD_Ct         KAKVEEVIAEEVPAVKAIIDEIRPRTEGKTAMLFVGGSRAHHYQDLFSE-LGMTTIAAGY 376
NifD_Ava        QAKTEEVIAKYEAQTKAVLDKYRSRLEGKTVALMVGGLRPRHVVPAFED-LGMKLIGTGY 389
NifD_Rs         QANAEAVIAKYQPLVDAVNAKYKPRLEGKKVMLYVGGLRPRHVVDAYHD-LGMEIVGTGY 389
BchY_Rd         AEDIAAAQNAVLPAIRGALG--ATPING-TITLSGYEGSELLVARLLIE-SGANVPYVGT 364
BchY_Ct         PETVKTVAEEERQKAKGMMAGFAERMHG-SVIVAGYEGNELPLVRLLLE-AGLDVPYAST 296
BchY_Rs         ADKVAAAQNAFLPAIRGALA--GAPIKG-RITLSGYEGSELIVARLLIE-SGAEVPYVGT 357
BchY_Rr         AAKVATAQNRFLPLIGEALA--KAPIRG-RITLSGYEGSELIVARVLVE-SGADVAYVGT 356
                                        *    .                 *      .

ChlN_Pm         PYLNREMMGP------------------------------------------------------ 327
BchN_Ct         AYINKKFHAR------------------------------------------------------ 321
ChlN_Te         PYMDKRYQAA------------------------------------------------------ 358
BchN_Rs         PFLHRGILGP------------------------------------------------------ 339
NifD_Av         EFAHNDDYDR------------------------------------------------------ 389
NifD_Ct         EFAHRDDYEGREVLPKIKIDADSKNIEELKVTADPELYNPRKSKAELEELKAKGLEINGY 436
NifD_Ava        EFGHNDDYKR------------------------------------------------------ 399
NifD_Rs         EFAHNDDYKR------------------------------------------------------ 399
BchY_Rd         ACANSPWSAD------------------------------------------------------ 374
BchY_Ct         SIARTALGEE------------------------------------------------------ 306
BchY_Rs         AAGRTPWSAA------------------------------------------------------ 367
BchY_Rr         ACPRTPWSED------------------------------------------------------ 366
```

```
ChlN_Pm         --ELDLLPQN--------TRIVEGQHVEKQLDRVREHHPDLVVCGMGLANPLEAEGISTK 377
BchN_Ct         --ELEALEG---------VKVVEQPNFHRQLEEIRATRPDMIVTSLMTANPFVGNGFIVK 370
ChlN_Te         --ELALLSQTCAEMGHPLPTIVEKPDNYNQLQRIKALQPDLVITGMAHANPLEARGISTK 416
BchN_Rs         --DLDLIAEG--------PVLSEGQDVERQLDRVRAARPDLTVCGLGLANPLEAEGFTTK 389
NifD_Av         --TMKEMGDS--------TLLYDDVTGYEFEEFVKRIKPDLIGSGIKEKFIFQKMGIPFR 439
NifD_Ct         EGMMKQMMKK--------TLVVDDISHYESEKLIEMYKPDIFCAGIKEKYVVQKMGVPLK 488
NifD_Ava        --TTHYVENG--------TLIYDDVSAYEFEQFVKALKPDLIASGIKEKYVFQKMALPFR 449
NifD_Rs         --TGHYIKEG--------TLIFDDVSGYELEKFVEAIRPDLVGSGIKEKYNTQKMGIPFR 449
BchY_Rd         --DAAWLEAKG-------VKVKYRASLEDDCAAMEAIQPDLAIGTTPVVQKAKQLGIPGL 425
BchY_Ct         --DHRLLTMLG-------TEVRYRKYLEEDMEAVLEHKPDLVIGTTSLDSFAKEHGIPAI 357
BchY_Rs         --DREWLEARG-------TVVKFRASLEDDLAAMQGFEPDLAVGTTPVVQKAKSLGIPSL 418
BchY_Rr         --DRAWLEARG-------VPVKFRASLEDDLAAVDALAPDLAIGTTPVVQHAKQKAIPAL 417
                      :             :            :    **:              ..

ChlN_Pm         WSIEMVFS-PIHGIDQASDLAELFARPLHRQNLLNKKT----LEAV-------------- 418
BchN_Ct         WSMEFTLM-SIHSWSGVFTLANLFVSPLLRRESLPEFDESVWLEGVMPSAQ--------- 420
ChlN_Te         WSVEFTFA-QIHGFGNARDILELVTRPLRRNQALAGLG---WQKLVAH------------ 460
BchN_Rs         WAIELVFT-PVHFYEQAGDLAGLFSRPVRRRAILRREA----AE---------------- 428
NifD_Av         QMHSWDYSGPYHGFDGFAIFARDMDMTLNNPCWKKLQAPWEASEGAEKVAASA------- 492
NifD_Ct         QLHSYDYGGPYTGFKGAVNFYKDIDRMVNNPVWKMIKAPWEKSEPESLEASYVAS----- 543
NifD_Ava        QMHSWDYSGPYHGYDGFAIFARDMDLALNSPTWSLIGAPWKK------------------ 491
NifD_Rs         QMHSWDYSGPYHGYDGYAIFARDMDLAINNPVWGMFDAPWKKTA---------------- 493
BchY_Rd         YFTNLISARPLMGVAGAGSLATVINAAIGNKERMAHMQEFFEGVGAGDTAGVWEGAPNLR 485
BchY_Ct         YYTNNISARPIFFASGAASVLGMIAGLLEKREIYGRMKEYFMPSA--------------- 402
BchY_Rs         YFTNLISARPLMGPAGAGSLAQVINAAIGNRERMSKMKAFFAGVGEGDTAGIWEGAPNLR 478
BchY_Rr         YFTNLISARPLMGPAGAGSLAQVINAALANKARFETMRAFFEGPAEG------EGGR--- 468
                   .               .   .   :

ChlN_Pm         ------------------------
BchN_Ct         ------------------------
ChlN_Te         ------------------------
BchN_Rs         ------------------------
NifD_Av         ------------------------
NifD_Ct         ------------------------
NifD_Ava        ------------------------
NifD_Rs         ------------------------
BchY_Rd         PDFRAQHQKKLDKLARAAKAQEMI 509
BchY_Ct         ------------------------
BchY_Rs         PDFRAAHQKKLEKAARAAKSEEMI 502
BchY_Rr         ------------------------
```

Appendix C

Alignment Subunit ChlB

```
ChlB_Pm         ------------------------------------------------------------M 1
BchB_Ct         ------------------------------------------------------------M 1
ChlB_Te         ------------------------------------------------------------M 1
BchB_Rs         ------------------------------------------------------------M 1
NifK_Av         MSQQVDKIKASYPLFLDQDYKDMLAKKRDGFEEKYPQDKIDEVFQWTTTKEYQELNFQRE 60
NifK_Ct         ----------------------MLLR--------------------HTTKEVKE-----RE 14
NifK_Ava        MPQNPERIVDHVDLFKQPEYTELFENKRKNFEGAHPPEEVERVSEWTKSWDYREKNFARE 60
NifK_Rs         MPQSAEKVLDHKDLFKEPEYQAMLEKKRATYENATPAETVAETADWTKSWDYREKNLARS 60
BchZ_Rd         ------------------------------------------------------------
BchZ_Ct         ------------------------------------------------------------MA 2
BchZ_Rs         ------------------------------------------------------------
BchZ_Rr         ------------------------------------------------------------

ChlB_Pm         ELTLWTYEGPPHIGAMRIATSMKGLHYVLHAPQGDTYADLLFTMIERRGSRPPVTYTTFQ 61
BchB_Ct         RLAFWLYEGTALHGVSRVTNSMKGVHTVYHAPQGDDYITATYTMLERTPEFPKLSISVVR 61
ChlB_Te         KLAYWMYAGPAHIGTLRIASSFKNVHGIMHAPLGDDYFNVMRSMLERERDFTPVTASIVD 61
BchB_Rs         KLTLWTYEGPPHVGAMRVATGMTGMHYVLHAPQGDTYADLLFTMIERRGKRPPVSYTTFQ 61
NifK_Av         ALTVNPAKACQPLGAVLCALGFEKTMPYVHGSQG-CVAYFRSYFNRHFREPVSCVSDSMT 119
NifK_Ct         GLTINPAKTCQPIGAMYAALGIHGCLPHSHGSQG-CCAYHRSTLTRHYKEPVMAATSSFT 73
NifK_Ava        ALTVNPAKGCQPVGAMFAALGFEGTLPFVQGSQG-CVAYFRTHLSRHYKEPCSAVSSSMT 119
NifK_Rs         CVTINPAKACQPLGAVFAAAGYDSTMSFVHGSQG-CVAYYRSHLARHFKEPSSAVSSSMT 119
BchZ_Rd         MLVTDHDRAGGYWGAVYAFCAVKGLQVVIDGPVG--CENLPVTSVLHYTDALPPHELPIV 58
BchZ_Ct         KTIRDESTASAYWAAVNTFCALKDVHVIADAPVG--CYNLAGVAVMDYTDAIPYLEN-LT 59
BchZ_Rs         MLVQDHDRAGGYWGAVYAFCAVKGLQVVIDGPVG--CENLPVTSVLHYTDALPPHELPIV 58
BchZ_Rr         MMLLDHDRAGGYWGAVYVFGALKGLQVVIDGPVG--CENLPVTAVLHYTDALPPHELPIV 58

ChlB_Pm         ARDLGGDTAELVKGHIFEAVERFKPEALLVGESCTAELIQDQPGSLAKG----MGLN--I 115
BchB_Ct         GQDLARGTS-RLPGTVEQVDKHYKPELIVVAPSCSTALLQEDLGQMAR-----ASGVDQS 115
ChlB_Te         RHVLARGSQEKVVDNIIRKDTEEHPDLIVLTPTCTSSILQEDLQNFVRR----ASLSTTA 117
BchB_Rs         ARDLGSDTAELFQSACRDAYERFQPQAIMVGSSCTAELIQDDTGGLADA----LSLP--V 115
NifK_Av         EDAAVFGGQQNMKDGLQNCKATYKPDMIAVSTTCMAEVIGDDLNAFINNSKKEGFIPDEF 179
NifK_Ct         EGASVFGGQANLLSAIETIFTVYDPEVIAVHSTCLSETIGDDLQQITKKASDDGKIPEGK 133
NifK_Ava        EDAAVFGGLNNMVEGMQVAYQLYKPKMIAVCTTCMAEVIGDDLGAFITNSKNAGSIPQDF 179
NifK_Rs         EDAAVFGGLNNMVEGLANTYALYSPKMIAVSTTCMAEVIGDDLNSFIIKSKEKESVPADF 179
BchZ_Rd         VTGLGEGEMG-SGTEESMKRAWDTLDPA-LPAVVVTGSIAEMIGGG--------VTPQGT 108
BchZ_Ct         PTSLTEREISSSGSSQIVQETIEKLMGSGKQLILVSSAESEMIGSDHQH----MLAMKYP 115
BchZ_Rs         VTGLGESEMS-EGTEASMSRAWKVLDPA-LPAVVVTGSIAEMIGGG--------VTPQGT 108
BchZ_Rr         VTGLGESELGRDGTEAAMTRAHATLDPS-RPAVVVTGSIAEMIGGG--------VTPAGT 109

ChlB_Pm         PIVSLELPAYSKKENWGASETFYQLIRGLLKEISEDSSNNAKQSWQEEGRRP-RVNLLGP 174
BchB_Ct         KIMVYAVNPFRVAENEAAEGLFTELVRRFAAEQ-------------PKTEKP-SVNLLGF 161
ChlB_Te         DVLLADVNHYRVNELQAADRTLEQIVQFYIDKARRQGTLGT-----SKTPTP-SVNIIGI 171
BchB_Rs         PVVHLELPSYQRKENFGADESFLQICRKLARPM-------------ERTEKV-SCNLLGP 161
NifK_Av         PVPFAHTPSFVGSHVTGWDNMFEGIARYFTLKSM----------DDKVVGSNKKINIVPG 229
NifK_Ct         YVIYASTPSYVGSHITGYANMVTSMTEQFAV--------------STGEKKDQVNVIAG 178
NifK_Ava        PVPFAHTPSFVGSHVTGYDNMMKGILSNLTE-------------GKKKATSNGKINIIPG 226
NifK_Rs         PVPFAHTPAFVGSHVDGYDNMQKGILSNFWK-------------DAPRTAGEG-LNIIPG 225
BchZ_Rd         NIQRFLPRTIDEDQWEAADRAMTWIFTEFGMTKGRMPPEKKR----GEGARP-RVNILGP 163
BchZ_Ct         SVRFFASDSLGENEWQGRDRALAWLFDQFDDGQ-------------PSQIEPGTVSIIGP 162
BchZ_Rs         NIQRFLPRTIDEDQWEAADRAMTWIFSEFGMTKGRMPPEAKR----PEGAKP-RVNILGP 163
BchZ_Rr         GLKRFLPRTIDEDQWQSADRALRWLWSEFGAGKRTKTP--AR----PAEAKP-RVNIIGP 162
```

```
ChlB_Pm         SLLGFRCRDDVLEIQKILGENGIDINVIAP------------------LGASPSDLMRLP 216
BchB_Ct         TSLGFHLRSNLTSLRRMLKTLGIEVNVVAP------------------WGAGIDDLKKLP 203
ChlB_Te         TTLGFHNQHDCRELKQLMADLGIQVNLVIP------------------AAATVHDLQRLP 213
BchB_Rs         TALGFRHRDDILEVTRLLEGMGIAVNAVAP------------------MGASPADIARLG 203
NifK_Av         FETY---LGNFRVIKRMLSEMGVGYSLLSDPEEVLDTPADGQFRMYA-GGTTQEEMKDAP 285
NifK_Ct         WMEP----SDMREIKSLASRLGVKIVLFPDTSDVLDAPQTGKHEFYPKGGITINELKSAG 234
NifK_Ava        FDTY---VGNNREVKRMLGVMGVDYTILSDSSDYFDSPNTGEYEMYP-GGTKLEDAADSI 282
NifK_Rs         FDGYC--VGNVREMKRMLGLMGVEATVLGDASDVYDTPSDGEYRMYA-GGTTQEEIKEAL 282
BchZ_Rd         MYGTFNMPSDLAEIRRLVEGIGCEVNMVLP------------------LGAHVAEMRNLV 205
BchZ_Ct         TYGCFNSPADLAEVKRLVTGAGGRVAHVYP------------------FESKAAEITKLK 204
BchZ_Rs         MYGVFNMASDLHEIRRLVEGIGAEVNMVMP------------------LGAHLAEMRHLV 205
BchZ_Rr         SYGMFNMWSDIAEIRRLVEGIGAEIALEFP------------------LGSHLDDVPRLA 204
                         :   :  :    *                            :

ChlB_Pm         KADANVCLYPEIAESTCLWLERNFKTPF-TKVVPIGVKATQDFLEELYELLGMEVSNSIS 275
BchB_Ct         AAWVNIAPFREIGCQAAGYLKEKFGMPS-ITEAPLGVNATLRWLRAIIAEVNKIGAEKGM 262
ChlB_Te         QAWFNLVPYREIGGLTAQYLEREFGQPS-VRITPMGVVETARCIRAIQGVLNAQGAGVNY 272
BchB_Rs         AAHFNVLLYPETGESAARWAEKTLKQPY-TKTVPIGVGATRDFVAEVAALAGVAP---VA 259
NifK_Av         NALNTVLLQPWHLEKTKKFVEGTWKHEVPKLNIPMGLDWTDEFLMKVSEISGQPIPASLT 345
NifK_Ct         DSKCSLAVGCISAEPAAIALEKKCKVPFETVDMPIGLSATDRFIMALSKAGSVKVPDEIT 294
NifK_Ava        NAKATVALQAYTTPKTREYIKTQWKQET-QVLRPFGVKGTDEFLTAISELTGKAIPEELE 341
NifK_Rs         NAKATLSLQEYCTRRTLAFCEEVGQETA-SFHYPMGVKATDEFLMKVSDLTGKEIPEALR 341
BchZ_Rd         NADVNICMYREFGRGLSELLAKPYLQ------APIGVESTTKFLRALGNLVGLDPEP--F 257
BchZ_Ct         NSAAIVVMYREFGAALAEKLGRPVLY------APFGIEETDRFIGKIGRLCGTPEQATRF 258
BchZ_Rs         NADANIVMYREFGRGLAEVLGKPYLQ------APIGVESTTAFLRRLGEILGLDPEP--F 257
BchZ_Rr         EADVNICLYREFGRGLCEALGKPYLQ------APIGLHSTTAFLRTLGQLLGLDPEP--F 256
                 :   :                          *:*:  *   :  :    .

ChlB_Pm         NSDQSKLP---------------WYSKSVDSNYLTGKRVFIFGDGTHVLAAARIANEELG 320
BchB_Ct         APMAMPELRDFSLDGQSAPSSVPWFARTADMESFSNKRAFVFGDATQVVGVTKFLKDELG 322
ChlB_Te         EAFIEQQTREVSQ--------AAWFSRSIDCQNLTGKKAVVFGDNTHAAAMTKILSREMG 324
BchB_Rs         DDSRLRQP---------------WWSASVDSTYLTGKRVFLFGDATHVIAAARVARDEMG 304
NifK_Av         KERGRLVD-----------------MMTDSHTWLHGKRFALWGDPDFVMGLVKFLLELGC 388
NifK_Ct         AERGRLVD-----------------VMVDMEQYFYGKKVALFGDPDQLIPLTEFLLDLGM 337
NifK_Ava        IERGRLVD-----------------AITDSYAWIHGKKFAIYGDPDLIISITSFLLEMGA 384
NifK_Rs         LERGRLID-----------------AMADSQAYLHGKTYAIFGDPDFVYAMARFVMEMGG 384
BchZ_Rd         ITQEKHSTIKPVWD----------LWRSVTQDFFATASFGIVANETYARGIRQFLENDLG 307
BchZ_Ct         IAEEKRTTLSPVWD----------LWRGPQSEWFPTIRFGVVASKSYADGIKHVLGDELG 308
BchZ_Rs         IEREKHSTLKPVWD----------LWRSVTQDFFGTANFGIVATETYARGIRNYLEGDLG 307
BchZ_Rr         IEREKQTTIKPLWD----------LWRSVTQDFFGTASFGIAANETYSRGVRHFLEEEMG 306
                                         :      : .

ChlB_Pm         FEVVGIGTYSREMARKVRAAATELGL-EALITNDYLEVEESIKECAPELVLGTQMERHSA 379
BchB_Ct         MKIIGAGTYLPKQADWVREQLEGYLPGELMVTDKFQEVSAFIEEEMPELVCGTQMERHSC 382
ChlB_Te         IHVVWAGTYCKYDADWFRAEVAGFCD-EVLITDDHTVVGDAIARVEPAAIFGTQMERHVG 383
BchB_Rs         FEVVGMGCYNREFARPMRAAAKGYGL-EALVTDDYLEVEEAIQALAPELILGTQMERHIA 363
NifK_Av         EPVHILCHN----------------------------GNKRWKKAVDAILAASPYGKNAT 420
NifK_Ct         IPAHIVSGT----------------------------PGLRFEKRMKEILERAP-GANFR 368
NifK_Ava        EPVHILCNN----------------------------GDDTFKKEMEAILAASPFGKEAK 416
NifK_Rs         EPKHCLATN----------------------------GGKDWEVQMKELLASSPFGEGCQ 416
BchZ_Rd         FPCAFAVARIAGKKTNNEEVRAMIGQ---------KKPLIVLGSINEKMYLAEQKAGFGP 358
BchZ_Ct         MQCLFSLDS---AEVDNNAVRKEIVQ---------KQPQFLYGRMPDKIYLAEADA---- 352
BchZ_Rs         LPCAFAVARKRGSKTDNEAVRGLIRQ---------HRPLVLMGSINEKIYLAELKAGHGP 358
BchZ_Rr         LPCRFSFARKAGSKTDNQAIRQAIKD---------TPPLVLFGSFNERMYLAEANG---- 353
```

```
ChlB_Pm         KRLGIPCAVISTPMHVQDVPARYSPQMGWEGANVIFDDWVHPLMMGLEEHLIGMFRHDFE 439
BchB_Ct         RKLDVPCMVISAPTHIENHLLGYYPFFGFDGADVMADRVYTSAKLGLEKHLIDFFGDAGL 442
ChlB_Te         KRLNIPCGVIAAPIHIQDFPVGYRPFLGYEGTNQLVDLIYNSFTLGMEDHLLEIFG---- 439
BchB_Rs         KRLGIPCAVISAPVHVQDFPARYSPQMGFEGANVLFDTWIHPLTMGLEEHLLTMFREDFE 423
NifK_Av         VYIGKDLWHLRSLVFTDKP----DFMIGNSYGKFIQRDTLHKGKEFEVPLIRIGFP---- 472
NifK_Ct         NGPQADMFLMHQWIKNEPV----DLLIGNTYGKYIARDED-------IPFVRFGFP---- 413
NifK_Ava        VWIQKDLWHFRSLLFTEPV----DFFIGNSYGKYLWRDTK-------IPMVRIGYP---- 461
NifK_Rs         VWAGKDLWHLRSILATEPA----DLLIGSSYGKYLERDCN-------VPLIRLTFP---- 461
BchZ_Rd         APAFIPASFPGAAIRRHTG----TPFMGYAGATYLLQEICN----GLFDALFHILP---- 406
BchZ_Ct         KSRFIPAGFPGPIVRRALG----TPFMGHSGVVWLVQEIVN----ALYDTLFNFLP---- 400
BchZ_Rs         QPSFIAASFPGAAIRRATG----TPVMGYAGATWLLQEVCN----ALFDALFHILP---- 406
BchZ_Rr         RGAYVPASFPGAIIRRHTG----TPFMGYSGATYLVQEVCN----ALFDMLFNILP---- 401
                                       :*      :             :

ChlB_Pm         FTDGH-QSHLGHLGGHASETKT-------------SSKGINQSPNNHSPAGES------I 479
BchB_Ct         EYEAEEPEAFTEPTMSGNGTVA----------------SVSSAEAPSEAAVVTATATGEL 486
ChlB_Te         ----------------GHDTKA----------------VIHKGLS----------ADSDL 457
BchB_Rs         FHDEAGPSHHGGKAVPASAPRADEAAEALPLTGAETAEGGSIPPEAVPPAEAAAVPAGEI 483
NifK_Av         ----------------------------------------------------IFDRHHLH 480
NifK_Ct         ----------------------------------------------------ILDRIGHS 421
NifK_Ava        ----------------------------------------------------LFDRHHLH 469
NifK_Rs         ----------------------------------------------------IFDRHHHH 469
BchZ_Rd         ---------------LGTDMDA----------------TDATLTPLRRDFPWDEDAQAML 435
BchZ_Ct         ---------------ITRRQQA----------------AAPTKP-----LKWTPEANAIL 424
BchZ_Rs         ---------------LGTEMDS----------------AAATPTTLRRDFPWDADAQAAL 435
BchZ_Rr         ---------------MARDLDA----------------VEATPSRMHDELPWDDEARAVL 430

ChlB_Pm         HWTSEGESELAKIPFFVRGKVRRNTEKYARQAGCREIDGETLLDAKAHFGA------- 530
BchB_Ct         SWTAEAEKMLGKVPFFVRKKVRKNTDNYAREIGEPVVTADVFRKAKEHLGG------- 537
ChlB_Te         TWTAAGLAELNKIPGFVRGKVKRNTEKFAREQGISEITVEVLYAAKEAVGA------- 508
BchB_Rs         VWLTDAERELKKIPFFVRGKARRNTEKFAAEKGLTRISLETLYEAKAHYAR------- 534
NifK_Av         RSTTLGYEGAMQILTTLVNSILERLDEETRGMQATDYNHDLVR---------------- 523
NifK_Ct         YFPNVGYSGSLRLVEKILGVLMDRQDR-----TSLEEKFELVM---------------- 459
NifK_Ava        RYSTLGYQGGLNILNWVVNTLLDEMDRSTNITGKTDISFDLIR---------------- 512
NifK_Rs         RFPTFGYQGAIQVLVKILDKIFDKLD------DESDISFDLTR---------------- 506
BchZ_Rd         DRIVETHPILTRIS--AAKSLRDAAEKAALAAGDERVVLSTVRALDPASAGPDLEDQT 491
BchZ_Ct         DGIVRKAPFISQIS--FGRELKRKAENLAASRGADTVTPDILQQLG------------ 468
BchZ_Rs         DRIVEEHPVLTRIS--AARALRDAAEKAALDAGAERVVRETVEALRGPGFGERKGENQ 491
BchZ_Rr         DRTVEAQPVVARIS--AAKRLRDAAERSARAAGEGQVTAARVIRLLDLQAGA------ 480
                          .:            :
```

Appendix D

Tab. S1: Amino Acid Sequence Identities of the individual subunits of DPOR, COR and nitrogenase. Amino acid sequences of the individual subunits of DPOR, COR and nitrogenase employed in the present study (compare Fig. 18 - 20) were aligned by using ClustalW method in MegAlign (DNASTAR) and sequence identities were calculated.

		DPOR			COR			nitrogenase		
		N	**B**	**L**	**Y**	**Z**	**X**	**NifD**	**NifK**	**NifH**
DPOR	**N**	37 – 58			15 – 18			12 – 20		
	B		34 – 62			15 – 22			14 – 18	
	L			51 – 69			31 – 35			31 – 38
COR	**Y**				35 – 78			13 – 15		
	Z					39 – 81			11 – 16	
	X						42 – 83			29 – 36
nitrogenase	**NifD**							17 – 70		
	NifK								37 – 58	
	NifH									67 – 75

DANKSAGUNG

Mein besonderer Dank gilt Prof. Dr. Dieter Jahn, der es mir ermöglicht hat, diese Arbeit in den letzten Jahren in seiner Arbeitsgruppe anzufertigen - und dabei stets mit hilfreichen Diskussionen und vor allem Motivation zur Seite stand.

Prof. Dr. Michael Steinert danke ich für sein Interesse an meiner Arbeit und seine Bereitschaft das Zweitgutachten dieser Dissertation zu übernehmen. Prof. Dr. Ralf Mendel sei gedankt für die Übernahme des Vorsitzes der Prüfungskommission.

Ganz besonderer Dank gilt Dr. Jürgen Moser für die hervorragende Betreuung, die sehr hilfreichen Diskussionen und fortwährende Unterstützung und Motivation.

Darüber hinaus bedanke ich mich bei Prof. Dr. Ribbe für die Bereitstellung der Nitrogenase-Untereinheit $NifH_2$, bei Prof. Dr. Forchhammer für die Zusammenarbeit bei der Herstellung der *S. elongatus* Mutanten, sowie bei Prof. Dr. Bauer für die Bereitstellung der *R. capsulatus* Mutante CB1200. Weiterhin danke ich der Arbeitsgruppe von Prof. Dr. Lendzian, insbesondere Miguel Saggu, für die Zusammenarbeit bei den ESR Messungen und Auswertungen für die COR. Außerdem geht Dank an Prof. Dr. Scheer und Prof. Dr. Rüdiger für die zur Verfügung gestellten Substratanaloga.

Ein großes Dankeschön an alle „Johnny's" für die nette Laboratmosphäre, die entspannenden Kaffeepausen und die Unterstützung.

Ein besonderes Dankeschön, an meine „Labormädels" Stefanie Klein und Simone Virus, sowie Dr. Corinna Lüer, Dr. Kalle Möbius und Dr. Rebekka Biedendieck für die ganzen Tipps, Tricks, Gespräche und Späße im und außerhalb des Labors, ohne die die ganze Zeit nur halb so schön gewesen wäre.

Allen Mitarbeitern der AG Jahn möchte ich für die nette Atmosphäre in der Arbeitsgruppe und die tolle Zeit danken.

Mein größter Dank gilt meiner Familie, insbesondere meinen Eltern, und meinen Freunden, die mich jederzeit unterstützt haben und immer für mich da waren und sind.